The Mre11-Rad50-Xrs2 Complex in the DNA Damage Response

Julyun Oh

Submitted in partial fulfillment of the
requirements for the degree
of Doctor of Philosophy
in the Graduate School of Arts and Sciences

COLUMBIA UNIVERSITY

2018

ABSTRACT

The Mre11-Rad50-Xrs2 Complex in the DNA Damage Response

Julyun Oh

DNA is continuously subjected to various types of damage during normal cellular metabolism. Among these, a DNA double-strand break (DSB) is one of the most cytotoxic lesions, and can lead to genomic instability or cell death if misrepaired or left unrepaired. The Mre11-Rad50-Xrs2/Nbs1 (MRX/N) complex orchestrates the cellular response to DNA damage through its structural, enzymatic, and signaling roles. It senses DSBs and is essential for both of the two major repair mechanisms: non-homologous end joining (NHEJ) and homologous recombination (HR). In addition, the complex tethers DNA ends, activates Tel1/ATM kinase, resolves hairpin capped DNA ends and maintains telomere homeostasis. Although significant progress has been made in characterizing the complex, many questions regarding the precise mechanism of how this highly conserved, multifunctional complex manages its various activities in chromosome metabolism remain to be solved. The overarching focus of this thesis is to further expand our understanding of the molecular mechanism and regulation of the MRX complex. Specifically, the contributions of Xrs2, Tel1, and Mre11 3'-5' dsDNA exonuclease in the multiple roles of the MRX complex are examined.

Xrs2/Nbs1, the eukaryotic-specific component of the complex, is required for the nuclear transport of Mre11 and Rad50 and harbors several protein-interacting domains. In order to define the role of Xrs2 as a component of the MRX complex once inside the nucleus, we fused a nuclear localization signal (NLS) to the C terminus of Mre11 and assayed for complementation of *xrs2Δ* defects. We found that nuclear localization of Mre11 (Mre11-NLS) is able to bypass several functions of Xrs2, including DNA end resection, meiosis, hairpin resolution, and cellular resistance to clastogens. Using purified components, we showed that the MR complex has the equivalent activity to MRX in cleavage of protein-blocked DNA ends. Although Xrs2 physically

interacts with Sae2, end resection in its absence remained Sae2 dependent in vivo and in vitro. MRE11-NLS was unable to rescue the xrs2Δ defects in Tel1 kinase signaling and NHEJ, consistent with the role of Xrs2 as a chaperone and adaptor protein coordinating interactions between the MR and other repair proteins.

To further characterize the role of Xrs2 in Tel1 activation, we fused the Tel1 interaction domain of Xrs2 to Mre11-NLS (Mre11-NLS-TID). Mre11-NLS-TID was sufficient to restore telomere elongation and Tel1 signaling to Xrs2-deficient cells, indicating that Tel1 recruitment and activation are separate functions of the MRX complex. Unexpectedly, we found a role for Tel1 in stabilizing Mre11-DNA association independently of its kinase activity. This stabilization function becomes important for DNA damage resistance in the absence of Xrs2. Moreover, while nuclear-localized MR complex is sufficient for HR without Xrs2, MR is insufficient for DNA tethering, stalled replication fork stability, and suppression of chromosomal rearrangements. Enforcing Tel1 recruitment to the MR complex fully rescued these defects, highlighting the important roles for Xrs2 and Tel1 in stabilizing the MR complex to prevent replication fork collapse and genomic instability.

Lastly, in order to decipher the functional significance of the Mre11 3'-5' dsDNA exonuclease activity in DSB repair, mre11 mutant alleles reported to be proficient endonuclease and deficient exonuclease were analyzed in vivo and in vitro. Although we did not observe a clear separation of the nuclease activities in vitro, our genetic analysis of the mutant allele is consistent with the current two-stepped, bidirectional model of end resection.

Table of Contents

List of Figures

List of Tables

Acknowledgement

First of all, I would like to thank my thesis advisor Dr. Lorraine Symington. Lorraine is everything and anything you could wish for in an ideal mentor; She is supportive, encouraging, patient, and caring. She holds your hand when you are about to fall and pushes you further once you learn how to run. She is a pure scientist and my ultimate role model. Her genuine curiosity and passion for science, as well as her sincere dedication to help her mentees find the joy of discovery is truly inspiring. I am forever grateful to have learned from her. Thank you.

I would also like to thank –

My thesis committee: Dr. Jean Gautier and Dr. Shan Zha for their insightful discussions throughout my dissertation; Dr. Rodney Rothstein and Dr. John Petrini for serving on my defense committee.

My collaborators for their contribution in my thesis and publications: Dr. Petr Cejka, Elda Cannavo, Dr. Rodney Rothstein, and So Jung Lee.

Members of the Rothstein, Ciccia, Ghosh, and Dworkin labs, for generously sharing space, equipment, and reagents.

The past and current members of the Symington lab: Amr Al-Zain, Huan Chen, Sarah Deng, Roberto Donnianni, Valerie Garcia, Eleanor Glancy, Robert Gnügge, Mike Kimble, Alicia Lam, Lea Marie, Sehyun Oh, Patrick Ruff, Beth Stivison, and Tai-Yuan Yu. Symington lab has always been a happy, fun, supportive family. In addition to insightful scientific discussions, I treasured our long, talkative teatimes/lunches, our spontaneous lab outings, and our silly jokes which made my days in the lab genuinely enjoyable. I am truly grateful to have made so many life-long friends here. Thank you for all of your friendship and support.

Lastly, I would like to thank my family –

Mom and Dad, for their unconditional love and endless encouragement. I am forever in debt for their sacrifice and support throughout my life.

My sister and all my dear friends, for their continuous support and love.

My husband Seung Won Suh, for sharing every step of this journey with me.

Thank you.

Chapter 1: Introduction

1.1 Formation and repair of DSBs

DNA is continuously subjected to exogenous and endogenous stresses that are capable of leading to various types of DNA damage. Among these, DNA double-strand breaks (DSBs) are one of the most cytotoxic lesions a cell could harbor. A DSB can arise spontaneously when a replication fork collapses or can be induced by exposure to genotoxic agents such as ionizing radiation (IR) or clastogens. Even though accidental DSBs are highly cytotoxic, DSBs are necessary intermediates in a number of programmed recombination events, such as during V(D)J recombination in lymphocyte development, meiosis, and mating-type switching in budding yeast. In all cases, DSBs need to be properly detected and repaired to maintain genomic integrity. For this reason, cells have evolved a sophisticated and highly conserved DNA damage response (DDR) system that consists of checkpoint signaling and various repair mechanisms. As one can imagine, defects in the factors involved in DDR are implicated in many human pathologies including cancer predisposition, neurodegeneration, and immunodeficiency (Aguilera and Gomez-Gonzalez, 2008).

There are two mechanistically distinct pathways of repairing DSBs: homologous recombination (HR) and non-homologous end joining (NHEJ) (Figure 1-1). HR utilizes an intact donor template with extensive sequence homology for accurate repair. In contrast, NHEJ directly re-ligates the two ends of the broken DNA, which can be accompanied by gain or loss of nucleotides at the junction. Both mechanisms are highly conserved throughout the eukaryotic evolution.

HR initiates with degradation of the 5'-terminated strands in a process referred to as end resection. The resulting 3' single-strand DNA (ssDNA) intermediates are initially coated with replication protein A (RPA), which protects the ssDNA from degradation and removes secondary structures (Chen et al., 2013). Then, the recombination mediators, Rad52 in yeast and BRCA2 in human, replace RPA with Rad51 recombinase to engage in homology search.

Once an intact homologous donor is found, usually the sister chromatid, the ssDNA bound by Rad51 pairs with the complementary strand of the donor duplex to form a displacement loop (D-loop) and the 3' end primes DNA synthesis. From this point, several sub-pathways of HR have been defined (Figure 1-1). In double-strand break repair (DSBR), the second 3' overhang is captured by the displaced strand of the D-loop and forms a double Holliday junction intermediate, which is eventually resolved through nucleolytic cleavage or dissolved by Sgs1/BLM helicase to form crossover or non-crossover products (Sarbajna and West, 2014; Svendsen and Harper, 2010; Szostak et al., 1983; Wu and Hickson, 2003). In synthesis-dependent strand annealing (SDSA), the extended invading strand is displaced and anneals to the complementary 3' overhang in the other side of the break (Ferguson and Holloman, 1996). The remaining gap is then filled and the nicks are ligated. Even though HR uses a homologous template, in certain sub-pathways, the outcomes can be mutagenic. In single-strand annealing (SSA), annealing between long direct repeats exposed by extensive resection results in the deletion of one of the repeats (Fishman-Lobell et al., 1992). In circumstances where only one end of the broken chromosome remains, the remaining end invades homologous sequences and synthesizes from the site of invasion to the telomere by a process referred to as break-induced replication (BIR) (Sakofsky and Malkova, 2017). This pathway features a long ssDNA intermediate and is, therefore, highly mutagenic (Deem et al., 2011; Smith et al., 2007).

Repair by NHEJ initiates with Ku heterodimer (Yku70-Yku80) binding to the DSB ends and antagonizing the end resection process (Mimitou and Symington, 2010; Wu et al., 2008). The two broken ends are then directly re-ligated by the DNA ligase IV complex (Lig4/Dnl4-Lif1/Xrcc4-Nej1/Xlf) (Chiruvella et al., 2013). The ligation can be precise or imprecise, depending on how the ends are processed before ligation (Daley et al., 2005). Vertebrate cells require additional factors to facilitate NHEJ, including the catalytic subunit of DNA-dependent protein kinase (DNA-PKcs) and Artemis. DNA-PKcs is recruited and activated by DSB-bound KU to trigger signaling cascade that promotes the repair process (Dynan and Yoo, 1998).

Artemis nuclease is activated by DNA-PKcs to trim back overhangs in preparation for ligation (Ma et al., 2002; Mohapatra et al., 2013). In the absence of these classical NHEJ factors, a distinctive alternative NHEJ (alt-NHEJ) pathway can occur using microhomology-mediated end joining (MMEJ). MMEJ can be viewed as a smaller-scaled SSA pathway as it uses short microhomologies (MHs) (5-25 nt in yeast; 1-16 nt in mammalian cells) to anneal and repair DSBs (Bennardo et al., 2008; Boboila et al., 2012; Sfeir and Symington, 2015; Truong et al., 2013; Yan et al., 2007). Similarly to SSA, MMEJ pathway requires end resection to expose the MHs internal to the break ends (Truong et al., 2013) (Figure 1-1). After annealing of the MHs, heterologous flaps are removed, DNA is synthesized to fill-in the gap, and then the ends are ligated to regenerate an intact chromosome (Sfeir and Symington, 2015).

The relative reliance on different repair mechanisms depends on the organism. Mammalian cells rely more on NHEJ than yeast cells presumably because its larger genome with more repetitive sequences makes homology search difficult and dangerous. In contrast, the yeast genome is compact with fewer repetitive sequences, allowing HR to be more efficient and error-free. Similarly, MMEJ occurs in significantly higher frequency in metazoans than in budding yeast (Ma et al., 2003; Robert et al., 2009; Sfeir and Symington, 2015; Yan et al., 2007; Yu and Gabriel, 2003). Yeast cells lack several NHEJ and MMEJ factors that are found in vertebrates, including DNA-PKcs, Artemins, and Polθ (promotes pairing of short microhomologies and is required for template addition of nucleotides at break sites), which potentially accounts for the different efficiencies of these repair mechanisms (Chan et al., 2010; Yu and McVey, 2010). The cell cycle phase also dictates the repair pathway choice. NHEJ is more prevalent in the G1 phase while HR is generally restricted to the S and G2 phases, when the sister chromatid is available to be used as a template (Barlow et al., 2008; Clerici et al., 2008; Karathanasis and Wilson, 2002; Zierhut and Diffley, 2008). Also, CDK-mediated phosphorylation upregulates several HR factors, such as end resection factor Sae2/CtIP and

Dna2, in the S and G2 phases (Chen et al., 2011; Huertas et al., 2008; Huertas and Jackson, 2009).

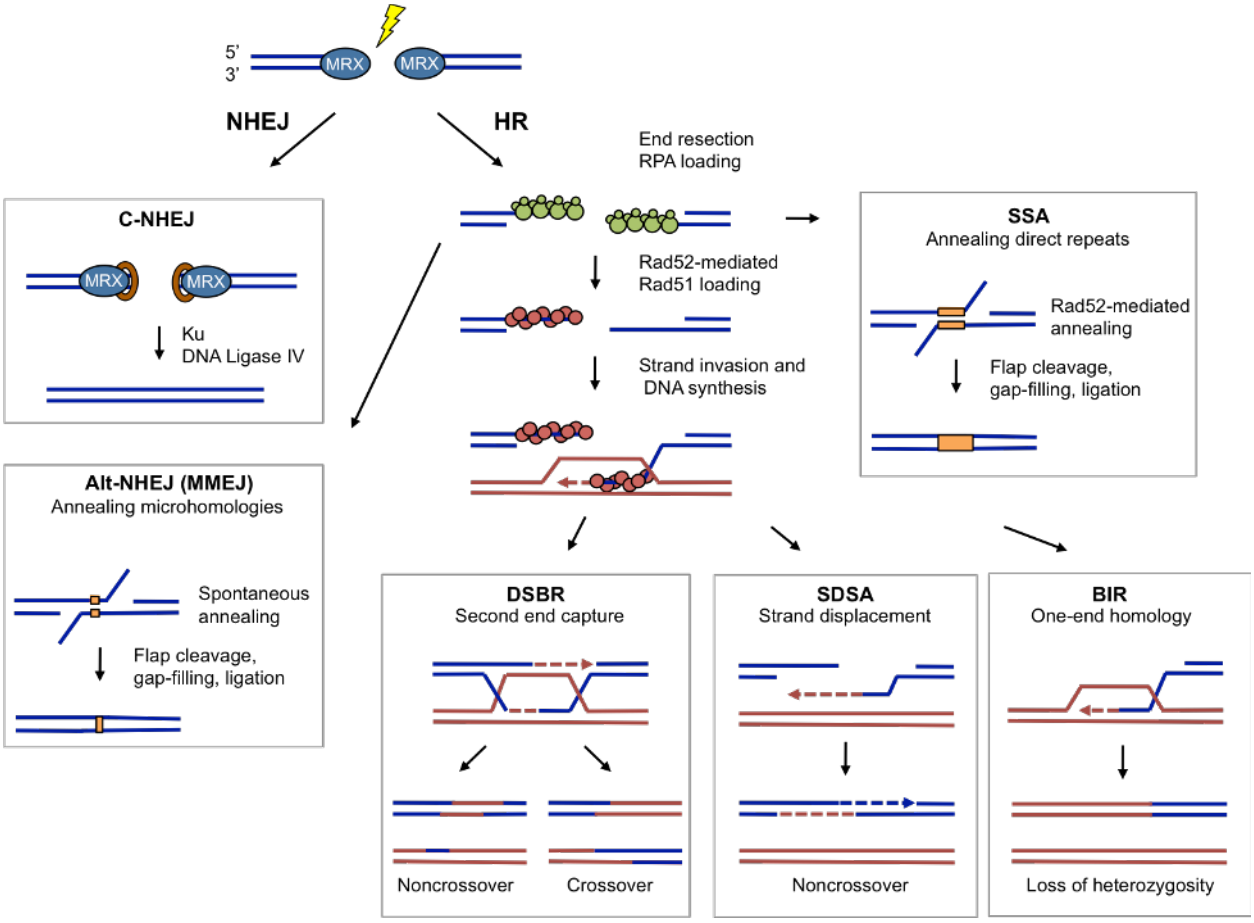

Figure 1-1. Overview of the DSB repair mechanisms

DSBs repair by two major pathways: NHEJ and HR. Classical NHEJ (C-NHEJ) directly re-ligates the two ends together while HR utilizes homologous template. HR initiates with end resection, followed by strand invasion and DNA synthesis through several sub-pathways: DSBR, SDSA, SSA, and BIR. Alternative NHEJ (Alt-NHEJ) anneals microhomologies after limited end resection.

1.2 Various roles of the Mre11 complex in DDR

Central to the DDR is the Mre11-Rad50-Xrs2/Nbs1 (MRX/N) complex. The complex orchestrates all stages of the DDR, including sensing the initial lesion, activating checkpoint signaling, driving specific repair pathways, and structurally bridging the participating DNA molecules together. The *MRE11, RAD50,* and *XRS2* genes were originally identified by their severe IR sensitivity and meiotic recombination defects in *Saccharomyces cerevisiae* (budding yeast) (Krogh and Symington, 2004). Mre11 and Rad50 are conserved in all domains of life whereas Xrs2/Nbs1 is less conserved than Mre11 and Rad50 and has only been identified in eukaryotes (Stracker and Petrini, 2011). The three proteins form a heterohexameric DNA binding complex containing dimers of each subunit (van der Linden et al., 2009; Williams et al., 2010). Hypomorphic mutations of human MRN complex components are associated with Nijmegen breakage syndrome (NBS) and Ataxia telangiectasia-like disorder (ATLD), which are characterized by cellular radiosensitivity, immune deficiency, and cancer proneness (Carney et al., 1998; Stewart et al., 1999; Stracker and Petrini, 2011). In mammals, the MRN complex is essential for cell viability, unlike in *S. cerevisiae,* in which the null mutations are viable (Luo et al., 1999; Xiao and Weaver, 1997; Zhu et al., 2001).

1.2.1 DSB detection and checkpoint activation

The cellular response to DSBs is initiated by detection of the lesions by the MRX/N complex, which binds to the broken DNA ends within minutes of the damage (Karlsson and Stenerlow, 2004). The complex is normally diffused evenly throughout the nucleus until a lesion induces the redistribution of the proteins to the damaged site in high concentration (Lisby et al., 2004; Maser et al., 1997; Nelms et al., 1998), indicating that the complex normally surveys the nucleus for a binding site. MRX/N scans along the DNA via facilitated diffusion to detect free ends (Myler et al., 2017). After binding to DSBs, the MRX/N complex recruits the central transducing kinase

Tel1/ATM and activates the DNA damage checkpoint signaling cascade (Figure 1-2) (Stracker and Petrini, 2011). Once resection proceeds and long tracts of RPA-coated ssDNA are generated, the Mec1/ATR kinase is recruited and activated through Ddc2/ATRIP to continue checkpoint signaling (Gobbini et al., 2013). The 9-1-1 checkpoint clamp, which is recruited to the ssDNA-dsDNA junction, also aids in Mec1/ATR kinase activation (Figure 1-2) (Majka et al., 2006; Melo et al., 2001). The two master DDR kinases, Tel1/ATM and Mec1/ATR, phosphorylate checkpoint mediators Rad9/53BP1, which in turn activate downstream checkpoint effectors such as Rad53/CHK2 (Harper and Elledge, 2007; Vialard et al., 1998). The signaling cascade arrests cell-cycle progression to ensures enough time for the repair to be completed and regulate activities of repair factors. In addition, chromatin elements, including H2A histone, are phosphorylated to trigger chromatin modification, which spreads surrounding the break and facilitate the accessibility of DNA to repair factors (Rogakou et al., 1998; van Attikum et al., 2004).

1.2.2 End resection

MRX/N competes with the Ku complex at DSB ends (Lee et al., 1998; Mimitou and Symington, 2010; Shim et al., 2010). To commit cells to HR, the MRX/N complex catalyzes the initiation of end resection, antagonizing Ku activity (Myler et al., 2017; Reginato et al., 2017; Wang et al., 2017). Generation of ssDNA prevents NHEJ and is necessary for the subsequent steps of recombination (Shim et al., 2010; Zierhut and Diffley, 2008). End resection follows a two-step, bidirectional mechanism (Figure 1-2). First, MRX/N, stimulated by its cofactor Sae2/CtIP, catalyzes an endonucleolytic cleavage internal to 5’ ends, generating a single-stranded nick. Then, the nick becomes an entry site for two parallel extensive resection machineries, the Exo1 5’-3’ exonuclease or the Sgs1/BLM helicase together with the Dna2 endonuclease, which will further degrade in a 5’ to 3’ direction. Meanwhile, MRX/N utilizes its 3’ to 5’ exonuclease activity to proceed back toward the DSB ends (Figure 1-2) (Cannavo and Cejka, 2014; Garcia et al.,

2011; Mimitou and Symington, 2008; Neale et al., 2005; Zhu et al., 2008). The initial endonucleolytic cleavage by MRX/N is critical for removing hairpin-capped ends or protein blocks from DSB ends (Lobachev et al., 2002; Reginato et al., 2017; Wang et al., 2017), while the long-range resection maintains DNA damage checkpoint and ensure fidelity by preventing recombination between short dispersed repeats (Chung et al., 2010; Gravel et al., 2008; Zhu et al., 2008).

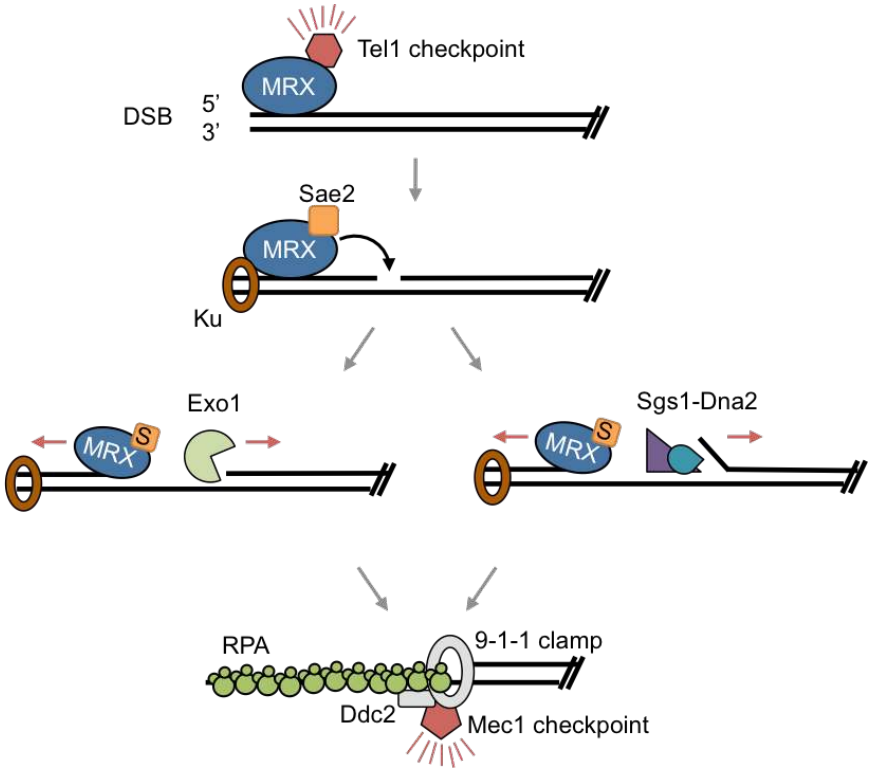

Figure 1-2. Process of end resection and checkpoint activation

The MRX complex detects DSBs and binds to the break ends. Xrs2 recruits Tel1 and checkpoint signaling is activated. Resection follows a two-step, bidirectional mechanism. MRX, together with its cofactor Sae2, initiates resection by endonucleolytic cleavage of the 5'-terminated strand, generating an entry site for long-range resection machineries, Exo1 and Sgs1-Dna2, to proceed in the 5' to 3' direction. Meanwhile, the MRX complex proceeds back towards the dsDNA end using its 3' to 5' exonuclease. ssDNA generated by resection is coated by RPA, which recruits Ddc2 and 9-1-1 clamp to activate Mec1 checkpoint kinase.

Besides its catalytic function, the MRX complex also physically recruits Exo1 and Sgs1-Dna2 nucleases to the damaged site (Mimitou and Symington, 2010; Shim et al., 2010). Mutations that eliminate the nuclease activity of the complex (*mre11-nd*) or *sae2Δ* mutant show a mild resection defect at DSB ends with no covalent modification because, in the absence of the endonucleolytic cleavage, Exo1 and Sgs1-Dna2 can initiate resection, albeit with some delay (Mimitou and Symington, 2009). However, *mre11Δ, rad50Δ,* and *xrs2Δ* mutants show a more severe resection defect, presumably because the absence of the complex attenuates recruitment of Exo1, Sgs1, and Dna2 to DSBs (Shim et al., 2010). The DNA damage sensitivity of *mre11-nd* and *sae2Δ* cells can also be rescued by deletion of *YKU70* as the elimination of Ku exposes the DSB ends to allow Exo1 to directly access the DNA ends and initiate resection (Mimitou and Symington, 2010). In *Schizosaccharomyces pombe* (fission yeast) and mammalian cells, *mre11-nd* confers greater defects in resection, HR, and resistance to DNA damaging agents than is observed in budding yeast (Buis et al., 2008; Langerak et al., 2011). This difference may be due to the differing extent of compensating activity by the long-range resection machineries or Ku may be more dominating in fission yeast and higher eukaryotes, thereby posing a greater barrier for resection.

End resection is a crucial regulatory process in the DSB response because it holds the key to repair pathway choice. Initiation of resection by MRX/N-Sae2/CtIP commits cells to HR in lieu of NHEJ by ejecting Ku from DSB ends and processing the substrate for end joining (Shibata et al., 2014; Wang et al., 2017). Furthermore, end resection orchestrates the DNA damage checkpoint signaling by mediating the switch from Tel1-dependent checkpoint signaling to Mec1, as mentioned in section 1.2.1

In *S. cerevisiae*, HR still occurs in Mre11-complex mutants. The lack of MRX delays but does not prevent mating-type switching, a specialized mitotic intrachromosomal gene conversion process (Ivanov et al., 1994). Moreover, while homozygous diploids of central HR

factors *rad51Δ* and *rad52Δ* are as sensitive to IR as haploid strains, homozygous *rad50Δ* diploid cells show increased IR resistance compared to haploid cells, indicating a proficiency in diploid-specific repair (Saeki et al., 1980). In fact, the absence of MRX in diploid yeast cells increases the rate of spontaneous heteroallelic recombination about 10-fold (Ajimura et al., 1993; Bressan et al., 1999). These observations suggest that the extent of resection in MRX-null cells is still sufficient to mediate strand invasion.

1.2.3 NHEJ

MRX is essential for NHEJ in budding yeast. *In vitro*, MRX tethers DNA ends and stimulates their ligation by the DNA ligase IV complex (Chen et al., 2001). Moreover, the complex has been shown to interact with Lif1 *in vitro*, suggesting that it recruits the DNA ligase IV complex to the lesion (Chen et al., 2001; Matsuzaki et al., 2008; Palmbos et al., 2008). In mammalian cells, MRN plays a supporting role in classical and alt-NHEJ. MRN localizes to RAG-mediated DSBs during V(D)J recombination and regulates the repair pathway choice (Deriano et al., 2009). Resection initiation by MRN and CtIP is an essential step for MMEJ as it reveals MHs (Lee-Theilen et al., 2011; Rass et al., 2009; Truong et al., 2013; Zhang and Jasin, 2011).

1.2.4 Meiotic recombination

During meiosis, DSBs are programmed in order to promote recombination and mixing of genetic material between homologous chromosomes. In addition, recombination during meiosis links chromosome homologs and ensures correct alignment and segregation during meiosis I. In budding yeast, the MRX complex plays at least two roles during meiotic recombination. First, the complex is required for the meiosis-specific topoisomerase-like protein, Spo11, to generate DSBs. This function is independent of the nuclease activity of the MRX complex. After DSB formation, Spo11 is covalently attached to the 5’ end at break sites. The second role of the Mre11 complex is to remove Spo11 from break ends by endonucleolytic cleavage, releasing

Spo11 attached to a short oligonucleotide (D'Amours and Jackson, 2002; Haber, 1998; Neale et al., 2005). This function requires the nuclease activity of the MRX complex. *mre11-nd*, *sae2Δ*, and *rad50S* show the same defect in processing Spo11-bound meiotic DSB ends, while lack of the complex prevents Spo11-mediated meiotic DSB formation. By coupling DSB formation and processing, MRX ensures timely and efficient crossover formation and restoration of genome integrity before the meiotic division. Unlike in budding yeast, fission yeast and vertebrate MRN is not required for meiotic DSB formation but is strictly required for DSB processing (Borde, 2007; Young et al., 2004). Interestingly, in *Caenorhabditis elegans,* Mre11 and Rad50 are required for both meiotic DSB formation and processing whereas Nbs1 is only required for the latter (Girard et al., 2018). The evolutionary reason for this differential requirement for MRX/N in meiotic DSB formation in different organisms is currently unknown.

After the removal of Spo11, MRX also stimulates recruitment of Exo1, either directly or indirectly by creating a substrate for Exo1. Unlike in mitotic DSB processing, Sgs1-Dna2 pathway does not appear to play an active role in meiotic end resection (Keelagher et al., 2011; Zakharyevich et al., 2010). The bidirectional model of end resection was proposed based on the phenotype of mre11 and exo1 mutants during meiosis. An *mre11* allele that encodes a protein proficient for endonuclease but defective for exonuclease activity *in vitro* (*mre11-H59S*) shows longer (41-300nt) Spo11-linked oligonucleotides compared to WT cells (12-40nt) (Garcia et al., 2011). In *exo1Δ* mutants, average resection tract length is ~300 nt, compared with ~800 nt in WT cells (Mimitou et al., 2017; Zakharyevich et al., 2010), longer than the predicted if MRX-Sae2 clipping removed only 12-40 nt from DSB ends. The combination of *mre11-H59S* with *exo1Δ* results in accumulation of DSBs and abrogation of meiotic end resection (Garcia et al., 2011). These observations demonstrate the bidirectional resection by MRX and Exo1 in which the Mre11 exonuclease is responsible for processing back towards the DSB ends from the single-stranded nick created by the Mre11 endonuclease ~300nt internal to the Spo11-bound end while Exo1 proceeds in a 5’-3’ direction away from the DSB.

1.2.5 Hairpin resolution

SbcD and SbcC, the *E. coli* homologs of Mre11 and Rad50, respectively, function primarily to cleave DNA hairpins formed by palindromic sequences (Connelly and Leach, 2002). DNA hairpins form on the lagging strand during DNA replication and after SbcCD cleavage, the resulting DSB is repaired by RecA-dependent sister-chromatid recombination, preserving the palindrome. Consistently, hairpin-capped DNA ends are resolved by MRX-Sae2 to prevent palindromic gene application and other chromosomal rearrangements in yeast (Chen et al., 2013; Deng et al., 2015; Lobachev et al., 2002; Narayanan et al., 2006; Rattray et al., 2005).

1.2.6 Replication stability

DNA replication forks are fragile structures where damage can arise easily. Indeed, spontaneous Rad52 foci form without any exogenous DNA damage in approximately 5% of cells during S phase (Lisby et al., 2003; Lisby et al., 2001), representing spontaneous DNA damage during replication. The DDR is responsible for stabilizing the fork, resolving the replicative stress, and completing DNA synthesis in order to avoid chromosomal rearrangements that lead to genomic instability (Harper and Elledge, 2007).

Given its pivotal role in the DDR, it is not a surprise that the Mre11 complex also plays a crucial role in the replication stress response. In mammalian cells, the MRN complex colocalizes with proliferating cell nuclear antigen (PCNA) and with sites of BrdU incorporation throughout an unperturbed S phase (Maser et al., 2001). Mre11 was also detected at unperturbed replication-origin-proximal sites by chromatin immunoprecipitation (ChIP) and by isolation of proteins on nascent DNA (iPOND), and its enrichment significantly increased near stalled forks (Maser et al., 2001; Sirbu et al., 2011). In *Xenopus laveis*, depleting the Mre11 complex during replication resulted in increased DNA breakage and DSB accumulation (Costanzo et al., 2001).

The Mre11 complex is most likely recruited to replication forks by RPA. Stable interactions between MRN and RPA have been observed at replication sites throughout S

phase with increased interaction at sites of stalled forks induced by hydroxyurea (HU) or ultraviolet light (UV) (Olson et al., 2007; Robison et al., 2004). A mutation in the N-terminal OB fold of Rfa1 subunit of yeast RPA (*rfa1-t11*) abolished MRX recruitment to replication forks, leading to collapse of stalled replication forks and separation of sister chromatids (Seeber et al., 2016). Another study demonstrated that the MRX complex stabilizes the association of essential replisome components at stalled forks independently of the S phase checkpoint or the nuclease activity of Mre11 (Tittel-Elmer et al., 2009). Disruption of the MRX complex led to a loss of fork recovery and a failure to properly complete DNA replication under replication stress while the nuclease-dead complex was fine (Tittel-Elmer et al., 2009). These observations indicate a structural contribution of the Mre11 complex during replication.

When a replication fork encounters a lesion, the fork may reverse its course and form a four-way junction structure, which protects the fork and allows for a restart (Neelsen and Lopes, 2015). Two SWI/SNF translocases, ZRANB3 and SMARCAL1, has been demonstrated to mediate such fork remodeling (Kolinjivadi et al., 2017; Taglialatela et al., 2017; Vujanovic et al., 2017). Fork reversal generates one-ended DSB that is subjected to degradation by MRE11 and EXO1. Rad51 accumulation at stalled forks depends on Mre11 nuclease activity, suggesting a requirement for end resection (Sirbu et al., 2011). Degradation by Mre11 at stalled forks may promote template switch –mediated repair or may amplify checkpoint signaling by enlarging ssDNA gaps. However, uncontrolled Mre11 nuclease activity can also be dangerous as it can lead to extensive nascent DNA degradation (Hashimoto et al., 2010; Vallerga et al., 2015). MRE11-mediated degradation of the reversed fork in *Brca*-deficient cells causes genome instability upon treatment with replication stress, demonstrating the toxicity of nucleolytic degradation at unprotected stalled forks (Chaudhuri et al., 2016). Such catastrophe is normally prevented by BRCA1 and BRCA2 in mammals, which protect nascent ssDNA from Mre11-mediated degradation by promoting formation of stable RAD51 nucleoprotein filament (Kolinjivadi et al., 2017; Lemacon et al., 2017; Mijic et al., 2017; Schlacher et al., 2011;

Taglialatela et al., 2017; Ying et al., 2012). Similarly to DSB end resection, CtIP initiates the MRE11-dependent degradation of the unprotected reversed fork and EXO1 further extends the degradation (Lemacon et al., 2017). Tel1 has also been reported to regulate the nuclease activity of Mre11 at replication fork that reverses after topoisomerase poisoning (Menin et al., 2018).

1.2.7 Cohesin loading

Cohesin is a structural maintenance of chromosomes (SMC) complex that keeps sister chromatids paired. In addition to ensuring proper chromosome segregation after replication, cohesin also contributes in DSB and stalled replication fork repair, presumably by maintaining sister chromatids in a conformation that favors efficient HR-mediated repair (Heidinger-Pauli et al., 2008; Kim et al., 2002; Sjogren and Nasmyth, 2001). DDR factors, including MRX, Tel1, and Mec1, regulate cohesin recruitment to DSBs and stalled forks (Strom et al., 2007; Strom and Sjogren, 2007; Unal et al., 2004; Unal et al., 2007). Mec1- and Tel1-dependent phosphorylation of histone H2AX generates a large domain along DSBs that enables cohesin binding (Unal et al., 2004). How MRX/N facilitates cohesin loading is unclear, as no physical interaction has been observed between the two complexes. Interestingly, structural features of Rad50 that are important for bridging sister chromatid, including the hook domain and coiled-coil region (see 1.3), are important for facilitating cohesin loading to forks during replication stress (Tittel-Elmer et al., 2012). MRX/N itself is structurally capable and sufficient of holding sister chromatid together at breaks at early time points (Seeber et al., 2016), suggesting that cohesin may simply load on to sisters initially held together by MRX/N. Nonfunctional or insufficient cohesin at damaged site causes sensitivity to IR and genotoxins (Sjogren and Nasmyth, 2001; Strom et al., 2007; Unal et al., 2004).

1.2.8 GCR suppression

A hallmark of cancer is the accumulation of gross chromosomal rearrangements (GCRs), such as translocations, interstitial deletions, and inverted duplications (Mitelman, 1991; Shikano et al., 1993). Genetic assays in *S. cerevisiae* that allow quantitative measurement of the accumulation of GCRs as well as identification of the spectrum of GCR event have been useful for identifying pathways that normally suppress the formation of GCRs (Chan and Kolodner, 2011; Chen and Kolodner, 1999; Kanellis et al., 2007; Putnam et al., 2009). In these assays, the loss of genetic markers on one arm of a chromosome is measured and analyzed. In the absence of *MRE11, RAD50*, or *XRS2,* the rate of GCR formation increases about 600-fold (Chen and Kolodner, 1999), demonstrating MRX role in normally suppressing GCRs. This effect is approximately 60-fold higher than that observed in simultaneous inactivation of HR factor *RAD51* and NHEJ factor *YKU70,* suggesting that the MRX complex acts beyond facilitating HR and NHEJ to prevent GCRs (Chen and Kolodner, 1999). *mre11-nd* and *sae2Δ* mutants show 13-fold and 5-fold increased GCR rates, respectively, (Deng et al., 2015) and loss of Tel1 has no significant effect on GCR rate (Myung et al., 2001b; Smith et al., 2005), indicating that the enzymatic and signaling functions of the MRX complex only mildly contributes in GCR suppression. A major class of GCR events recovered from *mre11-nd* and *sae2Δ* mutants is hairpin-mediated inverted duplication, which is a rare class in WT cells. Combining a hypomorphic allele of *RFA1* (encoding the largest subunit of the RPA complex), *rfa1-t33*, with *mre11-nd* or *sae2Δ* results in a >1000-fold increase in the rate of palindromic duplications (Deng et al., 2015). These observations led to the model where RPA normally prevents foldback structures between short inverted repeats at resected DSB ends and, when they do occasionally arise, the Sae2-dependent Mre11 endonuclease efficiently cleaves them to prevent the formation of inverted duplications (Deng et al., 2015).

1.2.9 Telomere maintenance

In addition to its role in DDR, MRX/N is also required for telomere homeostasis. Telomeres are specialized nucleoprotein structures that cap the ends of each chromosome to prevent degradation and fusions (Palm and de Lange, 2008). Telomerase maintains the length of telomeres by adding telomeric repeats to the terminal ssDNA tail using RNA template. In budding yeast, recruitment of telomerase to short telomeres requires MRX and Tel1. As in DSB repair, MRX first binds to telomeric ends and recruits Tel1 via Xrs2, which in turn recruits telomerase through phosphorylation of Cdc13 (Tseng et al., 2006; Wellinger and Zakian, 2012). Null mutations in any of the components of the MRX complex results in short telomeres similar to as in *tel1Δ* cells (Hector et al., 2007; Ritchie and Petes, 2000). Tel1 association to telomeres is counteracted by Rif2, which negatively regulates telomere length (Levy and Blackburn, 2004; Wotton and Shore, 1997). Rif2 also interacts with C-terminus of Xrs2 (Hirano et al., 2009), suggesting that Rif2 may inhibit Tel1 localization to telomeres by interfering with MRX-Tel1 interaction. Unlike in *S.cerevisae,* mammalian ATM is not required for association of telomerase to short telomeres (Feldser et al., 2006). However, MRN has been shown to mediate ATM-dependent response at dysfunctional telomeres (Takai et al., 2003). In addition, MRX/N is essential for processing telomeric DNA ends to generate 3' ssDNA overhangs, which impairs NHEJ and prevents fusions (Celli and de Lange, 2005).

1.3 Structural and biochemical properties of the Mre11 complex

Mre11 interacts independently with both Rad50 and Xrs2/Nbs1 and dimerizes with itself to form the core of the complex (Chamankhah and Xiao, 1999; Johzuka and Ogawa, 1995; Usui et al., 1998). The protein consists of phosphodiesterase motifs in the N-terminal region and displays manganese-dependent ssDNA endonuclease and 3'-5' dsDNA exonuclease activities *in vitro* (Figure 1-3A) (Furuse et al., 1998; Moreau et al., 1999; Paull and Gellert, 1998; Usui et al., 1998). Mutations in the conserved residues within the phosphoesterase domain (e.g., Asp16, Asp56, His125, and His213 of ScMre11) completely eliminate the endo-and exo-nuclease activities *in vitro* (Arthur et al., 2004; Moreau et al., 1999; Ohta et al., 1998; Usui et al., 1998). *mre11-nd* mutants with intact complex stability are proficient for telomere length maintenance and DDR, showing only mild IR sensitivity. However, *mre11-nd* mutants show severe defects in meiosis and hairpin resolution, similar to the *mre11Δ* cells, highlighting the importance of the nuclease activity in these functions (Lobachev et al., 2002; Moreau et al., 1999; Rattray et al., 2001). Mre11 forms a dimer in solution mediated via the phosphodiesterase domain (Hopfner et al., 2001). Disrupting Mre11 dimerization sensitizes cells to DNA damaging agents, demonstrating the importance of the dimeric form in the overall complex function (Williams et al., 2008). Moreover, structural analysis suggests that Mre11 dimerization coordinate short-range DNA bridging (Williams et al., 2008).

Rad50 is a member of the structural maintenance of chromosome (SMC) family of proteins, characterized by ATPase motifs at the N and C termini separated by a long coiled-coil domain (Figure 1-3A) (Stracker and Petrini, 2011). At the apex of the coiled-coil domain is a zinc-binding CxxC motif, referred to as a zinc hook, which facilitates dimerization with a second hook domain via the chelation of zinc ion (Figure 1-3A) (de Jager et al., 2001; Hopfner et al., 2002a). This hook-mediated dimerization of Mre11-complex tethers the two DSB ends and bridges the sister chromatids together (Hohl et al., 2011; Seeber et al., 2016; Wiltzius et al.,

2005). Maintaining close proximity of DNA ends may promote NHEJ by stimulating ligation. Indeed, the Mre11 complex has been shown to directly stimulate the activity of yeast DNA ligase IV complex *in vitro* (Chen et al., 2001). Bridging sister chromatids at DSBs may promote homology search for recombination and prevent the damaged chromatid from physically separating from the rest of the chromosome. Consistent with this view, Rad50 hook domain is crucial to prevent a DSB from becoming a chromosome break (Hohl et al., 2011; Lobachev et al., 2004; Wiltzius et al., 2005) and mutants with reduce end tethering ability show reduced efficiency in DSB-induced SDSA and SSA (Cassani et al., 2018; Cassani et al., 2016). Moreover, the absence of the MRX complex in diploid yeast cells increases the rate of spontaneous heteroallelic recombination about 10-fold, while the nuclease-defective Mre11 complex does not (Ajimura et al., 1993; Bressan et al., 1999). This observation can be explained by Rad50-mediated-bridging channeling DSB repair to the sister chromatid and suppressing the interhomolog recombination.

The long coiled-coil domain of Rad50 links the two ATPase motifs and the hook domain. The coiled-coils could extend up to approximately 500 Å, or 1,000 Å in the hook-mediated dimeric state (de Jager et al., 2004; Hopfner et al., 2002b). The length of the coiled-coil is critical for the Mre11 complex functions. Truncation of the coiled-coil domain abolishes meiotic DSB formation and telomere length maintenance (Hohl et al., 2011). Interestingly, short coiled-coil affects HR and NHEJ functions of the Mre11 complex differently. While truncation of ~300 amino acids severely impairs NHEJ, HR-related functions are largely intact (Hohl et al., 2011). Shortening the domain further (~500 amino acids removal) completely abolishes HR, suggesting that flexibility in the coiled-coils is important for mediating recombination (Hohl et al., 2011).

The globular DNA binding domain of the Mre11-Rad50 complex is comprised of an Mre11 dimer associated with the ATPase cassettes of a Rad50 dimer (Hopfner et al., 2000; Lee et al., 2003; Trujillo et al., 2003). The ATPase activity triggers conformational changes in the

Mre11-Rad50 complex, which are crucial for regulating the nuclease activity and the diverse functions of the complex (Figure 1-3B). ATP binding induces the “closed” conformation, in which Rad50 head domains dimerize and block the nuclease active site of Mre11. In this conformation, DNA tethering, ligation, and Tel1/ATM activation are promoted. ATP hydrolysis drives a disengagement of the Rad50 dimer, allowing the Mre11 active site to access DNA for its nuclease activity, thus promoting end resection (Deshpande et al., 2014; Lammens et al., 2011; Lim et al., 2011; Mockel et al., 2012). Consistently, the hairpin-opening activity and endonucleolytic cleavage internal to a protein-blocked DNA ends require ATP *in vitro* (Cannavo and Cejka, 2014; Hopfner et al., 2001; Paull and Gellert, 1998). Mutating the ATP-binding domain of Rad50 results in null-phenotype, highlighting the importance of conformation changes for the function of the MR complex (Alani et al., 1990; Hopfner et al., 2000). Mutation of residues near the ATPase domain generated a class of *rad50* mutants, referred to as *rad50S*, which confer similar phenotypes as *mre11-nd* and *sae2Δ* mutants (Alani et al., 1990). The *rad50S* mutants are proficient in ATPase activity and the molecular basis of the end-processing defect is currently not understood, but it is speculated that it may be impaired in protein-protein interactions.

Xrs2/Nbs1 is the eukaryote-specific component of the Mre11 complex. It harbors a number of protein-protein interaction motifs (Figure 1-3A), suggesting it functions as a chaperone and scaffold (Carney et al., 1998; Tsukamoto et al., 2005). The C-terminal region of Xrs2/Nbs1 contains Mre11 and Tel1/ATM interaction domains (Figure 1-3A) (Falck et al., 2005; Nakada et al., 2003; Tsukamoto et al., 2005; You et al., 2005). Deletion of the Tel1 interaction domain at the C terminus of Xrs2 (*xrs2-11*) results in a phenotype similar to the *tel1Δ* mutant, including defects in Tel1-dependent DNA damage signaling and short telomeres (Nakada et al., 2003). Mutation of residues within the Mre11 interaction motif that prevent binding to Mre11 confers a phenotype indistinguishable from *xrs2Δ* and *mre11Δ* null mutations in budding yeast and leads to embryonic lethality in mice (Demuth et al., 2004; Zhu et al., 2001). The Mre11

interaction domain is comprised of two regions: Interaction domain 1 wraps around the outside of the Mre11 phosphodiesterase domains in a highly extended conformation; Interaction domain 2 includes a highly conserved NFKxFxK motif that binds across the Mre11 dimer interface (Figure 1-3B). Interestingly, two Xrs2/Nbs1 molecules bind to an Mre11 dimer through interaction domain 1 while only one of the two Xrs2/Nbs1 molecules additionally binds to Mre11 via interaction domain 2. This second interaction is mediated by the eukaryotic-specific loop insertion, referred to as the latching loop, within the phosphoesterase domain that is absent from bacteria and archaeal proteins (Park et al., 2011; Schiller et al., 2012). It is suggested that the Xrs2/Nbs1 binding to the latching loop stabilizes the Mre11 dimeric form (Schiller et al., 2012). Indeed, expression of just a 108 amino acid fragment of murine Nbs1, encompassing the Mre11 interaction domain, is sufficient to sustain cell viability and improve dimer stability (Kim et al., 2017). The N-terminal region of Xrs2/Nbs1 contains a forkhead-associated (FHA) domain, which binds to phosphorylated Sae2 /CtIP and Lif1/Xrcc4 (Chen et al., 2001; Liang et al., 2015; Lloyd et al., 2009; Matsuzaki et al., 2008; Palmbos et al., 2008; Wang et al., 2013; Williams et al., 2009). The FHA domain is directly fused to a tandem BRCT domain (Becker et al., 2006; Lloyd et al., 2009). In mammals, checkpoint adaptor MDC1 interacts simultaneously with FHA and BRCT domains to engage with phosphorylated H2AX and amplify the DNA damage checkpoint (Stracker and Petrini, 2011; Xu et al., 2008). *In vitro*, Xrs2/Nbs1 promotes the DNA binding and nucleolytic hairpin processing abilities of Mre11-Rad50 (Lee et al., 2003; Paull and Gellert, 1999; Trujillo et al., 2003). Mammalian Nbs1 *in vitro* stimulates Mre11-Rad50-catalyzed endo- and exonucleolytic cleavage of DNA containing 5’ adducts (Deshpande et al., 2016), generating clean DSB ends that are available for further resection. Importantly, Xrs2/Nbs1 is the only component of the complex harboring a nuclear localization signal (NLS) and its interaction with Mre11 is necessary for translocation of Mre11-Rad50 into the nucleus (Carney et al., 1998; Desai-Mehta et al., 2001; Tsukamoto et al., 2005). Consistently, NBS patients with 657del5

allele, which confers reduced amounts of mutated protein, have Mre11 mislocalized to the cytoplasm (Carney et al., 1998; Tauchi et al., 2001).

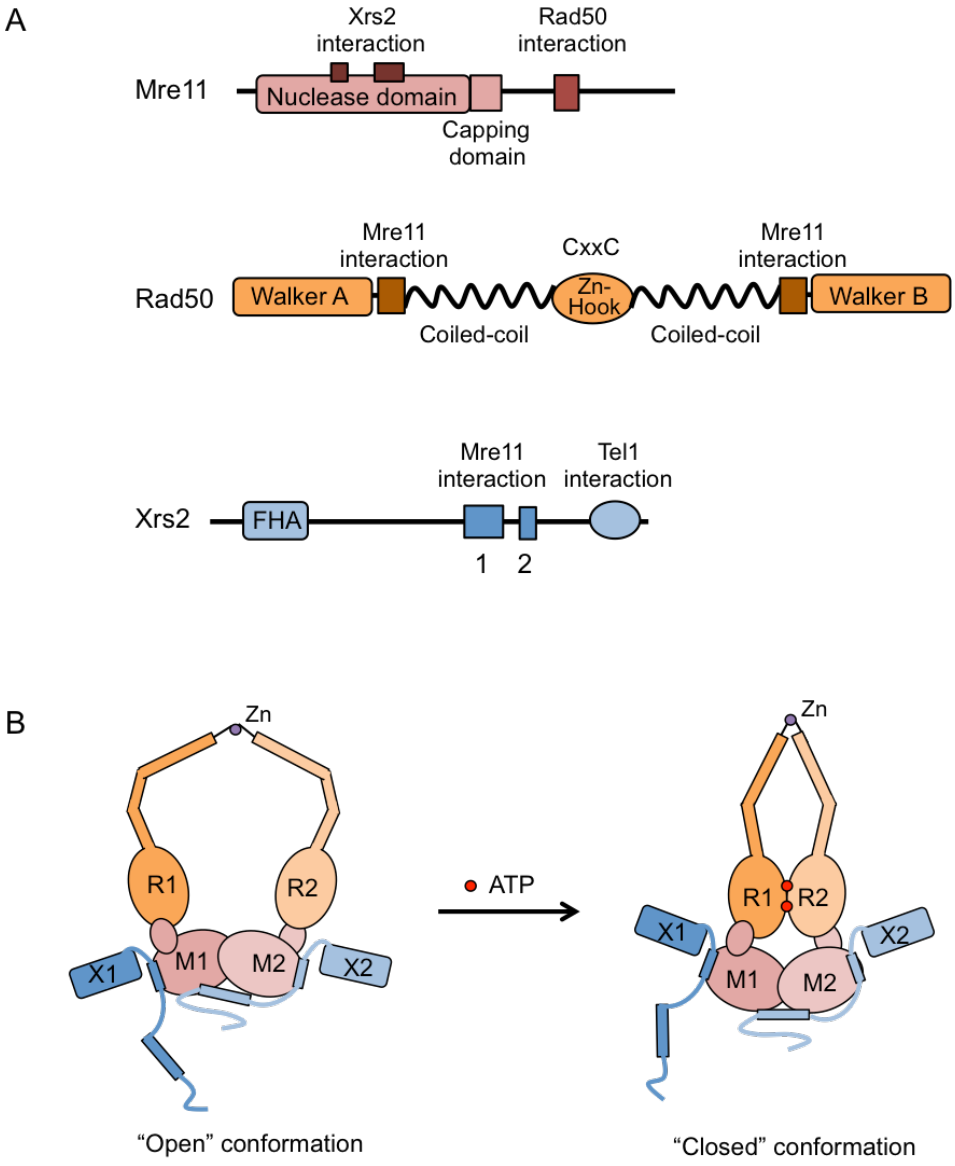

Figure 1-3. Domains and architecture of the MRX complex

(A) Mre11 consists a conserved phosphodiesterase nuclease domain and a capping domain at the N-terminus. The hydrophobic interaction domain for Rad50 resides towards the C-terminal region. Rad50 consists a bipartite ABC-ATPase domain at the N and C termini separated by a long coiled-coil domain. At the apex of the coiled-coil domain is a zinc hook CxxC motif. Xrs2 harbors FHA domain at the N-terminus and Mre11 and Tel1 interacting domains at the C-terminus. (B) Mre11, Rad50, and Xrs2 forms a 2:2:2 heterohexameric complex The MRX complex undergoes a dramatic conformation change upon ATP binding.

1.4 Sae2/CtIP and the Mre11 complex

Sae2/CtIP is a cofactor of the Mre11 complex and is essential for stimulating the dsDNA-specific endonuclease activity of Mre11 *in vitro* (Anand et al., 2016; Cannavo and Cejka, 2014). Indeed, *sae2Δ* exhibits the same defects as *mre11-nd* and *rad50S* cells in meiotic DSB processing and hairpin resolution (Keeney and Kleckner, 1995; Lobachev et al., 2002; McKee and Kleckner, 1997b; Prinz et al., 1997). Sae2/CtIP needs to be phosphorylated by CDK to be able to stimulate Mre11 endonuclease (Cannavo and Cejka, 2014; Huertas et al., 2008). In addition to regulating the Mre11 endonuclease, a recent *in vitro* study showed that Sae2 also stimulates the exonucleolytic activity of MRX at a DNA nick (Wang et al., 2017). At a mechanistic level, it is still unknown how Sae2/CtIP stimulates the endo- and exonuclease activities of Mre11.

Independent of its stimulatory effect on Mre11 endonuclease, recombinant Sae2 has been reported to harbor intrinsic ssDNA endonuclease that processes hairpin DNA (Lengsfeld et al., 2007). CtIP also has been reported to possess a 5' flap endonuclease activity on branched DNA structures *in vitro* (Makharashvili et al., 2014; Wang et al., 2014). However, nuclease-free recombinant Sae2 and CtIP have also been reported (Anand et al., 2016; Cannavo and Cejka, 2014; Niu et al., 2010; Wang et al., 2017), and no nuclease activity is associated with Ctp1, the functional ortholog of Sae2/CtIP in fission yeast (Andres et al., 2015). Further studies need to be done to verify the intrinsic nuclease activity of Sae2/Ctp1/CtIP.

In vivo, the absence of Sae2 does not significantly impair resection at HO- or I-SceI-endonuclease generated breaks because the presence of MRX is sufficient for the direct recruitment of Exo1 and Dna2-Sgs1, which can initiate resection at "clean" ends (Clerici et al., 2005; Mimitou and Symington, 2008; Shim et al., 2010). In contrast, the loss of Ctp1 or CtIP severely impairs resection and HR (Limbo et al., 2007; Sartori et al., 2007; Zhang and Jasin, 2011). Furthermore, deletion of CtIP in mouse leads to early embryonic lethality, indicating that

CtIP is required for cell proliferation (Chen et al., 2005). These observations reflect a stronger dependency on CtIP/Ctp1 for cell viability in higher eukaryotes.

Sae2/Ctp1/CtIP physically interacts with Xrs2/Nbs1 via its FHA domain (Liang et al., 2015; Lloyd et al., 2009; Williams et al., 2009) and weak interaction with Mre11 has also been observed (Cannavo and Cejka, 2014; Ghodke and Muniyappa, 2013). Sae2 has intrinsic DNA binding activity and can localize to DSBs independently of MRX (Lisby et al., 2004). Sae2 is required for the proper turnover of Mre11 at DSB ends. Mre11 foci persist longer at damaged sites and the enrichment of Mre11 at the vicinity of DSB is significantly higher in *sae2Δ* cells (Clerici et al., 2006; Kim et al., 2008; Langerak et al., 2011; Lisby et al., 2004). *mre11-nd* and *rad50S* cells also confer the persistent and hyper-enrichment of Mre11 at DSB ends, suggesting that the nuclease activity of Mre11 is required for timely eviction of the complex (Langerak et al., 2011; Lisby et al., 2004). Persistent accumulation of MRX sensitizes cells to DNA damage through hyper-activation of checkpoint signaling. *sae2Δ* is more sensitive to DNA damaging agents than *mre11-nd* and *rad50S,* and over-expression of Mre11 causes DNA damage sensitivity only in the absence of Sae2, suggesting that in addition to removing MRX from DSB ends, Sae2 also promote DNA damage resistance by attenuating a hyper-active checkpoint signal (Chen et al., 2015; Puddu et al., 2015).

X-ray crystal structures have revealed that Ctp1 and CtIP exist as a stable homotetramer and that this architecture is essential for effective end resection and repair by HR (Andres et al., 2015; Davies et al., 2015). Sae2 has also been shown to oligomerize in response to post-translational modifications (Fu et al., 2014). The oligomerized architecture of Sae2, Ctp1, and CtIP is structurally capable of binding and bridging DNA (Andres et al., 2015; Davies et al., 2015; Forment et al., 2015). Consistently, purified Ctp1 showed effective DNA linking activity *in vitro* (Andres et al., 2015). As mentioned before, the Mre11 complex also bridges DNA (Deshpande et al., 2014; Hopfner et al., 2002a; Williams et al., 2008). The precise roles of the

two DNA-tethering activities within the MR-Sae2/Ctp1/CtIP complex in coordinating DNA molecules are currently unknown.

1.5 Tel1/ATM and the Mre11 complex

Tel1/ATM is a member of the PIKK family, characterized as a serine/threonine protein kinase with an N-terminal HEAT repeat domain and C-terminal kinase domain (Lempiainen and Halazonetis, 2009). Mutations in the ATM gene are associated with ataxia telangiectasia (A-T), a human syndrome characterized by neurodegeneration, sensitivity to IR, immunodeficiency, and predisposition to cancer (Shiloh, 1997). The cellular phenotype and clinical manifestation of A-T are similar to NBS and ATLD.

Tel1/ATM is recruited to DSBs by the Mre11 complex. The N-terminal HEAT domain of Tel1/ATM physically interacts with the conserved Tel1/ATM-interacting motifs on the C-terminus of Xrs2/Nbs1 (Falck et al., 2005; Nakada et al., 2003; Tsukamoto et al., 2005; You et al., 2005). In *S. cerevisiae* Xrs2*,* The C-terminal 161 amino acids are necessary and sufficient for Tel1 interaction (Nakada et al., 2003). In *S. pombe* and *Xenopus laevis* Nbs1, a highly conserved FXF/Y motif preceded by an acidic patch of amino acids was shown to be essential for $Tel1^{ATM}$ binding (You et al., 2005). The conserved FATC domain on the C-terminus has also been shown to play a role in localization to DNA ends, possibly through affecting the overall structure of the HEAT repeats (Ogi et al., 2015). The physical interaction between Xrs2/Nbs1 and Tel1/ATM is crucial for the kinase activity and in yeast, Tel1 kinase activity is stimulated by MRX binding to protein-bound DNA ends (Fukunaga et al., 2011). The nuclease activity of the Mre11 complex is dispensable for the activation of Tel1/ATM (Buis et al., 2008) and the ATP-driven conformational changes in the MRN complex have been shown to regulate the ATM kinase activity (Lee et al., 2013), suggesting that distinct allosteric effect stimulates the kinase activity. Human ATM undergoes intermolecular autophosphorylation upon interaction with the MRN

complex, which results in dissociation of the inactive dimer into active monomers (Bakkenist and Kastan, 2003). The exact molecular mechanism of ATM/Tel1 activation remains to be elucidated. Tel1/ATM activation independently of the conserved Xrs2-interaction motif has been observed in murine cells and fission yeast (Difilippantonio et al., 2007; Limbo et al., 2018; Stracker et al., 2007), suggesting there may be an additional pathway in which Tel1/ATM can be activated.

The attenuation of Tel1/ATM kinase activity temporally correlates with the initiation of end resection. Once ssDNA is generated, Mec1/ATR checkpoint kinase is activated and in turn, Tel1/ATM signaling is inhibited (Nakada et al., 2005; Zou and Elledge, 2003). In the absence of Sae2 or Mre11 nuclease activity, Tel1 is hyper-activated and persists longer at the damage site (Clerici et al., 2005; Usui et al., 2001). *sae2Δ* and *mre11-nd* cells also show increased retention of MRX at DSB ends, consistent with the model where eviction of the Mre11 complex at DSB ends via resection turns off Tel1 activity. The significance of the Tel1/ATM to Mec1/ATR switch in response to DSBs remains to be fully understood.

In budding yeast, Tel1 checkpoint activity is functionally redundant with Mec1 activity but Mec1 is considered to be the principal PIKK. Lack of Tel1 does not sensitize cells to DNA damaging agents and only slightly reduces the resection efficiency (Lee et al., 2008; Mantiero et al., 2007). Moreover, phosphorylation of Rad53 is unperturbed as long as Mec1-dependent checkpoint pathway is active, unlike in mammals where ATM is required for Chk2 activation (Mantiero et al., 2007). This minor role of Tel1 in DSB signaling may reflect the efficient initiation of resection in *S. cerevisiae* and, thus, the preference to stimulate Mec1 kinase activity. Tel1-dependent phosphorylation of Mre11 and Xrs2 in response to DNA damage has been observed (D'Amours and Jackson, 2001; Usui et al., 2001), though its functional significance is not understood completely. Elimination of all the SQ and TQ motifs in Xrs2 does not cause any defects in telomere maintenance and DNA damage response (Mallory et al., 2003). In mammalian cells, ATM-dependent phosphorylation of Nbs1 appears to be necessary for S

phase checkpoint signaling (Lim et al., 2000; Zhao et al., 2000). ATM and ATR dependent phosphorylation of *Xenopus* Mre11 triggers the dissociation of MRN from chromatin, suggesting that it acts as a negative feedback loop to limit MRN activity (Di Virgilio et al., 2009).

Apart from its signaling activity, Tel1 also plays a structural role to stabilize MRX-DSB association. Deletion of Tel1 impairs MRX association at telomeric DNA ends and at DSBs (Cassani et al., 2016; Hirano et al., 2009), while kinase-dead mutant (*tel1-kd*) show comparable enrichment as in WT cells (Gobbini et al., 2015). Moreover, a screen for mutants that require Tel1 to survive genotoxic agents identified a mutation in Rad50 (*rad50-V1269M*), which results in reduced Mre11 and Rad50 association with DSBs. Deletion of Tel1, but not *tel1-kd*, further reduced the enrichment of MRX, indicating that Tel1 promotes and stabilizes the MRX-DSB association (Cassani et al., 2016). Interestingly, the activity of Rif2 in modulating MRX-Tel1 interaction is not restricted to telomeres. Rif2 is also recruited to intrachromosomal DSBs and counteracts Tel1 function in promoting MRX association to DSBs (Cassani et al., 2016).

1.6. Objectives

The MRX/N complex plays a central role in all aspects of the DDR, providing structural, enzymatic, and signaling roles. Defects in the human MRN complex are associated with the chromosome instability syndromes, Nijmegen breakage syndrome, and AT-like disorder, highlighting the importance of MRN function. The overarching objective of this thesis is to expand our understanding of the molecular mechanism and regulation of the MRX/N complex using genetic, biochemical, and molecular assays with *S. cerevisiae* as a model organism.

The enzymatic core of the complex is composed of Mre11 and Rad50, which are both found in all domains of life. Xrs2/Nbs1 is only found in eukaryotes with no enzymatic activities and several scaffolding domains, suggesting that it mediates eukaryote-specific functions as an adaptor. Xrs2/Nbs1 physically interacts with Tel1/ATM and is responsible for its recruitment to

DSBs. *In vitro*, Xrs2/Nbs1 influences the DNA binding and hairpin processing abilities of Mre11-Rad50. However, the precise role of Xrs2/Nbs1 in the various MRX/N complex functions is not fully defined in a molecular level. The aim of Chapter 3 is to define Xrs2 dependent and independent roles of Mre11-Rad50 complex functions in DDR. This study also sheds light into current gaps of our knowledge on the complex, such as the regulation of Mre11 nuclease activity and the activation of the Tel1/ATM kinase.

Tel1/ATM works closely with the MRX/N complex in DDR. It is recruited and activated by the complex, and Tel1 provides a positive feedback loop by stabilizing MRX association to DSBs. The significance of this Tel1-dependent stabilization has not been fully explored, partly because the lack of Tel1 does not confer obvious sensitivity to genotoxic agents in budding yeast. Chapter 4 aims to examine the consequence of Tel1 recruitment to Mre11 independently of Xrs2. This study expands our understanding of MRX-dependent Tel1 activation and the role of Tel1 and MRX in promoting efficient DNA tethering, replication fork stability, and genome stability.

Mre11 exhibits ATP-dependent ssDNA endonuclease activity and ATP-dependent 3'-5' dsDNA exonuclease activity, both of which participate in the bidirectional end resection process. The Mre11 endonuclease activity is essential for resolving "dirty ends" with protein abducts or secondary structures, and it commits cells to HR in lieu of NHEJ. The Mre11 exonuclease acts downstream of the endonucleolytic cleavage and is suggested to further enhance resection efficiency. However, the functional relevance of the Mre11 exonuclease during DNA repair has not been fully examined. The objective of Chapter 5 is to address these questions.

Chapter 2: Materials and Methods

2.1 Media and growth conditions

Media and growth conditions were as described previously (Amberg, 2005). Experiments were carried out with log-phase cells, unless otherwise indicated. Cells were grown at 30°C for all the experiments except for the end tethering assay, in which cells were grown at 23°C. For DNA damage sensitivity assays, cells grown overnight were diluted to 0.5 OD_{600}. 10-fold serial dilutions were made and were 4µl were spotted onto media with or without indicated DNA damaging drugs.

2.2 Yeast strains and plasmids

Yeast strains used in this study are listed in Table 2-1.

The strain containing *MRE11-NLS* integrated into the endogenous locus was constructed by one-step gene targeting. A PCR fragment containing a sequence encoding a monopartite NLS (CCAAAAAAGAAGAGAAAGGTC) in the 3' end of the *MRE11* ORF, along with 759bp of the upstream and 59bp of the downstream region of the *MRE11* locus, was transformed into an *mre11::URA3* strain, selecting for 5-fluoroorotic acid resistance. PCR and DNA sequencing were used to confirm clones with correct integration of the *MRE11-NLS* allele. Other W303 derivatives were constructed by crossing isogenic strains present in our laboratory collection to produce the indicated genotypes. For non-W303 strains, one-step gene replacement with PCR products was used to construct desired mutations. pRS416-*mre11-H125N-NLS* was constructed by site-directed mutagenesis of pRS416-*MRE11-NLS* (Schiller et al., 2012)

For the Mre11-NLS-X164 and Mre11-NLS-X85 strains, overlapping PCR was performed to fuse C-terminal 164 amino acid and 85 amino acid fragments of Xrs2 to the C-terminus of Mre11-NLS with 5xGly as a linker. The resulting Mre11-NLS-X164 and Mre11-NLS-X85 constructs were cloned into pRG205MX (Gnugge et al., 2016), along with the promoter (450bp

upstream) and 3'UTR (599bp downstream) of *MRE11,* and were integrated into the *LEU2* locus of *mre11::TRP1* strain. Integration was confirmed by PCR and DNA sequence analysis, and expression of the fusion proteins was analyzed by western blot using α-Mre11 polyclonal antibodies (Krogh et al., 2005). For the X224 strain, a 224 amino acid C-terminal fragment of Xrs2 was amplified and cloned into pRG205MX, along with the *XRS2* promoter (504bp upstream) and 3'UTR (468bp downstream), and was integrated into the *LEU2* locus of an *xrs2::kanMX* strain. X224-MYC strain was constructed by one-step targeting of a PCR fragment containing a sequence encoding 13 repeats of MYC.

For the end tethering assay strain (W11278-23B), a tandem array of Tet operators (TetOx336) was integrated in *ura3* on chromosome V, and an I-*Sce*I cut site was integrated 4 kb to the left of *ura3* in iYEL023, as described (Lisby et al., 2003). The TetO array was visualized by TetR-mRFP, which is integrated in the intergenic region iYGL119 on chromosome VII. A tandem array of Lac operators (LacOx256) was integrated in iYEL024, 4 kb to the left of the I-*Sce*I cut site. The LacO array was visualized by YFP-LacI integrated in *his3*. The I-*Sce*I endonuclease gene is under the transcriptional control of *GAL1-10* promoter, integrated in *lys2* (Frank-Vaillant and Marcand, 2002). The Rad52 C-terminus was tagged with GAx3 linker and yeast codon optimized mTurquoise2, which is an improved variant of CFP. The protein sequence of mTurquoise2 is from (Goedhart et al., 2012) and yeast codon optimization was ordered from GenScript. Integration was accomplished with pop-in, pop-out using *K. lactis URA3*. All other W303-derived strains were obtained from crossing appropriate haploid strains. Strains used for the GCR assay were made by transformation with linear DNA fragments to generate gene disruptions, or to integrate Mre11 or Xrs2 constructs.

For generating the GST-tagged Mre11-H125N, Mre11-H59S, and Mre11-H59N, QuickChange II site-directed mutagenesis (Agilent Technologies) was performed on GST fusion vector, pEG(KT), containing *MRE11* ORF (Moreau et al., 1999). For generating the *mre11-*

H59S-NAT strain (LSY3329), PCR product consisting *mre11-H59S* tagged with NAT was transformed into *mre11::klURA3* strain (LSY1427).

2.3 Physical monitoring of end resection

The physical monitoring of end resection was performed as described (Gnugge et al., 2018). Yeast cells were grown in YP medium containing 2% lactate (YPL) to log phase and were arrested in G2/M phase with the addition of nocodazole (15 µg/ml) to the medium. Then, galactose was added to a final concentration of 2% for HO induction. Cells were collected at 30-60 min intervals after HO induction and genomic DNA was extracted. Genomic DNA was digested with StyI restriction enzyme and fragments were separated by neutral agarose gel electrophoresis. DNA fragments were transferred to nylon membranes and hybridized with a probe that recognizes *MAT* sequence distal to the HO-cut site (coordinates 201176-201580 on chromosome III). A probe corresponding to coordinates 173285-173654 on chromosome VII sequence was used for normalization of band intensities by ImageJ. DSB end resection for each time point was estimated as a percentage of signal intensity corresponding to that before induction and represents the mean of three independent experiments.

The real-time PCR assay was performed as described with primers flanking the StyI site located 0.7 kb away from the HO cut site (Gnugge et al., 2018; Zierhut and Diffley, 2008). A control primer pair was used to amplify a region on chromosome XV that does not contain StyI sites. The PCR reaction program and calculation of the fraction of DNA resected were done in the same manner as described (Chen et al., 2013; Gnugge et al., 2018). The mean of three independent experiments is presented.

2.4 Chromatin immunoprecipitation – real-time PCR (ChIP-qPCR)

For HA-Tel1, Mre11, and Dna2-Myc ChIP at *MAT* locus in Chapter 3, yeast cells were grown in YP medium containing 2% lactate (YPL) to log phase and were arrested in G2/M phase with the addition of nocodazole (15 µg/ml) to the medium. Then, galactose was added to a final concentration of 2% for HO induction. Cells were collected at 0, 1, and 3 hrs after HO induction. For For HA-Tel1, Mre11, and Scc1-Pk ChIP at *MAT* locus in Chapter4, cells were grown in YP medium containing 2% lactate (YPL) to log phase. Cells were collected before (-HO) and 90 minutes after (+HO) addition of galactose to a final concentration of 2% for HO induction. For Polα-Flag and Mre11 ChIP at replication origin ARS607, cells were arrested in G1 using α-factor and released into YPD containing 0.2M HU. Cells were collected at 20 min intervals after release. To perform ChIP, collected cells were crosslinked with 1% formaldehyde and were then lysed in lysis buffer (50mM HEPES, 140mM NaCl, 1mM EDTA, 1% IGEPAL CA-630, 0.1% Sodium deoxycholate, 1mM PMSF) using FastPrep-24 (MP Biomedicals). Chromatin was fragmented by water bath sonication and immuno-precipitation was carried out with Pierce A magnetic beads or Pierce A/G magnetic beads coupled to Anti-Mre11 (Krogh et al., 2005), anti-HA (ab9110), anti-cMyc 9E10 (Santa Cruz Biotechnology), anti-Flag M2 (Sigma), or anti-V5 [SV5-pk1] (ab27671) antibodies overnight at 4°C. qPCRs were carried out by the SYBR green system using primer pairs complementary to DNA sequences corresponding to ARS607 and sites 0.2 kb and 1 kb from the HO-cut site at *MAT* (DSB). DNA sequences located 66 kb from *MAT* and 14 kb from ARS607 were amplified as background controls. Fold enrichment was calculated by $2^{\Delta\Delta Cq}$, where ΔΔCq = (Cq(IP, control) − Cq(input, control)) − (Cq(IP, DSB) − Cq(input, DSB)).

2.5 Recombinant proteins, DNA substrates, and nuclease assays

Recombinant Mre11-Rad50-Xrs2 was purified as a complex using baculoviruses coding for his-tagged Mre11, FLAG-tagged Xrs2 and untagged Rad50 as described previously (Cannavo and Cejka, 2014). Mre11-Rad50 heterodimer was prepared using his-tagged Mre11 and untagged Rad50 constructs. The soluble extract preparation and binding to Ni-NTA resin was carried out as described previously for the heterotrimer (Cannavo and Cejka, 2014). The Ni-NTA resin bound by Mre11-Rad50 was washed with Wash buffer I (Tris-HCl, pH 7.5, 50 mM; β-mercaptoethanol, 2 mM; NaCl, 0.2 M; phenylmethylsulphonyl fluoride, 1 mM; leupeptin, 10 $\mu g.ml^{-1}$; glycerol, 10%; imidazole, 25 mM), followed by Wash buffer II ($KHPO_4$, pH 7.4, 20 mM; β-mercaptoethanol, 2 mM; KCl, 80 mM; glycerol, 10%, phenylmethylsulphonyl fluoride, 1 mM) containing 25 mM imidazole. The heterodimer was eluted with Wash buffer II supplemented with 300 mM imidazole. Fractions containing Mre11-Rad50 were pooled and diluted with 5 volumes Wash buffer II without imidazole and 1 volume of H_2O. The sample was loaded on a pre-equilibrated 1 ml HiTrap SP column (GE Healthcare). The column was washed with SP buffer A ($KHPO_4$, pH 7.4, 20 mM; dithiothreitol, 1 mM; KCl, 100 mM; glycerol, 10%, phenylmethylsulphonyl fluoride, 1 mM). The protein was eluted with a 20 ml gradient in the same buffer with increasing KCl concentration (0.1 to 1 M). Samples were analyzed on SDS-PAGE gels and fractions containing protein (1.8 ml) were diluted with 10 ml Wash buffer II without imidazole and 10 ml H_2O. The sample was loaded on a pre-equilibrated 1 ml HiTrap Q column (GE healthcare), washed and eluted as above but with only 12 ml KCl gradient. Fractions containing recombinant Mre11-Rad50 were pooled, frozen in liquid nitrogen and stored at -80°C. Xrs2 was similarly expressed in *S. frugiperda* 9 cells and prepared by applying the soluble extract on anti-FLAG M2 affinity resin (Sigma). The resin was extensively washed with de-gassed Wash buffer (Tris-HCl, pH 7.5, 30 mM; β-mercaptoethanol, 0.3 mM; NaCl, 0.3 M; phenylmethylsulphonyl fluoride, 1 mM; leupeptin, 10 $\mu g.ml^{-1}$; glycerol, 10%; NP40, 0.1%),

and then with the same buffer without NP40. Xrs2 was eluted with wash buffer without NP40 but with FLAG peptide (Sigma, 200 μg.ml^{-1}). Fractions containing Xrs2 were pooled, frozen in liquid nitrogen and stored at -80°C. Recombinant Sae2, DNA substrates and nuclease assays were used as described previously(Cannavo and Cejka, 2014).

2.6 *In vivo* hairpin opening assay

The rate of Lys^{+} recombinants was derived from the median recombination frequency determined from eight different isolates of each strain as described (Lobachev et al., 2002).

2.7 End-joining assay

Yeast cells were transformed with 250 ng of *BamHI*-digested or undigested plasmid pRS414 (*ARS-CEN, TRP1)*. Transformation efficiency was calculated as a ratio of the number of transformants with digested plasmid DNA to that with undigested plasmid DNA. The chromosomal end-joining assay was performed as described (Deng et al., 2014).

2.8 Western blot and Rad53 phosphorylation assay

Protein extracts for western blot analysis were prepared by TCA precipitation. Anti-Mre11 (Krogh et al., 2005), anti-Rad53 (gift from M. Foiani), anti-Rfa1 (Agrisera), and anti-cMyc 9E10 (Santa Cruz Biotechnology) were used for western blot analysis. For checkpoint activation, cells were collected after one hour in a media containing 500 μg/ml of zeocin (Invitrogen).

2.9 Telomere blot

Genomic DNA was purified from an O/N culture and digested with XhoI restriction enzyme. The products were separated on 1% agarose gel and were examined by Southern blot anlysis with a probe that hybridizes to the repeated Y' element sequence. Wild-type strains yield a terminal restriction fragment of 1.3 kb, which includes ~400 bp of the G1–3T telomeric repeat.

2.10 End tethering assay

Cells were grown to log phase in SC medium containing 2% raffinose at 23°C. Then, galactose was added to a final concentration of 2% for I-SceI induction. Cells were collected and washed after 4 hr of growth at 23°C. Cells were re-suspended in a small volume of SC medium containing 2% glucose and were immobilized on a microscope slide by mixing them with a solution of 1.2% low melting agarose in SC medium. Live cell fluorescent imaging was performed on Leica DM5500B upright microscope with 100x Leica oil-immersion 1.46NA objective, using 100W mercury arc lamp as the light source. Chroma bandpass filter sets were used to visualize RFP (41002c), YFP (41028), and CFP (31044v2). Images were acquired with Hamamatsu ORCA-ER-1394 camera using Volocity software. 14 z-sections at 0.3μm intervals were taken for each channel.

2.11 DNA combing

DNA combing was performed as described (Hélène Tourrière, 2017). Cells were arrested in G1 using α-factor. BrdU was added to a final concentration of 40 μg/ml and 200mM HU 15 min before release cells into S phase using 50 μg/ml Pronase. After 3 hrs in 30°C, cells were collected and genomic DNA was prepared in 1% low melting point agarose DNA combing was performed on a Combicoverslip with the FiberComb Molecular Combing System (Genomic

Vision). BrdU was detected with a rat monoclonal antibody (ab6326) followed by a secondary antibody coupled to Alexa 488 (A11006, Molecular Probes). DNA molecules were detected with an anti-ssDNA antibody (MAB3034) followed by an anti-mouse IgG coupled to Alexa 546 (A11030, Molecular Probes). DNA fibers were analyzed on a Zeiss Axio Imager 2 microscope equipped with AxioCam MRc and a 63x Zeiss oil-immersion objective. Image acquisition was performed with AxioVision software. At least 100 BrdU tract lengths were measured for each genotype with ImageJ and representative DNA fibers were assembled with Image J. Significance was measured by Mann-Whitney rank sum test.

2.12 GCR assay

The rate of GCRs was measured by fluctuation assay as previously described (Putnam and Kolodner, 2010). Cells were grown to saturation and plated on YPD or 5FOA Can plates. Plates were incubated in 30°C and colonies were counted after 3-5 days. Two or more independent experiments using sets of at least five independent cultures were performed. Significance was determined by a Student's t test.

2.13 Recombination assays

The direct repeat recombination assay was performed as previously described (Ruff et al., 2016). Cells were grown to log phase in synthetic complete medium lacking tryptophan (SC-trp) supplemented with raffinose and then plated on YPD or 2% galactose (YPGal). Plates were incubated at 30°C and counted after 2–4 days. Colonies from YPGal were replica plated to SC-trp to determine the fraction due to gene conversion. Cell viability after I-SceI induction was determined by dividing the number of Trp+ and Trp- colonies on YPGal by that on YPD. Significance was determined by a Student's t test using the mean values of at least three

independent trials. For the diploid recombination assay, diploids were grown to log phase and plated on YPD or SC-ADE. Plates were incubated at 30°C and counted after 3-4 days. Fluctuation assay was used to determine the heteroallelic recombination rate. Three independent experiments using sets of eight independent cultures were performed. Significance was determined by a Student's t test.

2.14 Purification of GST-Mre11

The GST fusion plasmids were transformed into LSY0269. Transformants were grown in SC-URA/Raffinose to log phase and Galactose was added to a final concentration of 2%. Cells were harvested after 12 hours, resuspended in lysis buffer with acid glass beads, and lysed by FastPrep (MPbio). The lysate was clarified by centrifugation and the soluble fraction was mixed with Glutathione Sepharose 4B (GE Healthcare) for at least 4 hours at 4°C. The beads were collected by centrifugation and washed three times with lysis buffer. The GST fusion proteins were recovered from the beads by elution with 10 mM glutathione.

2.15 *In vitro* nuclease assays

For the *in vitro* endonuclease assay, 300 ng of ΦX174 viral DNA was incubated for 30 minutes at 30°C in a 30 µl reaction mixture volume containing 25 mM Tris-HCl [pH 8.0], 0.1 mM DTT, 5 mM $MnCl_2$, 100 µg BSA/ml, with 1 µg of purified Mre11 protein. To terminate the reaction, 0.3% SDS, 5 mM EDTA, and 50 mg/ml proteinase K were added and incubated in 37°C for 10 minutes. The reaction products were ran on 0.8% agarose gel for analysis.

For the *in vitro* exonuclease assay, a 5'-radiolabelled 55bp oligonucleotide was hybridized with its reverse complement to generate a dsDNA substrate. The substrate was incubated with ~0.3pmoles of purified proteins in 37°C for 30 minutes. The reaction was

stopped as in the endonuclease assay, denatured by boiling with loading dye, and separated by running through 6M urea / 12% polyacrylamide in 1x TBE.

Table 2-1. Yeast strains used

Strain	Genotype	Source
W303-1A	*MATa*	R. Rothstein
W303-1B	*MATα*	R. Rothstein
LSY2992	*MATα xrs2::KanMX*	This study
LSY2993	*MATa xrs2::KanMX*	This study
LSY3289	*MATa MRE11-NLS*	This study
LSY3386-1A	*MATα MRE11-NLS*	This study
LSY3386-8D	*MATa xrs2::URA3 MRE11-NLS*	This study
LSY3386-4A	*MATα xrs2::URA3 MRE11-NLS*	This study
LSY2363-28C	*MATa mec1::TRP1 sml1::HIS3*	Lab collection
LSY3616-4C	*MATα xrs2::URA3 MRE11-NLS sae2::KanMX*	This study
LSY3616-12C	*MATa xrs2::URA3 MRE11-NLS sae2::KanMX*	This study
LSY3399-9C	*MATα mec1::TRP1 sml1::HIS3 MRE11-NLS*	This study
LSY3399-20B	*MATα mec1::TRP1 sml1::HIS3 xrs2::URA3*	This study
LSY3399-16C	*MATa mec1::TRIP1 sml1::HIS3 xrs2::URA3 MRE11-NLS*	This study
LSY2346	*MATa lif1::KanMX*	This study
LSY1996	*MATa tel1::hphMX*	This study
LSY3543-4C	*MATa tel1::hphMX lif1::KanMX*	This study
LSY3543-8D	*MATα tel1::hphMX lif1::KanMX*	This study
LSY3344-15D	*MATa leu2::Gal-HO-LEU2 hmlΔ hmrΔ*	This study
LSY3464-1A	*MATa leu2::Gal-HO-LEU2 hmlΔ hmrΔ*	This study
LSY3387-1D	*MATa leu2::Gal-HO-LEU2 hmlΔ hmrΔ MRE11-NLS*	This study
LSY3464-1C	*MATa leu2::Gal-HO-LEU2 hmlΔ hmrΔ MRE11-NLS*	This study
LSY3083-22D	*MATa leu2::Gal-HO-LEU2 hmlΔ hmrΔ xrs2::KanMX*	This study
LSY3464-4C	*MATa leu2::Gal-HO-LEU2 hmlΔ hmrΔ xrs2::KanMX*	This study
LSY3327	*MATa leu2::Gal-HO-LEU2 hmlΔ hmrΔ MRE11-NLS xrs2::KanMX*	This study
LSY3464-2C	*MATa leu2::Gal-HO-LEU2 hmlΔ hmrΔ MRE11-NLS xrs2::KanMX*	This study
LSY3494-5C, 18B	*MATa leu2::Gal-HO-LEU2 hmlΔ hmrΔ MRE11-NLS sae2::KanMX*	This study
LSY3387-9A	*MATa leu2::Gal-HO-LEU2 hmlΔ hmrΔ MRE11-NLS xrs2::KanMX sae2::KanMX*	This study
LSY3387-10A, 21B	*MATα leu2::Gal-HO-LEU2 hmlΔ hmrΔ MRE11-NLS xrs2::KanMX sae2::KanMX*	This study
LSY3565-1C, 2A	*MATa leu2::Gal-HO-LEU2 hmlΔ hmrΔ MRE11-NLS tel1::hphMX*	This study
LSY3565-3A	*MATα leu2::Gal-HO-LEU2 hmlΔ hmrΔ MRE11-NLS tel1::hphMX*	This study
LSY3589-1B, 3D	*MATa leu2::Gal-HO-LEU2 hmlΔ hmrΔ MRE11-NLS tel1::hphMX sae2::KanMX*	This study
LSY3589-2D	*MATα leu2::Gal-HO-LEU2 hmlΔ hmrΔ MRE11-NLS tel1::hphMX sae2::KanMX*	This study
LSY3576-5B	*MATa leu2::Gal-HO-LEU2 hmlΔ hmrΔ DNA2-TEV-9MYC-HIS3 MRE11-NLS*	This study
LSY3576-	*MATα leu2::Gal-HO-LEU2 hmlΔ hmrΔ DNA2-TEV-9MYC-HIS3*	This study

12D	*MRE11-NLS*	
LSY3576-2A	*MATa leu2::Gal-HO-LEU2 hmlΔ hmrΔ DNA2-TEV-9MYC-HIS3 xrs2::KanMX*	This study
LSY3576-5D	*MATα leu2::Gal-HO-LEU2 hmlΔ hmrΔ DNA2-TEV-9MYC-HIS3 xrs2::KanMX*	This study
LSY3576-1C	*MATa leu2::Gal-HO-LEU2 hmlΔ hmrΔ DNA2-TEV-9MYC-HIS3 MRE11-NLS xrs2::KanMX*	This study
LSY3576-4B	*MATα leu2::Gal-HO-LEU2 hmlΔ hmrΔ DNA2-TEV-9MYC-HIS3 MRE11-NLS xrs2::KanMX*	This study
LSY3576-1A, 12B	*MATa leu2::Gal-HO-LEU2 hmlΔ hmrΔ DNA2-TEV-9MYC-HIS3 MRE11-NLS xrs2::KanMX sae2::KanMX*	This study
LSY3584-9A	*MATa leu2::Gal-HO-LEU2 hmlΔ hmrΔ DNA2-TEV-9MYC-HIS3 MRE11-NLS sae2::KanMX*	This study
LSY3584-2C	*MATα leu2::Gal-HO-LEU2 hmlΔ hmrΔ DNA2-TEV-9MYC-HIS3 MRE11-NLS sae2::KanMX*	This study
LSY3576-1A, 12B	*MATa leu2::Gal-HO-LEU2 hmlΔ hmrΔ DNA2-TEV-9MYC-HIS3 MRE11-NLS xrs2::KanMX sae2::KanMX*	This study
LSY3685-3B	*MATα leu2::Gal-HO-LEU2 hmlΔ hmrΔ HA-TEL1-URA3*	This study
LSY3685-5D	*MATα leu2::Gal-HO-LEU2 hmlΔ hmrΔ HA-TEL1-URA3 MRE11-NLS*	This study
LSY3685-5A	*MATα leu2::Gal-HO-LEU2 hmlΔ hmrΔ HA-TEL1-URA3 xrs2::kanMX*	This study
LSY3685-3D	*MATα leu2::Gal-HO-LEU2 hmlΔ hmrΔ HA-TEL1-URA3 MRE11-NLS xrs2::kanMX*	This study
ALE94	*MATα ade5-1 his7-2 leu2-3,112::p305L3 (LEU2) trp1-289 ura3-Δ lys2::AluIR*	(Lobachev et al., 2002)
ALE108	*MATα ade5-1 his7-2 leu2-3,112::p305L3 (LEU2) trp1-289 ura3-Δ lys2::AluIR sae2::HgrB*	(Lobachev et al., 2002)
LSY2930	*MATα ade5-1 his7-2 leu2-3,112::p305L3 (LEU2) trp1-289 ura3-Δ lys2::AluIR mre11::TRP1*	(Chen et al., 2015)
LSY3109	*MATα ade5-1 his7-2 leu2-3,112::p305L3 (LEU2) trp1-289 ura3-Δ lys2::AluIR mre11::TRP1 xrs2::KanMX*	This study
LSY3174	*MATα ade5-1 his7-2 leu2-3,112::p305L3 (LEU2) trp1-289 ura3-Δ lys2::AluIR mre11::TRP1 xrs2::KanMX sae2::HgrB*	This study
ALE1	*MATα ade5-1 his7-2 leu2-3,112::p305L28 (LEU2) trp1-289 ura3-Δ lys2::AluIR*	(Lobachev et al., 2000)
LSY3553	*MATα ade5-1 his7-2 leu2-3,112::p305L28 (LEU2) trp1-289 ura3-Δ lys2::AluIR sae2::KanMX*	This study
LSY3557	*MATα ade5-1 his7-2 leu2-3,112::p305L28 (LEU2) trp1-289 ura3-Δ lys2::AluIR tel1::HphMX*	This study
LSY2611-23D	*MATa ade2-ISIR-10MH lys2::P_{GAL}-I-SceI*	This study
LSY3529-2C	*MATα ade2-ISIR-10MH lys2::P_{GAL}-I-SceI MRE11-NLS*	This study
LSY3529-1B	*MATα ade2-ISIR-10MH lys2::P_{GAL}-I-SceI xrs2::URA3*	This study
LSY3529-5A	*MATα ade2-ISIR-10MH lys2::P_{GAL}-I-SceI MRE11-NLS xrs2::URA3*	This study
LSY3529-15C	*MATa ade2-ISIR-10MH lys2::P_{GAL}-I-SceI MRE11-NLS xrs2::URA3*	This study
LSY3542	*MATa ade2-ISIR-10MH lys2::P_{GAL}-I-SceI xrs2-S47A-H50A*	This study
LSY1532	*MATα mre11::TRP1*	Lab collection
LSY1996	*MATa tel1::hphMX4*	Lab collection
LSY2590-14D	*MATa tel1-kd-LEU2*	Lab collection
LSY4066	*MATα mre11::TRP1 xrs2::kanMX6 leu2::MRE11-NLS-X164-*	This Study

	k.l.LEU2	
LSY4069	*MATα mre11::TRP1 xrs2::kanMX6 leu2::MRE11-NLS-X85-k.l.LEU2*	This Study
LSY4020-1	*MATα xrs2::kanMX6 leu2::X224-k.l.LEU2*	This Study
LSY4161	*MATα xrs2::kanMX6 leu2::X224-MYC-k.l.LEU2*	This Study
LSY4068	*MATα mre11::TRP1 xrs2::kanMX6 leu2::MRE11-NLS-X164-k.l.LEU2 tel1::hphMX4*	This Study
LSY4070	*MATα mre11::TRP1 xrs2::kanMX6 leu2::MRE11-NLS-X85-k.l.LEU2 tel1::hphMX4*	This Study
LSY4035-15C	*MATα xrs2::kanMX6 leu2::X224-k.l.LEU2 tel1::hphMX4*	This Study
LSY4086-5D	*MATα mre11::TRP1 xrs2::kanMX6 leu2::MRE11-NLS-X164-k.l.LEU2 tel1-kd-LEU2*	This Study
LSY4087-1A	*MATα mre11::TRP1 xrs2::kanMX6 leu2::MRE11-NLS-X85-k.l.LEU2 tel1-kd-LEU2*	This Study
LSY4045-1B	*MATα xrs2::kanMX6 leu2::X224-k.l.LEU2 tel1-kd-LEU2*	This Study
LSY4168-1A	*MATa mre11::TRP1 xrs2::kanMX6 leu2::MRE11-NLS-X164-k.l.LEU2 sae2::kanMX6*	This Study
LSY4169-8A	*MATα mre11::TRP1 xrs2::kanMX6 leu2::MRE11-NLS-X85-k.l.LEU2 sae2::kanMX6*	This Study
LSY4050-2B	*MATα xrs2::kanMX6 leu2::X224-k.l.LEU2 sae2::kanMX6*	This Study
LSY4092-2B	*MATα mec1::TRP1 sml1::HIS3 mre11::TRP1 xrs2::kanMX6 leu2::MRE11-NLS-X164-k.l.LEU2*	This Study
LSY4093-2A	*MATα mec1::TRP1 sml1::HIS3 mre11::TRP1 xrs2::kanMX6 leu2::MRE11-NLS-X85-k.l.LEU2*	This Study
LSY4051-19B	*MATa mec1::TRP1 sml1::HIS3 xrs2::kanMX6 leu2::X224-k.l.LEU2*	This Study
LSY4076-4D	*MATα ade3:: Gal-HO hmlΔ hmrΔ*	This Study
LSY4076-16A	*MATα ade3:: Gal-HO hmlΔ hmrΔ xrs2::kanMX6*	This Study
LSY4076-14D	*MATa ade3:: Gal-HO hmlΔ hmrΔ xrs2::kanMX6 MRE11-NLS*	This Study
LSY4104-2C	*MATa ade3:: Gal-HO hmlΔ hmrΔ tel1::hphMX4*	This Study
LSY4091-1B	*MATα ade3::Gal-HO hmlΔ hmrΔ mre11::TRP1 xrs2::kanMX6 leu2::MRE11-NLS-X164-k.l.LEU2*	This Study
LSY4088-3A	*MATα ade3::Gal-HO hmlΔ hmrΔ mre11::TRP1 xrs2::kanMX6 leu2::MRE11-NLS-X85-k.l.LEU2*	This Study
LSY4052-23D	*MATα ade3::Gal-HO hmlΔ hmrΔ xrs2::kanMX6 leu2::X224-k.l.LEU2*	This Study
LSY4101-4C	*MATα ade3::Gal-HO hmlΔ hmrΔ HA-TEL1-URA3 mre11::TRP1 xrs2::kanMX6 leu2::MRE11-NLS-X164-k.l.LEU2*	This Study
LSY4100-2D	*MATα ade3::Gal-HO hmlΔ hmrΔ HA-TEL1-URA3 mre11::TRP1 xrs2::kanMX6 leu2::MRE11-NLS-X85-k.l.LEU2*	This Study
LSY4075-1A	*MATα ade3::Gal-HO hmlΔ hmrΔ HA-TEL1-URA3 xrs2::kanMX6 leu2::X224-k.l.LEU2*	This Study
W11278-23B	*MATa lys2::GAL-I-SceI URA3-TetO LEU2-LacO(YEL023) HIS3-YFP-LacI TetR-RFP RAD52-CFP*	This Study
LSY3903	*MATa lys2::GAL-I-SceI URA3-TetO LEU2-LacO(YEL023) HIS3-YFP-LacI TetR-RFP RAD52-CFP MRE11-NLS*	This Study
LSY3904	*MATa lys2::GAL-I-SceI URA3-TetO LEU2-LacO(YEL023) HIS3-YFP-LacI TetR-RFP RAD52-CFP xrs2::kanMX6*	This Study
LSY3905	*MATa lys2::GAL-I-SceI URA3-TetO LEU2-LacO(YEL023) HIS3-YFP-LacI TetR-RFP RAD52-CFP MRE11-NLS xrs2::kanMX6*	This Study
LSY3939	*MATa lys2::GAL-I-SceI URA3-TetO LEU2-LacO(YEL023) HIS3-*	This Study

	YFP-LacI TetR-RFP RAD52-CFP tel1::hphMX4	
LSY4008-18A	*MATa lys2::GAL-I-SceI URA3-TetO LEU2-LacO(YEL023) HIS3-YFP-LacI TetR-RFP RAD52-CFP tel1-kd-LEU2*	This Study
LSY4085-8C	*MATα lys2::GAL-I-SceI URA3-TetO LEU2-LacO(YEL023) HIS3-YFP-LacI TetR-RFP RAD52-CFP mre11::TRP1 xrs2::kanMX6 leu2::MRE11-NLS-X85-k.l.LEU2*	This Study
LSY4033-14C	*MATα lys2::GAL-I-SceI URA3-TetO LEU2-LacO(YEL023) HIS3-YFP-LacI TetR-RFP RAD52-CFP xrs2::kanMX6 leu2::X224-k.l.LEU2*	This Study
LSY4166-2A	*MATα lys2::GAL-I-SceI URA3-TetO LEU2-LacO(YEL023) HIS3-YFP-LacI TetR-RFP RAD52-CFP mre11::TRP1 xrs2::kanMX6 leu2::MRE11-NLS-X85-k.l.LEU2 tel1::hphMX4*	This Study
LSY4055-8D	*MATα lys2::GAL-I-SceI URA3-TetO LEU2-LacO(YEL023) HIS3-YFP-LacI TetR-RFP RAD52-CFP xrs2::kanMX6 leu2::X224-k.l.LEU2 tel1::hphMX4*	This Study
LSY4294-1C	*MATα lys2::GAL-I-SceI URA3-TetO LEU2-LacO(YEL023) HIS3-YFP-LacI TetR-RFP RAD52-CFP mre11::TRP1 xrs2::kanMX6 leu2::MRE11-NLS-X85-k.l.LEU2 tel1-kd-LEU2*	This Study
LSY4295-5D	*MATα lys2::GAL-I-SceI URA3-TetO LEU2-LacO(YEL023) HIS3-YFP-LacI TetR-RFP RAD52-CFP xrs2::kanMX6 leu2::X224-k.l.LEU2 tel1-kd-LEU2*	This Study
LSY4293-20A	*MATα ade3::Gal-HO hmlΔ hmrΔ SCC1-9PK::TRP*	This Study
LSY4293-15C	*MATα ade3::Gal-HO hmlΔ hmrΔ SCC1-9PK::TRP xrs2::kanMX6*	This Study
LSY4299-5A	*MATα ade3::Gal-HO hmlΔ hmrΔ SCC1-9PK::TRP xrs2::kanMX6 MRE11-NLS*	This Study
LSY 4298-11A	*MATα ade3::Gal-HO hmlΔ hmrΔ SCC1-9PK::TRP xrs2::kanMX6 leu2::MRE11-NLS-X85-k.l.LEU2*	This Study
LSY4300-8B	*MATα ade3::Gal-HO hmlΔ hmrΔ SCC1-9PK::TRP xrs2::kanMX6 leu2::X224-k.l.LEU2*	This Study
ZGY2565	*MATa bar1::hisG POL1-5Flag::kanMX6 URA3::BrdU-Inc*	(Yu et al., 2014)
LSY4152-2A	*MATa bar1::hisG POL1-5Flag::kanMX6 URA3::BrdU-Inc xrs2::kanMX6*	This Study
LSY4147-13A	*MATa bar1::hisG POL1-5Flag::kanMX6 URA3::BrdU-Inc xrs2::kanMX6 MRE11-NLS*	This Study
LSY4153-1	*MATa bar1::hisG POL1-5Flag::kanMX6 URA3::BrdU-Inc mre11::TRP1 xrs2::kanMX6 leu2::MRE11-NLS-X85-k.l.LEU2*	This Study
LSY4149-2D	*MATa bar1::hisG POL1-5Flag::kanMX6 URA3::BrdU-Inc xrs2::kanMX6 leu2::X224-k.l.LEU2*	This Study
LSY4285	*MATa bar1::hisG POL1-5Flag::kanMX6 URA3::BrdU-Inc tel1::hphMX4*	This Study
LSY4286	*MATa bar1::hisG POL1-5Flag::kanMX6 URA3::BrdU-Inc mre11::TRP1 xrs2::kanMX6 leu2::MRE11-NLS-X85-k.l.LEU2 tel1::hphMX4*	This Study
LSY4287	*MATa bar1::hisG POL1-5Flag::kanMX6 URA3::BrdU-Inc xrs2::kanMX6 leu2::X224-k.l.LEU2 tel1::hphMX4*	This Study
LSY4296-6C	*MATa bar1::hisG POL1-5Flag::kanMX6 URA3::BrdU-Inc tel1-kd-LEU2*	This Study
LSY4301-16A	*MATa bar1::hisG POL1-5Flag::kanMX6 URA3::BrdU-Inc mre11::TRP1 xrs2::kanMX6 leu2::MRE11-NLS-X85-k.l.LEU2 tel1-kd-LEU2*	This Study
4302-16A	*MATa bar1::hisG POL1-5Flag::kanMX6 URA3::BrdU-Inc xrs2::kanMX6 leu2::X224-k.l.LEU2 tel1-kd-LEU2*	This Study
RDK3695	*MATa yel069C::URA3*	(Chen and

		Kolodner, 1999)
LSY3980	*MATa yel069C::URA3 MRE11-NLS-hphMX4*	This Study
LSY3991	*MATa yel069C::URA3 xrs2::kanMX6*	This Study
LSY3992	*MATa yel069C::URA3 xrs2::kanMX6 MRE11-NLS-hphMX4*	This Study
LSY4231	*MATa yel069C::URA3 mre11::TRP1 xrs2::kanMX6 leu2::MRE11-NLS-X85-k.l.LEU2*	This Study
LSY4229	*MATa yel069C::URA3 xrs2::kanMX6 leu2::X224-k.l.LEU2*	This Study
LSY4283	*MATa MATa yel069C::URA3 mre11::TRP1 xrs2::kanMX6 leu2::MRE11-NLS-X85-k.l.LEU2 tel1::hphMX4*	This Study
LSY4284	*MATa yel069C::URA3 xrs2::kanMX6 leu2::X224-k.l.LEU2 tel1::hphMX4*	This Study
LSY3440-62D	*MATα ade2-n::TRP1::ade2-I-SceI lys2::GAL-I-SceI*	(Ruff et al., 2016)
LSY1709-9D	*MATa ade2-n::TRP1::ade2-I-SceI lys2::GAL-I-SceI rad51::LEU2*	(Mimitou and Symington, 2008)
LSY4105-14C	*MATα ade2-n::TRP1::ade2-I-SceI lys2::GAL-I-SceI MRE11-NLS-hphMX4*	This Study
LSY4195-5D	*MATα ade2-n::TRP1::ade2-I-SceI lys2::GAL-I-SceI MRE11-NLS-hphMX4 rad51::LEU2*	This Study
LSY4105-18A	*MATa ade2-n::TRP1::ade2-I-SceI lys2::GAL-I-SceI xrs2::kanMX6*	This Study
LSY4105-13D	*MATα ade2-n::TRP1::ade2-I-SceI lys2::GAL-I-SceI xrs2::kanMX6 rad51::LEU2*	This Study
LSY4105-12D	*MATa ade2-n::TRP1::ade2-I-SceI lys2::GAL-I-SceI MRE11-NLS-hphMX4 xrs2::kanMX6*	This Study
LSY4105-17B	*MATa ade2-n::TRP1::ade2-I-SceI lys2::GAL-I-SceI MRE11-NLS-hphMX4 xrs2::kanMX6 rad51::LEU2*	This Study
LSY0269	*MATa leu2 trp1 ura3-52 prb1-1122 pep4-3 prc1-407 GAL+*	Lab Collection
LSY3329	*MATα mre11-H59S-NAT*	This Study
LSY3373-2B	*MATα mre11-H59S-NAT exo1::KanMX6*	This Study
LSY3373-1C	*MATα mre11-H59S-NAT sgs1::HIS3*	This Study
LSY3375-3B	*MATa mre11-H59S-NAT exo1::kanMX6 hdf1::HIS3*	This Study
LSY3375-6B	*MATα mre11-H59S-NAT sgs1::HphMX4 hdf1::HIS3*	This Study
LSY3371-8D	*MATa mre11-H59S-NAT exo1::kanMX6 sgs1::HIS3*	This Study
LSY1714	*MATa mre11-H125N*	Lab Collection
LSY3374-14C	*MATα mre11-H125N exo1::kanMX6*	This Study
LSY3374-8A	*MATα mre11-H125N sgs1::HIS3*	This Study
LSY3390-10B	*MATα mre11-H125N-NAT exo1::URA3 hdf1::HIS3*	This Study
LSY3390-4B	*MATα mre11H125N-NAT sgs1::HphMX4 hdf1::HIS4*	This Study
LSY2401-1B	*MATa exo1::kanMX6*	Lab Collection
LSY1475	*MATa sgs1::HIS3*	Lab Collection
LSY2956-1C	*MATa ade2-ISIR-12MH lys2::pGAL-ISceI*	(Deng et al., 2014)
LSY2957-2B	*MATa ade2-ISIR-12MH lys2::pGAL-ISceI sae2::kanMX6*	(Deng et al., 2014)
LSY3006-3B	*MATa MATa ade2-ISIR-12MH lys2::pGAL-ISceI mre11-H125N-URA3*	(Deng et al., 2014)
LSY3439	*MATa ade2-ISIR-12MH lys2::pGAL-ISceI mre11-H59S-NAT*	This Study
LSY3458-3D	*MATa ade2-ISIR-12MH lys2::pGAL-ISceI mre11-H59S-NAT*	This Study

	sae2::kanMX6	
LSY3013-17B	*MATα ade2-ISIR-12MH lys2::pGAL-ISceI exo1::URA3 sgs1::HphMX4*	Lab Collection
LSY3701-1B	*MATa ade2-ISIR-12MH lys2::pGAL-ISceI mre11-H59S-NAT exo1::URA3*	This Study
LSY3701-2C	*MATa ade2-ISIR-12MH lys2::pGAL-ISceI mre11-H59S-NAT sgs1::HphMX4*	This Study
LSY3326-14B	*MATα leu2::Gal-HO-LEU2 hmlΔ hmrΔ mre11-H125N*	This Study
LSY3292	*MATα leu2::Gal-HO-LEU2 hmlΔ hmrΔ mre11-H59S-NAT*	This Study

* Most strains are of the W303 background (*trp1-1 his3-11,15 can1-100 ura3-1 leu2-3,112 ade2-1 RAD5*). ALE94, ALE108, ALE1, LSY2930, LSY3109, LSY3174, LSY3553 and LSY3557 are isogenic to CGL strain (*ade5-1, his7-2, leu2-3,112, trip1-289, ura3-Δ*). RDK3695, LSY3980, LSY3991, LSY3992, LSY4231, LSY4229, LSY4283, and LSY4284 are S288C background (*ura3-52 leu2Δ1 trp1Δ63 his3Δ200 lys2ΔBgl hom3-10 ade2Δ1 ade8*). Only the mating type and differences from these genotypes are shown.

Chapter 3: Xrs2 dependent and independent functions of the Mre11-Rad50 Complex

The results presented in this chapter have been published as:

Oh, J., Al-Zain, A., Cannavo, E., Cejka, P., & Symington, L. S. (2016). Xrs2 Dependent and Independent Functions of the Mre11-Rad50 Complex. *Molecular Cell, 64*(2), 405-415.

(A.A.-Z. constructed the *MRE11-NLS* strain, performed pilot experiments of growth and end resection, and the data presented in Figure 3-9E.
E.C. and P.C. performed the experiments shown in Figure 3-8.)

3.1 Introduction

This chapter aims to define the contribution of Xrs2 in the various Mre11-Rad50 complex functions once inside the nucleus. As mentioned in Chapter 1, Xrs2 is required for the nuclear localization of Mre11 (Schiller et al., 2012; Tsukamoto et al., 2005). In addition, a previous study demonstrated that nuclear localization of Mre11 via fusion to the Gal4 DNA binding domain (GBD) could partially bypass the requirement for Xrs2 in DNA repair (Tsukamoto et al., 2005). However, the mechanism by which nuclear Mre11 mediates DNA repair in the absence of Xrs2 was not investigated. Here we show that localization of Mre11 to the nucleus suppresses the slow growth, DNA damage sensitivity and meiotic defects of the *xrs2Δ* mutant by restoring Mre11 nuclease and Sae2-dependent end resection. However, Xrs2 is crucial for NHEJ and Tel1 signaling functions of the MRX complex.

3.2 Nuclear Mre11 rescues *xrs2Δ* slow growth and genotoxin sensitivity

To investigate the contribution of Xrs2 to MR activities, independently of Mre11 nuclear translocation, we fused a nuclear localization signal (NLS) to the C-terminus of Mre11 expressed from the endogenous locus and assayed for complementation of *xrs2Δ* defects. The steady-state protein level of Mre11-NLS was about two-fold lower than Mre11 in *XRS2* and *xrs2Δ* backgrounds (Figure 3-1A). Nevertheless, expression of *MRE11-NLS* suppressed the growth defect of *xrs2Δ* and this suppression was completely dependent on *RAD50* and *SAE2* (Figure 3-1B). A previous study had shown that expression of Mre11-GBD restores partial resistance to methyl methane sulfonate (MMS) to the *xrs2Δ* mutant (Tsukamoto et al., 2005). We found that *MRE11-NLS* partially suppresses the camptothecin (CPT) and MMS sensitivity of the *xrs2Δ* mutant in a *RAD50*-dependent manner, indicating that Xrs2 is dispensable for DNA repair once Mre11 and Rad50 are present in the nucleus (Figure 3-1C). Furthermore, Sae2 and Mre11 nuclease are required for DNA damage resistance in the *MRE11-NLS xrs2Δ* context,

even though the *sae2Δ* and *mre11-H125N* single mutants are not sensitive to the same low dose of CPT or MMS (Figure 3-1C,D), indicating that the nuclease activity of Mre11 is essential for DNA repair in the absence of Xrs2.

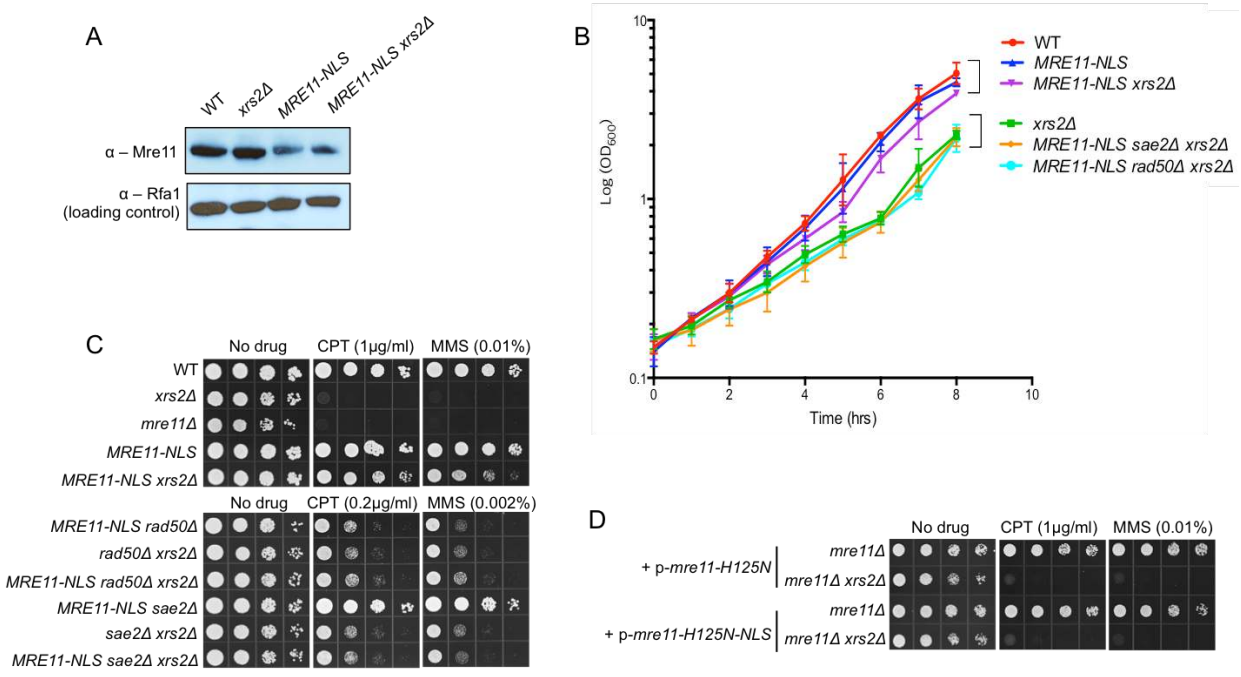

Figure 3-1. *MRE11-NLS* rescues *xrs2Δ* in growth and sensitivity to DNA damaging agents

(A) Steady-state protein levels of Mre11 and Rfa1 (loading control) of indicate strains measured by western blot analysis. (B) Growth curves representing cell concentration measured by OD600 at the indicated time points. (C) 10-fold serial dilutions of the indicated strains were spotted onto rich medium without drug or medium containing CPT or MMS at the indicated concentrations. (D) 10-fold serial dilutions of *mre11*D derivatives transformed with indicated plasmids were spotted onto selective plates containing 1 mg/mL CPT or 0.01% MMS.

Because the suppression by *MRE11-NLS* is incomplete, and the protein is expressed at lower steady-state level than Mre11, we over-expressed *MRE11-NLS* using a 2-micron plasmid construct but did not see further suppression of the DNA damage sensitivity of the *xrs2Δ* mutant (Figure 3-2A,B). Furthermore, the *MRE11-NLS* strain showed equivalent DNA damage

resistance to the *MRE11* parental strain, even at high MMS concentration, indicating that the reduced protein level is sufficient for normal activity (Figure 3-2C).

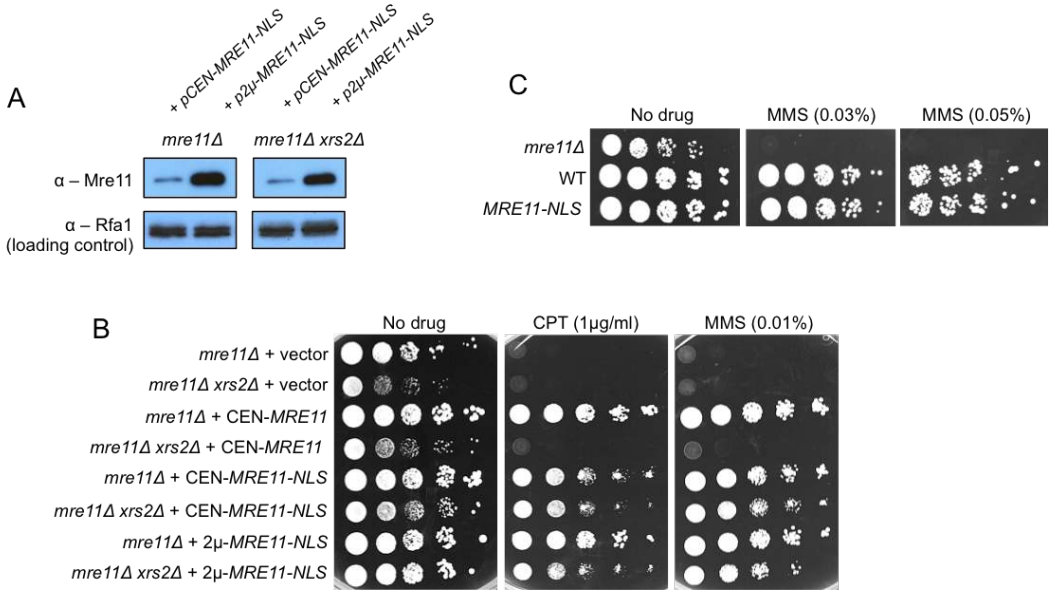

Figure 3-2. Mre11-NLS is not limiting for DNA repair

(A) Overexpression of *MRE11-NLS* using a 2-micron plasmid construct compared with expression from a single copy (*CEN*) plasmid. (B) Tenfold serial dilutions of the indicated strains harboring *CEN* or 2-micron plasmids were spotted onto selective plates containing 1μg/ml CPT or 0.01% MMS. (C) Tenfold serial dilutions of the indicated strains were spotted onto selective plates containing 0.03% or 0.05% MMS.

3.3 Xrs2 is required for Tel1 activation and NHEJ

Xrs2/Nbs1 is the only component of the complex known to directly interact with Tel1/ATM (Falck et al., 2005; Nakada et al., 2003). To test whether this physical interaction is required for Tel1 activation, phosphorylation of the downstream effector kinase, Rad53, was measured following acute zeocin treatment. The strains used contain *mec1Δ* and *sml1Δ* mutations to eliminate the main pathway for Rad53 activation (the *sml1Δ* mutation is required to suppress lethality caused by *mec1Δ*) (Gobbini et al., 2013; Zhao et al., 1998). As expected, there was no activation of Rad53 in the *mec1Δ xrs2Δ* mutant, and *MRE11-NLS* was unable to rescue this defect (Figure 3-

3A). Consistent with the lack of Tel1 activation, Tel1 was not recruited to a site-specific DSB in *xrs2Δ MRE11-NLS* cells (Figure 3-3B). We also showed that *MRE11-NLS* does not restore normal telomere length to the *xrs2Δ* mutant, in agreement with a previous study (Figure 3-3C) (Tsukamoto et al., 2005). These data indicate that Tel1 binding to the MR complex through its interaction with Xrs2 is necessary for Tel1-dependent checkpoint signaling and telomere maintenance functions.

In budding yeast, the MRX complex is essential for NHEJ (Boulton and Jackson, 1998; Moore and Haber, 1996). To determine whether Xrs2 is directly involved in facilitating NHEJ, we used a plasmid-ligation assay. A self-replicating plasmid linearized with BamHI is efficiently recircularized by NHEJ when transformed into yeast cells (Boulton and Jackson, 1998). Repair was completely eliminated in the *xrs2Δ* mutant and expression of *MRE11-NLS* did not complement this defect, indicating that Xrs2 has a direct role in promoting NHEJ (Figure 3-3D). The FHA domain of Xrs2/Nbs1 was previously shown to directly interact with Lif1/Xrcc4 *in vitro* (Chen et al., 2001; Matsuzaki et al., 2008; Palmbos et al., 2008); thus defective Lif1 binding could contribute to the *xrs2Δ* NHEJ defect. Consistent with this hypothesis, ablating Lif1 interaction by mutation of conserved residues within the Xrs2 FHA domain (*xrs2-SH* mutant) reduced NHEJ by 10-fold (Figure 3-3D). To verify these results in a chromosomal context we also determined the efficiency of repair using a substrate with an inverted duplication of I-SceI cut sites that measures imprecise NHEJ (Deng et al., 2014). Because I-SceI is continuously expressed, the NHEJ products recovered are inaccurate and mostly utilize a 2 bp microhomology within the 4-bp 3' overhangs produced by I-SceI cleavage (Deng et al., 2014). Minor classes of end joining products are also recovered that utilize microhomologies flanking the DSB. Consistent with the plasmid assay, *MRE11-NLS* was unable to suppress the *xrs2Δ* NHEJ defect and the *xrs2-SH* mutant displayed a similar defect to that seen using the plasmid assay (Figure 3-3E).

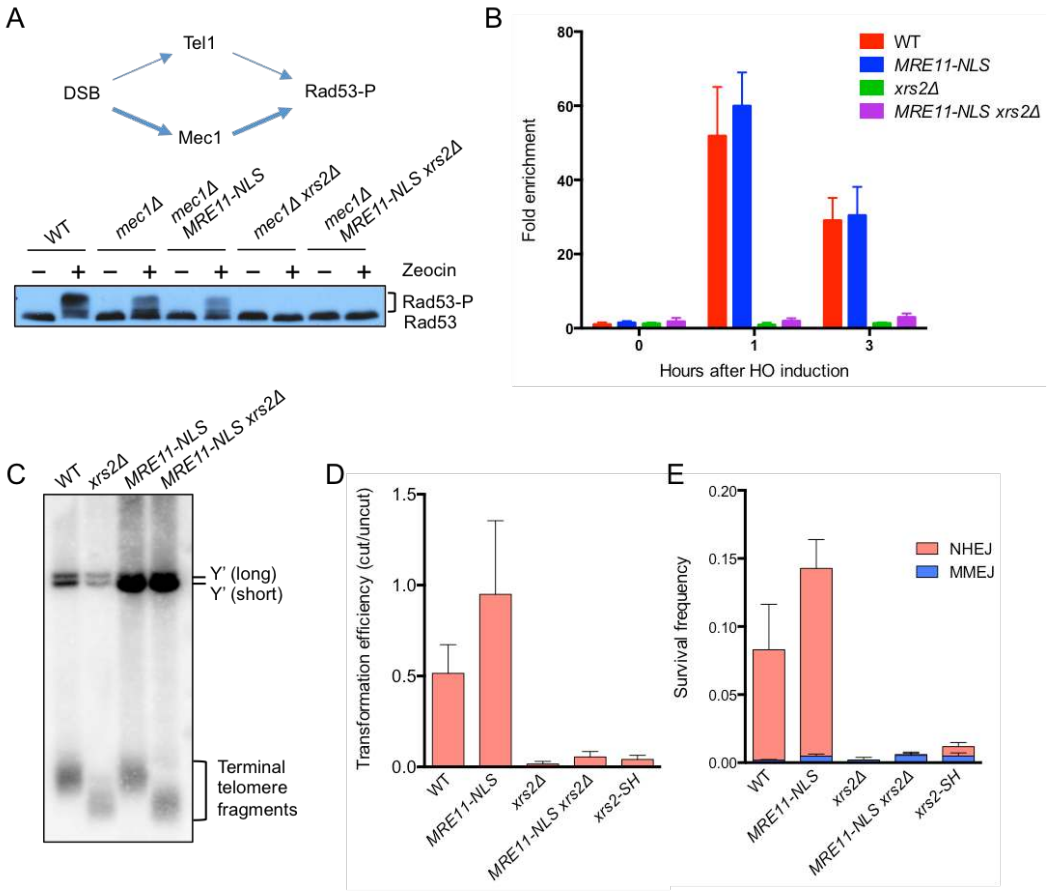

Figure 3-3. Xrs2 is required for end joining and Tel1 signaling functions of the MRX complex

(A) Model of Rad53 phosphorylation (Rad53-P) in response to DNA damage. Tel1/ATM responds to MRX/N bound DSBs, whereas Mec1/ATR is activated by RPA bound to the ssDNA formed at resected DSBs. Western blot analysis showing Rad53-P in response to zeocin treatment in the indicated strains. (B) ChIP-qPCR for HA-Tel1 0.2 kb from the DSB. The error bars indicate SD (n = 3). (C) Genomic DNA of indicated strains was digested with XhoI and separated on a 1% agarose gel. The DNA fragments were transferred to a nylon membrane and hybridized with a Y' element probe. The Y' long and Y' short refer to the two classes of subtelomeric Y' repeats. (D) Transformation efficiency of BamHI-digested linear plasmid DNA measured by the plasmid-ligation assay. The transformation efficiency was calculated as a ratio of the number of transformants with BamHI-digested pRS414 DNA to that with undigested DNA. The error bars indicate SD (n = 4). (E) Frequency of chromosomal NHEJ. The error bars indicate SD (n = 3).

Since the *xrs2Δ MRE11-NLS* strain is deficient for Tel1 signaling and NHEJ we asked whether combining these defects results in DNA damage sensitivity. The *lif1Δ tel1Δ* double mutant was more resistant to CPT and MMS than the *xrs2Δ MRE11-NLS* strain indicating that loss of NHEJ and Tel1 signaling is not responsible for the residual DNA damage sensitivity of *xrs2Δ MRE11-NLS* cells (Figure 3-4).

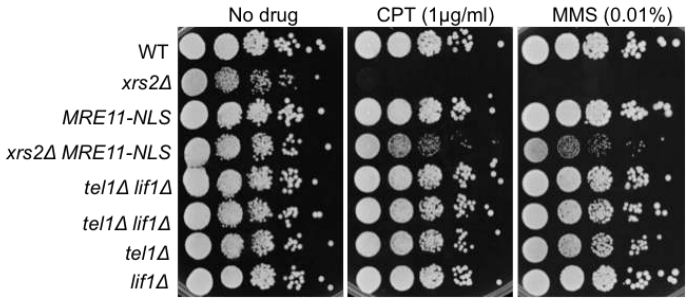

Figure 3-4. The DNA damage sensitivity of the *MRE11-NLS xrs2Δ* mutant is not due to loss of Tel1 signaling and NHEJ

Ten-fold serial dilutions of the indicated strains were spotted onto rich medium without drug, or medium containing CPT or MMS at the indicated concentrations.

3.4 Rescue of the *xrs2Δ* resection defect by *MRE11-NLS*

The MRX complex promotes HR by initiating end resection. To analyze resection activity of the MR complex in the absence of Xrs2, we monitored formation of ssDNA following DSB formation at the *MAT* locus. The strains used express *HO* from the galactose-inducible *GAL1* promoter, allowing synchronous DSB formation, and the *HML* and *HMR* loci were deleted to prevent repair by gene conversion. As resection proceeds, the StyI restriction enzyme site located 0.7 kb distal to the DSB becomes single-stranded and resistant to digestion, which results in disappearance of the 0.7 kb restriction fragment over time (Figure 3-5A). Resection was also measured by the accumulation of StyI-resistant ssDNA by real-time PCR (Zierhut and Diffley, 2008). Kinetic analysis of resection using both assays revealed that expression of *MRE11-NLS* restores resection to the wild-type level in the *xrs2Δ* mutant (Figure 3-5B,C,D). In the absence of Sae2, the suppression was completely abolished, indicating that Sae2 is still critical for resection in the absence of Xrs2 (Figure 3-5B,C,D). Because Tel1 signaling is defective in *xrs2Δ* derivatives, we tested resection in the *sae2Δ tel1Δ MRE11-NLS* strain and found it was reduced relative to *sae2Δ MRE11-NLS*, but not to the same extent as observed for *sae2Δ xrs2Δ MRE11-NLS* cells indicating a requirement for Xrs2 independent of Tel1 (Figure 3-5D).

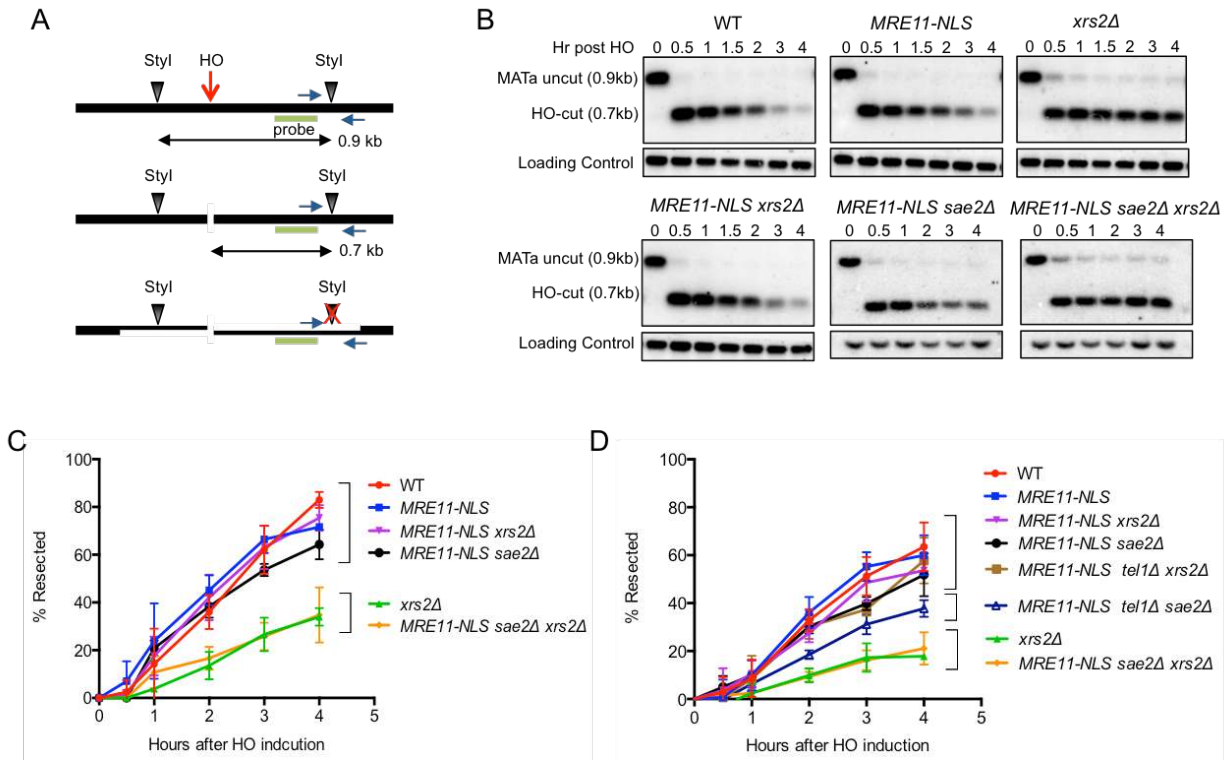

Figure 3-5. Xrs2 is dispensable for end resection of HO-induced DSBs

(A) Representation of the *MAT* locus used to measure end resection after introduction of a targeted DSB. The green bar shows the location of the probe used for hybridization and the blue arrows show primers used for real-time PCR. (B) Southern blot analysis of the genomic DNA from the indicated strains. (C) Quantification of the Southern blot data. The error bars indicate SD (n = 3). (D) qPCR analysis of end resection in the indicated strains. Error bars indicate s.d. (*n*=3).

To determine whether Mre11-NLS is recruited normally to DSBs we measured Mre11 binding to sequences 1 kb from the HO cut site by chromatin immunoprecipitation (ChIP). While the enrichment of Mre11 at the DSB was comparable in *MRE11* and *MRE11-NLS* cells, less Mre11-NLS was retained at the DSB in the *xrs2Δ* background at the 1 hr time point ($P<0.05$) (Figure 3-6A). Since Tel1 signaling is abrogated in the *xrs2Δ MRE11-NLS* mutant, and Tel1 is required for retention of Mre11 at DSBs (Gobbini et al., 2015), we considered the possibility that the Mre11 localization defect in *xrs2Δ MRE11-NLS* cells could be due to loss of Tel1 recruitment. Indeed, we found that Mre11 enrichment at the HO-induced DSB was the same in *MRE11-NLS xrs2Δ* and *MRE11-NLS* cells *tel1Δ* (Figure 3-6A). Note that resection is at almost

the wild-type level in *MRE11-NLS xrs2Δ* and *MRE11-NLS tel1Δ xrs2Δ* cells, indicating that Mre11 localization to DSBs is not limiting for resection initiation and loss of Tel1 signaling does not impair Sae2 activity (Figure 3-5D). We observed greater enrichment of Mre11-NLS in the *sae2Δ* mutant as compared with *SAE2* cells, consistent with previous studies (Clerici et al., 2006; Langerak et al., 2011; Lisby et al., 2004), and this was dependent on Xrs2 and Tel1 ($P<0.05$) (Figure 3-6A).

Previous studies implicate Sgs1-Dna2 in resection initiation when Sae2 or the Mre11 nuclease is absent (Bonetti et al., 2015; Budd and Campbell, 2009; Ferrari et al., 2015; Mimitou and Symington, 2010; Shim et al., 2010); thus, the dependence of resection on Sae2 in the *MRE11-NLS xrs2Δ* strain could be because the Sgs1-Dna2 mechanism is disabled. If this were the case, we would predict similar resection products in *exo1Δ MRE11-NLS xrs2Δ* and *exo1Δ sgs1Δ* mutants. We did not detect the characteristic end clipped products in *exo1Δ xrs2Δ MRE11-NLS* cells that are observed when Exo1 and Sgs1 are absent indicating that Sgs1-Dna2 is active, at least when Sae2 is present (Figure 3-6B). A previous study showed that Sgs1-Dna2 recruitment to DSBs is MRX dependent (Shim et al., 2010). Therefore, the decreased enrichment of Mre11 at DSBs in the *MRE11-NLS sae2Δ xrs2Δ* mutant could potentially result in reduced Sgs1-Dna2 recruitment and explain the decreased end resection relative to *MRE11-NLS sae2Δ* cells. Interestingly, we found the level of Dna2 enrichment 1 kb from the DSB was not significantly decreased in the *MRE11-NLS xrs2Δ* strain, despite the decrease in Mre11, whereas Dna2 enrichment was barely above background in *MRE11-NLS sae2Δ xrs2Δ* cells (Figure 3-6A). The decreased Dna2 binding in the *MRE11-NLS sae2Δ* mutant could be due to delayed resection initiation or Rad9 inhibition (Ferrari et al., 2015; Gobbini et al., 2015). We suggest that there are normally two modes of Sgs1-Dna2 recruitment to DSBs: via MRX interaction and by RPA interaction after MRX-Sae2 dependent cleavage creates ssDNA (Figure 3-6C) (Chen et al., 2013; Shim et al., 2010). Although Mre11 binding is reduced in *MRE11-NLS xrs2Δ* cells, resection still initiates by MR-Sae2 dependent cleavage and Dna2 is recruited to the

substrate generated. When Sae2 is absent, Mre11 accumulates at DSBs facilitating Sgs1-Dna2 recruitment and resection initiation. However, reduced Mre11 localization to DSBs and absence of clipping in the *MRE11-NLS sae2Δ xrs2Δ* strain results in diminished Sgs1-Dna2 activity.

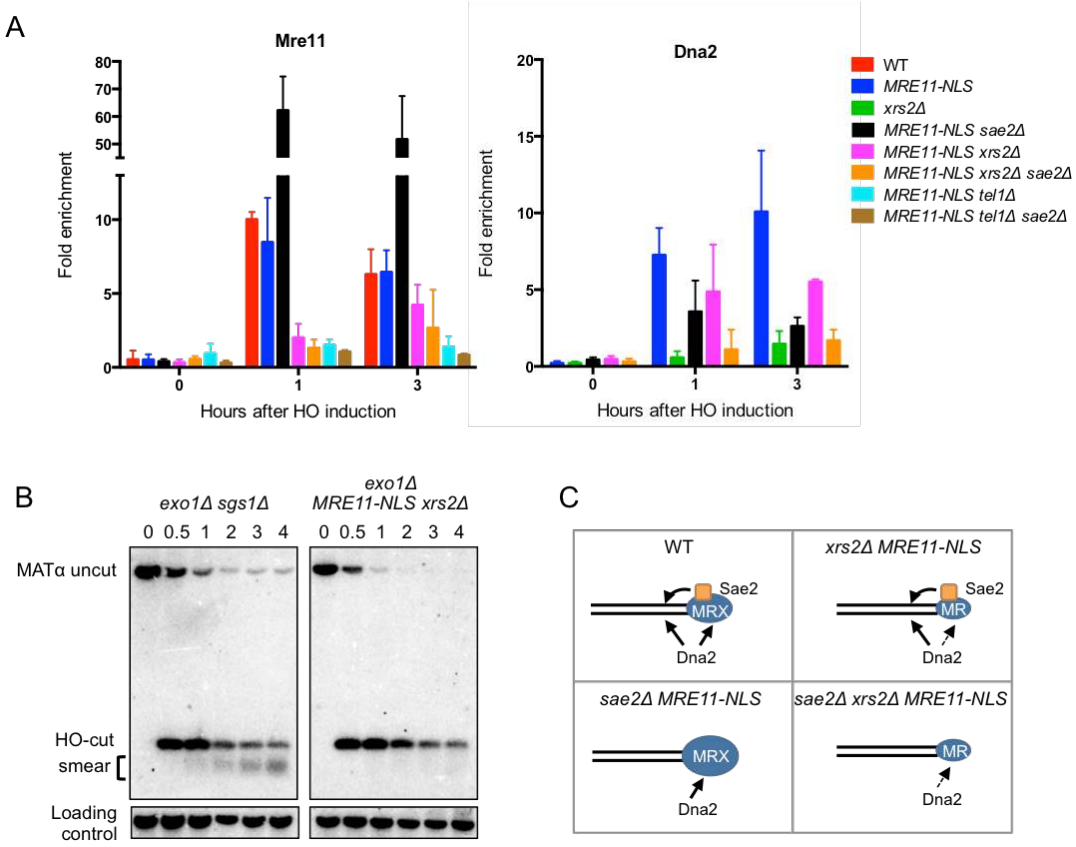

Figure 3-6. Mre11 binding at DSB ends is reduced in *xrs2Δ MRE11-NLS* cells

(A) ChIP-qPCR for Mre11 and Dna2-Myc 1 kb from the DSB. The error bars indicate SD (n = 3). **(**B) Southern blot of StyI digested DNA from *exo1Δ sgs1Δ* and *exo1Δ MRE11-NLS xrs2Δ* strains. The smear indicates MRX-Sae2 cleavage products in the absence of extensive resection. (C) Model for Sae2-dependent end resection in *xrs2Δ MRE11-NLS* cells. In WT cells, Dna2 is recruited via MRX and also by MRX-Sae2 clipping, which creates a substrate for RPA. Dna2 is recruited by MRX in *sae2Δ MRE11-NLS* cells and can bypass the need for Sae2 to initiate resection. Less Mre11 is recruited to ends in the *xrs2Δ MRE11-NLS* strain, but Sae2 clipping can still initiate resection and Dna2 loading. In the absence of Sae2 and Xrs2, MR poorly recruits Dna2 due to no clipping and reduced stabilization of Mre11 at ends.

3.5 Xrs2 is dispensable for meiosis

The Spo11 protein creates DSBs at meiotic recombination hotspots by covalent linkage to the 5' ends at break sites and is then removed by endonucleolytic cleavage releasing Spo11 attached to a short oligonucleotide (Neale et al., 2005). *mre11Δ, rad50Δ,* and *xrs2Δ* diploids fail to generate meiosis-specific DSBs and do not progress through meiosis in the W303 strain background, while *mre11-H125N* and *sae2Δ* diploids are able to form meiotic DSBs, but are unable to remove Spo11 from ends and consequently arrest during meiotic prophase with unrepaired DSBs (Mimitou and Symington, 2009). To determine the requirement for Xrs2 during meiosis, homozygous diploid strains were generated and grown under conditions to induce sporulation. Around 30% of wild-type cells sporulated and 97% of the dissected ascospores were viable; similar values were obtained for the *MRE11-NLS* homozygous diploid (Figure 3-7A). We found that expression of *MRE11-NLS* partially rescued the sporulation defect of *xrs2Δ* (7% of cells formed tetrads), and, remarkably, 70% of the spores were viable indicating formation and repair of meiosis-specific DSBs (Figure 3-7A,B). Restoration of sporulation in the *MRE11-NLS xrs2Δ* strain was dependent on *SAE2*, consistent with the Sae2 requirement to process Spo11-bound ends (Figure 3-7A,B).

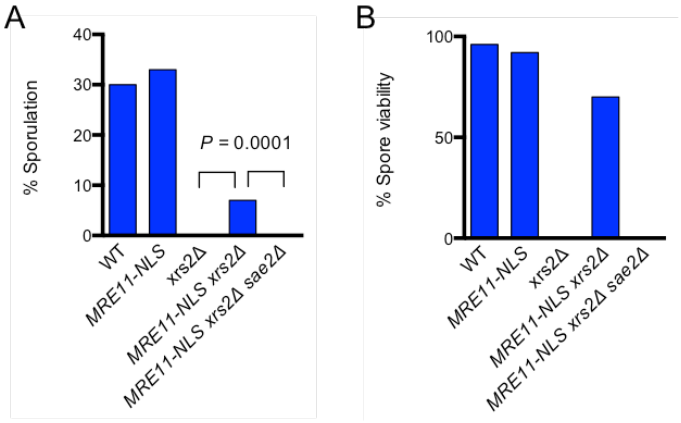

Figure 3-7. Xrs2 is not required for meiosis

(A) Sporulation percentage determined by counting cells that contain three or four visible spores out of at least 700 total cells counted. (B) Spore viability determined by dissection of asci and counting spores germinating to give visible colonies. No fewer than 50 asci were dissected for each strain.

3.6 The MR complex is competent for Sae2-dependent resection initiation *in vitro*

Previously, Mre11 within the MRX complex was found to possess a Sae2-stimulated endonuclease activity on dsDNA in the vicinity of protein-blocked DNA ends (Cannavo and Cejka, 2014). This reaction is believed to recapitulate the initial steps in DNA end resection that require the Mre11 nuclease. To determine whether Xrs2 is also required for dsDNA clipping by Mre11, we prepared recombinant MR complex and compared its activity with the MRX heterotrimer (Figure 3-8A,B). We used a DNA substrate with fully blocked DNA ends to prevent the Mre11 3'-5' exonuclease activity. We found that both MRX and MR complexes possess endonuclease activities that are strongly stimulated by Sae2 (Figure 3-8B). The MR complex appeared to be even more active than MRX (Figure 3-8C), however this may be due to different preparation procedures and specific activities of MR and MRX, respectively. The addition of recombinant Xrs2 did not have a significant inhibitory effect on the MR and Sae2-dependent cleavage of dsDNA (Figure 3-8D). Very similar results were obtained with a DNA substrate containing a single protein block, which allows both endonuclease as well as exonuclease activities of MR/MRX (Figure 3-8E,F). Therefore, Mre11 dependent cleavage in the vicinity of protein-blocked DNA *in vitro* requires Sae2, but not Xrs2, in agreement with the *in vivo* data.

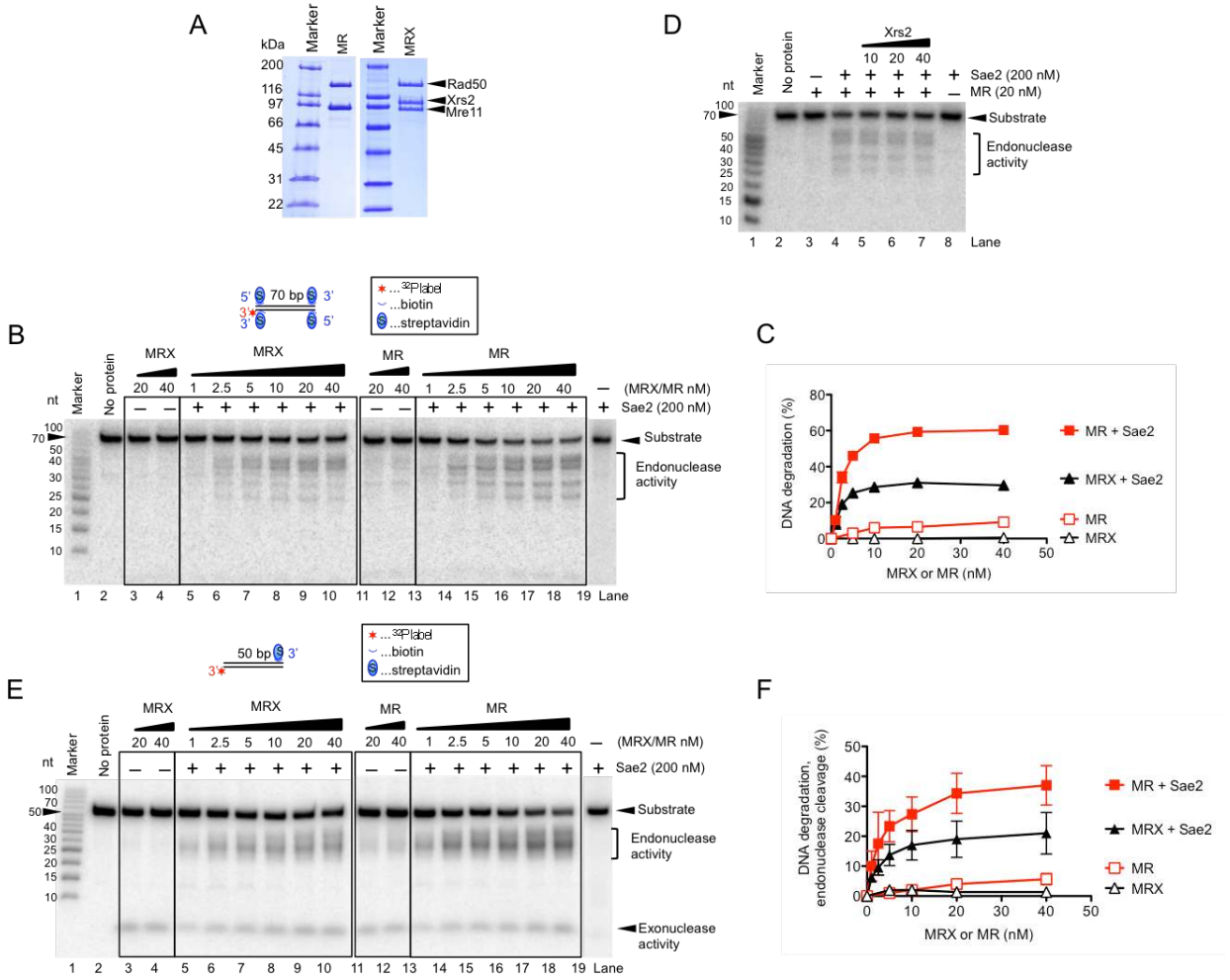

Figure 3-8. Xrs2 is not required for Sae2- and Mre11-Rad50-dependent endonuclease activity in the vicinity of protein-blocked DNA ends

(A) Recombinant Mre11-Rad50 (MR) and Mre11-Rad50-Xrs2 (MRX) used in this study. (B) Nuclease assay with Mre11-Rad50 (MR), Mre11-Rad50-Xrs2 (MRX), and Sae2, as indicated. (C) Quantitation of data from panel B. The error bars indicate SEM (n = 2). (D) The effect of various concentrations of Xrs2 (nM) on the endonuclease activity of Mre11-Rad50 in the presence of Sae2, as indicated. (E) Nuclease assay with Mre11-Rad50 (MR), Mre11-Rad50-Xrs2 (MRX) and Sae2, as indicated. (F) Quantitation of data from panel E. Error bars indicate SEM (*n* = 2).

3.7 Sae2-dependent and independent hairpin resolution

The MRX complex and Sae2 also play an important role in resolving hairpin-capped DNA ends.

Hairpin resolution in *MRE11-NLS* derivatives was measured using a genetic assay developed

by Lobachev and colleagues (Figure 3-9A) (Lobachev et al., 2002). Inverted Alu elements inserted in the *lys2* gene stimulate ectopic recombination with a truncated *lys2* gene by ~1000-fold relative to a strain with a direct repeat of Alu elements inserted at the same site in *lys2*, and this stimulation is largely dependent on the MRX complex, the Mre11 nuclease and Sae2 (Lobachev et al., 2002). The inverted repeats are thought to extrude to form a hairpin or cruciform that is cleaved by an unknown nuclease to form a hairpin-capped end, or to form a foldback structure following resection of a nearby DSB, which is then opened by MRX-Sae2 and stimulates recombination generating Lys^+ cells. Expression of *MRE11-NLS* increased the recombination rate of the *xrs2Δ* mutant by 20-fold (P = 0.01) (Figure 3-9B). Because the steady-state protein level of Mre11-NLS is reduced and could be the cause of the partial suppression, *MRE11-NLS* was overexpressed using a plasmid construct; however, this did not restore recombination to the wild-type rate (Figure 3-9C).

Interestingly, expression of *MRE11-NLS* in the *sae2Δ xrs2Δ* background enhanced the recombination rate by 10-fold (P = 0.04) compared to expression of *MRE11*. The increased rate of Lys^+ recombinants observed in the *sae2Δ* mutant was dependent on the Mre11 nuclease activity indicating that it is the Mre11 nuclease, and not Sae2, that promotes hairpin cleavage. Previous studies have demonstrated structure-selective nuclease activity for Sae2, and postulated a direct role for Sae2 in cleaving hairpin structures (Lengsfeld et al., 2007); by contrast, our data indicate that hairpin cleavage is catalyzed by Mre11 nuclease. Our data also suggest the possibility that Sae2 is required to relieve an inhibitory effect of Xrs2 on hairpin cleavage *in vivo* because the rate of Lys^+ recombinants when *MRE11-NLS* was expressed in the *mre11Δ sae2Δ* background was lower than in the *mre11Δ sae2Δ xrs2Δ* mutant (Figure 3-9D). These data show a separation of Sae2 function in regulating Mre11 nuclease activity, and are consistent with the finding that MR and MRX/N complexes cleave DNA hairpins *in vitro* independently of Sae2/CtIP (Cannavo and Cejka, 2014; Paull and Gellert, 1999; Trujillo and Sung, 2001).

Previous studies have shown redundancy between Mec1 and Tel1 for damage-induced Sae2 phosphorylation (Baroni et al., 2004). Since Tel1 signaling is abrogated in *xrs2Δ MRE11-NLS* cells, we tested whether the *tel1Δ* mutation results in decreased hairpin opening (Figure 3-9E). The *tel1Δ* mutant exhibited a small (*P*=0.0017) decrease in formation of Lys^{+} recombinants, but the frequency was 100-fold higher than the *sae2Δ* mutant indicating that Tel1-mediated phosphorylation of Sae2 is not required for hairpin opening. Similarly, the *tel1Δ* diploid exhibits close to normal sporulation and spore viability (Carballo et al., 2008), in contrast to the sporulation-defective *sae2Δ* diploid.

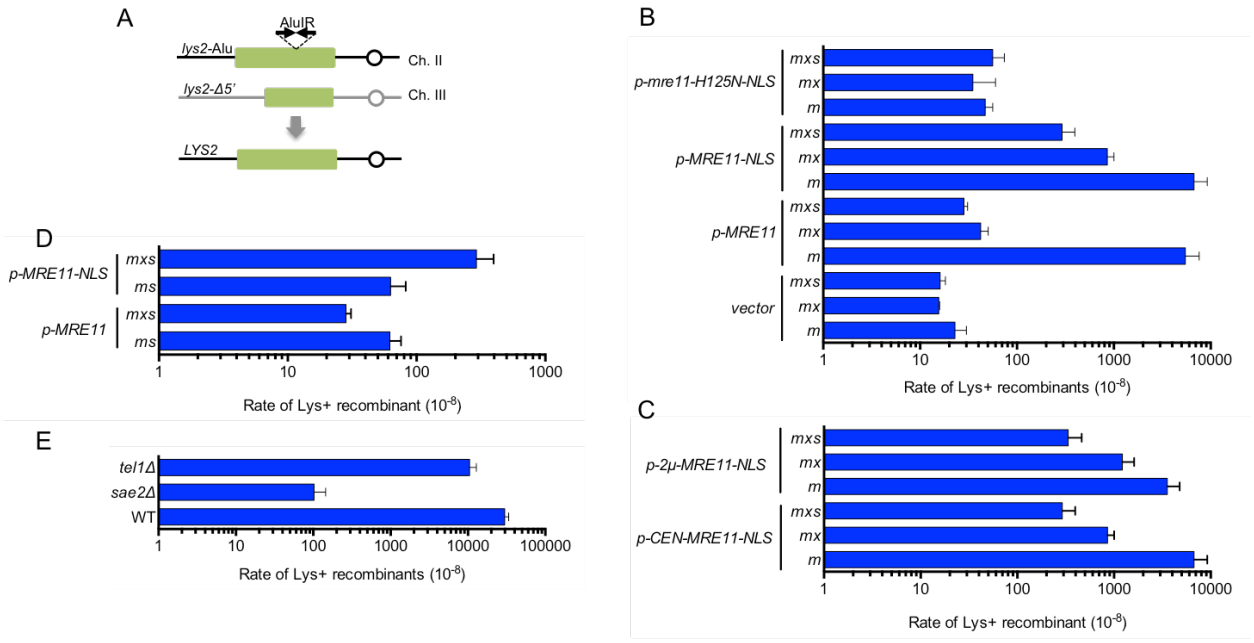

Figure 3-9. Hairpin resolution is independent of Xrs2 and partially Sae2 independent

(A) Cartoon representation of the *lys2-AluIR* ectopic recombination assay. (B) Recombination frequencies of strains with the *lys2-AluIR* and *lys2-Δ5*0 ectopic recombination reporter system. The rate of Lys+ recombinants was derived from the median recombination frequency determined from eight different isolates of each strain. The error bars indicate SD (n = 3). *mre11Δ*, *m*; *mre11Δ xrs2Δ*, *mx*; *mre11Δ xrs2Δ sae2Δ*, *mxs*. (C) IR-stimulated recombination rates for the indicated strains with *MRE11-NLS* expressed from a single copy (*CEN*) or high copy number plasmid (2-micron). The error bars indicate SD (n = 3). (D) IR-stimulated recombination rates for p*MRE11* or p*MRE11-NLS* expressed in *mre11Δ sae2Δ* and *mre11Δ sae2Δ xrs2Δ* derivatives. The error bars indicate SD (n = 3). (E) Recombination frequencies of *sae2Δ* and *tel1Δ* derivatives. The error bars indicate SD (n = 3).

3.8 Discussion

Previous studies have shown that Xrs2/Nbs1 is a flexible scaffold that binds to several DNA repair proteins, including Mre11, Tel1/ATM, Sae2/Ctp1/CtIP and Lif1 (Liang et al., 2015; Lloyd et al., 2009; Matsuzaki et al., 2008; Nakada et al., 2003; Palmbos et al., 2008; Tsukamoto et al., 2005; Williams et al., 2009). Xrs2 binding to Mre11 is required for its nuclear localization, raising the question of the contribution of Xrs2 to MR functions once the complex is in the correct cellular compartment. Here we show that localizing Mre11 to the nucleus in the absence of Xrs2 restores functions associated with MR nuclease activity including DNA end resection, hairpin resolution and meiotic recombination. However, *MRE11-NLS* is unable to rescue the end joining and Tel1 activation defects of the *xrs2Δ* mutant indicating an essential role for Xrs2 in these processes (Figure 3-10).

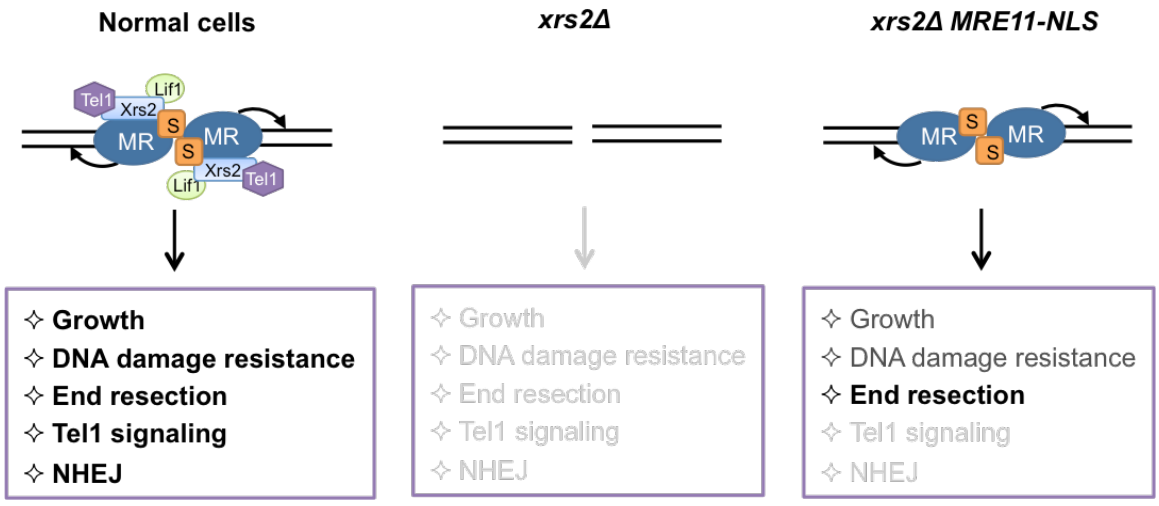

Figure 3-10. Summary of Xrs2 dependent and independent functions of the Mre11-Rad50 complex

Xrs2 is dispensable for nuclease-associated functions of the Mre11-Rad50 complex. Tel1 recruitment and NHEJ requires direct contribution of Xrs2.

Mre11 and Rad50 are conserved in all domains of life and together form an ATP-regulated nuclease involved in DNA end processing. In *Escherichia coli*, the main function of SbcCD (Rad50-Mre11) is to resolve hairpin-capped ends formed by closely spaced inverted repeats and the complex has no known function in 5'-3' end resection (Connelly and Leach, 1996; Eykelenboom et al., 2008). MRX shares the hairpin cleavage activity with SbcCD and in addition facilitates 5'-3' end resection, either directly by endonucleolytic cleavage internal to protein-blocked DNA ends or indirectly by recruitment of Exo1 and Dna2 nucleases (Cannavo and Cejka, 2014; Lobachev et al., 2002; Shim et al., 2010). Our data show that Xrs2 is not essential for hairpin resolution or end resection of HO and Spo11-induced DSBs consistent with MR comprising the core nuclease activity and the finding that Xrs2 is absent from bacteria and archaea.

DNA damage resistance and meiosis were not restored to wild type levels, and this could be due to either a direct role for Xrs2 in promoting MR activity or reduced localization of Mre11-NLS to DSBs in the absence of Xrs2. Previous studies have shown Xrs2/Nbs1 binds to DNA, and to the Mre11 latching loop, potentially stabilizing the Mre11 dimer at ends (Paull and Gellert, 1999; Schiller et al., 2012; Trujillo et al., 2003). Mre11 retention was equally reduced in the *MRE11-NLS xrs2Δ* and *MRE11-NLS tel1Δ* mutants suggesting the *xrs2Δ* defect could result from failure to recruit Tel1 (Gobbini et al., 2015). However, it is important to note that *tel1Δ* mutants are proficient for end resection, hairpin resolution and meiosis indicating that the reduction in Mre11 retention at DNA ends is of no consequence for these Mre11-dependent functions (Carballo et al., 2008; Iwasaki et al., 2016): thus, Xrs2 must contribute in some way to Mre11 activity, independent of the role of Tel1 stabilization of Mre11 at ends.

The sporulation and spore viability defects of the *xrs2Δ* diploid were partially rescued by *MRE11-NLS* indicating that Xrs2 is not essential for meiotic DSB formation and subsequent Spo11 removal. Our data contradict an earlier study in which it was shown that expression of GBD-Mre11 (nuclear localized) from a plasmid failed to suppress the meiotic defect of the *xrs2Δ*

mutant, even though it was able to partially complement MMS sensitivity (Tsukamoto et al., 2005). There are several possible explanations for this discrepancy. First, we created a chromosomal version of *MRE11-NLS* instead of expressing it from a plasmid and the plasmid might have been unstable during meiosis. Second, we used a different strain background to the one used by Tsukomoto et al (Tsukamoto et al., 2005). In *S. pombe*, the MRN complex is dispensable for meiotic DSB formation, but is required for Spo11 removal (Milman et al., 2009; Young et al., 2004). The *nbs1Δ* mutant displays a temperature-sensitive defect for Spo11 clipping and meiotic recombination indicating a separation of MR nuclease activity from Nbs1 (Milman et al., 2009). The finding that Xrs2 is not integral to MR nuclease activity explains why no separation-of-function alleles of *XRS2* have been identified in genetic screens for mutants proficient for meiotic DSB formation but deficient for Spo11 release, in contrast to *MRE11* and *RAD50* (Alani et al., 1990; McKee and Kleckner, 1997a; Nairz and Klein, 1997; Prinz et al., 1997).

Surprisingly, we found that end resection by the MR complex retains the requirement for Sae2 even though the FHA domain of Xrs2/Nbs1 was thought to recruit Sae2/Ctp1 to sites of DNA damage (Liang et al., 2015; Lloyd et al., 2009; Williams et al., 2009). A recent study found no defect in Sae2 recruitment to an HO-induced DSB in the *xrs2-SH* mutant (Iwasaki et al., 2016), and a weak interaction between purified Sae2 and Mre11 was detected by co-immunoprecipitation (Cannavo and Cejka, 2014), potentially accounting for Sae2-dependent end resection. Resection is only mildly impacted by the *sae2Δ* mutation in budding yeast, yet resection in *MRE11-NLS sae2Δ xrs2Δ* cells was reduced to the same extent as in the absence of the MRX complex, suggesting that resection initiation by Sgs1-Dna2 is compromised. Consistent with this idea, we found reduced localization of Dna2 to DSBs in *MRE11-NLS sae2Δ xrs2Δ* cells.

In contrast to MR-catalyzed end resection, which is Sae2 dependent, we found a partial restoration of hairpin opening by Mre11-NLS in the absence of Sae2 and Xrs2. Expression of

Mre11-NLS in cells lacking only Sae2 did not restore hairpin opening suggesting Sae2 is required to overcome an inhibitory role of Xrs2. *In vitro*, MR can cleave hairpin structures independently of Sae2, raising the question of why hairpin cleavage *in vivo* requires Sae2. We speculate that in normal cells, MRX and Sae2 promote cleavage of hairpin-capped ends at a distance from the end, analogous to protein-bound DSBs. Xrs2 has been shown to bind to branched-DNA structures *in vitro* and could potentially shield the ssDNA region of a DNA hairpin from MR cleavage (Trujillo et al., 2003). By this model, MR endonuclease could cleave the exposed ssDNA at the hairpin without Sae2 only when Xrs2 is absent, whereas MRX cleavage would require Sae2. As noted above, *E. coli* SbcCD cleaves hairpins *in vivo* independently of Xrs2 or Sae2-like functions and has no role in end resection. We suggest that the acquisition of end resection by the MR complex in eukaryotes coincided with evolution of Sae2, a regulatory subunit to coordinate end resection with the cell cycle (Huertas et al., 2008). How Sae2 converts the Mre11 endonuclease from being ssDNA specific to clipping the 5' terminated strand of duplex DNA is currently unknown.

Chapter 4: Xrs2 and Tel1 independently contribute to Mre11 and Rad50-mediated DNA tethering and replisome stability

The results presented in this chapter have been submitted for publication.

Julyun Oh, So Jung Lee, Rodney Rothstein and Lorraine S. Symington

(S.J.L. and R.R. constructed the strain used for the end tethering assay and contributed to data collection and analysis for Figure 4-5 and Figure 4-6.)

4.1 Introduction

Previous chapter has shown that fusing Mre11 to an NLS (Mre11-NLS) partially suppresses the slow growth and DNA damage sensitivity of Xrs2-deficient cells by restoring Mre11 nuclease and Sae2-dependent end resection (Oh et al., 2016; Tsukamoto et al., 2005); however, NHEJ and Tel1 activation are not restored, highlighting the role of Xrs2 as an Mre11 chaperone and scaffold protein, recruiting factors necessary for these functions (Oh et al., 2016). The goal of this chapter was to determine the role of Xrs2 in Tel1 activation. We found that fusing the Tel1 interaction domain from Xrs2 to Mre11-NLS (Mre11-NLS-TID) is sufficient to restore telomere elongation and Tel1 signaling to Xrs2-deficient cells. The Mre11- NLS-TID fusion proteins improve Mre11 association with DSBs and further suppress the DNA damage sensitivity of *xrs2Δ* cells. The suppression is dependent on Tel1, but partially independent of the kinase activity, suggesting a structural role of Tel1 in DNA repair. Moreover, *MRE11-NLS xrs2Δ* cells exhibit a severe DNA end tethering defect and instability of stalled replication forks, which are again rescued by enforcing Tel1 recruitment to the Mre11 complex. Together, our data suggest a model whereby Xrs2 and Tel1 independently contribute to Mre11 complex stabilization at DSBs and stalled replication forks to promote genome integrity through efficient DNA bridging.

4.2 Enforcing Tel1 recruitment to the Mre11-Rad50 complex

Our previous study showed that *MRE11-NLS xrs2Δ* cells are unable to recruit and activate Tel1 upon DSB formation, and are defective for telomere maintenance (Oh et al., 2016). In addition, Mre11 enrichment at DSBs is reduced compared to wild-type (WT) cells, similar to a *tel1Δ* mutant (Gobbini et al., 2015). Because Tel1 is required for the normal retention of Mre11 at DSBs, we asked if enforcing Tel1 recruitment in the absence of Xrs2 could restore Tel1 signaling and stabilize the MR complex at DSBs.

To address these questions, we fused the Tel1 interacting domain (TID) of Xrs2 to the C-terminus of Mre11-NLS. A previous study showed that the C-terminal 161 amino acids of Xrs2 are necessary and sufficient for Tel1 interaction (Nakada et al., 2003); however, the precise TID within the C-terminal fragment of Xrs2 is not strictly defined. In *Schizosaccharomyces pombe* and *Xenopus laevis* Nbs1, a highly conserved FXF/Y motif preceded by an acidic patch of amino acids was shown to be essential for $Tel1^{ATM}$ binding (You et al., 2005), and a recent study showed that fusing the C-terminal 60 amino acids of *S. pombe* Nbs1 to Mre11 is sufficient to restore Tel1 signaling to Nbs1-deficient cells (Limbo et al., 2018). *S. cerevisiae* Xrs2 has two such motifs, one located 100 amino acids from the C-terminus and another within the C-terminal 15 amino acids. For this reason, we constructed Mre11-NLS-TID fusion proteins with two differing lengths of the Xrs2 C-terminus: 164 amino acids, consisting of both FXF motifs, and 85 amino acids with only the most C-terminal FXF motif (Figure 4-1A). The *MRE11-NLS-X164* and *MRE11-NLS-X85* constructs were integrated at the *leu2* locus on chromosome III with the *MRE11* promoter and 3' UTR sequences in a strain with a deletion of the endogenous *MRE11* locus. Expression of the TID fusion proteins is slightly lower than Mre11, similar to Mre11-NLS (Figure 4-1B).

Because a previous study found that a short C-terminal fragment of Xrs2, including the Mre11 binding domain and Tel1 binding domain (residues 630-854), is able to rescue DNA damage sensitivity and partially restore telomere length when expressed in an *xrs2Δ* background (Tsukamoto et al., 2005), we constructed the same fragment and integrated it into the chromosome with the *XRS2* promoter and 3' UTR sequences (X224) (Figure 4-1A). Additionally, we constructed a derivative of the X224 fragment fused to a MYC epitope to compare steady state protein levels to full-length Xrs2-MYC; both proteins are expressed at similar levels (Figure 4-1C). There are two predicted NLS sequences in Xrs2, a monopartite NLS at residues 350-360 and a bipartite NLS located at the C-terminus (residues 816-849) of the protein (predicted by cNLS Mapper). The fusion proteins and the X224 fragment all contain

the predicted bipartite and lack the monopartite NLS. The observation that X224 is able to partially complement *xrs2Δ* demonstrates that the predicted bipartite NLS alone is able to facilitate nuclear localization of the MRX complex (Tsukamoto et al., 2005).

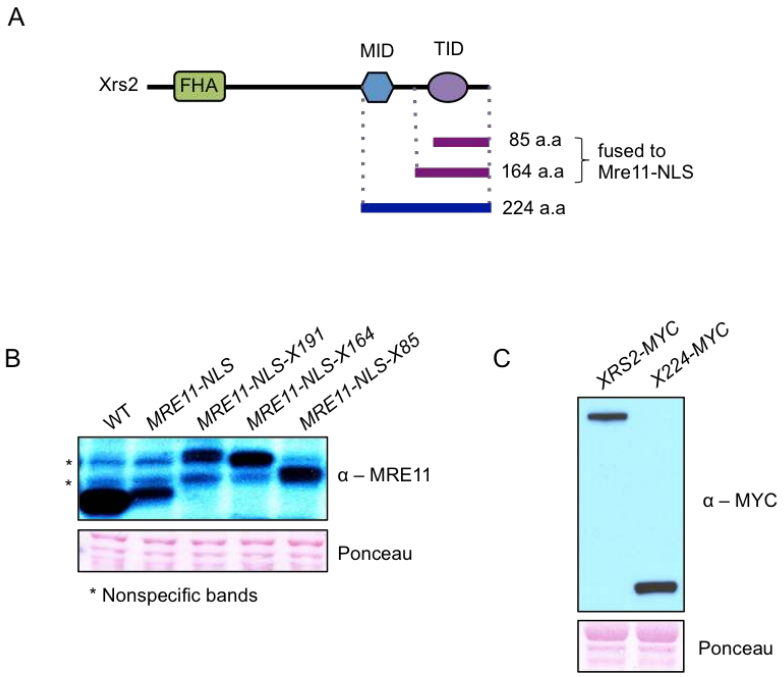

Figure 4-1. Constructs to enforce recruitment of Tel1 to Mre11 in *xrs2Δ* cells

(A) Schematic representation of Xrs2 protein binding domains and the C-terminal fragments used in this study. FHA: forkhead-associated domain; MID: Mre11 interaction domain; TID: Tel1 interaction domain. (B) Steady-state protein levels of Mre11 and fusion proteins measured by western blot analysis. (C) Steady-state protein levels of Xrs2 and X224 peptide measured by western blot analysis.

Recruitment of Tel1 to sequences adjacent to the HO endonuclease cut site at the *MAT* locus was measured by chromatin immunoprecipitation (ChIP). In these strains, the galactose-inducible *GAL1-10* promoter regulates expression of the HO endonuclease, and *HML* and *HMR* are deleted to prevent homology-dependent repair of the DSB. Tel1 binding was measured prior to and 90 min after HO induction. Expression of both of the fusion proteins in the *xrs2Δ* background restores Tel1 enrichment to the WT level, while expression of the *X224* fragment only partially suppresses the *xrs2Δ* Tel1 recruitment defect (Figure 4-2A). Consistently,

telomeres are restored to WT length in cells expressing the fusion proteins while the *X224* fragment only partially rescues the short telomere phenotype (Figure 4-2B). To examine Tel1 activity in response to DNA damage, phosphorylation of the downstream effector kinase Rad53 was measured following acute zeocin treatment. Rad53 is activated by Tel1 bound to MRX at DSBs or by Mec1-Ddc2 associated with RPA-coated ssDNA generated as a result of end resection. Because the Mec1 pathway is dominant in yeast, it was necessary to use *mec1Δ* strains to detect Rad53 activation by the Tel1 pathway (all the strains also have a *sml1Δ* mutation to suppress lethality caused by *mec1Δ* (Zhao et al., 1998)). Cells expressing the fusion proteins show reduced but visible Rad53 phosphorylation while Rad53 does not show an obvious mobility shift in cells expressing the *X224* fragment (Figure 4-2C). These data indicate that fusion of TID to Mre11-NLS is able to recruit and activate Tel1 in the absence of Xrs2, and that the *X224* fragment has reduced ability to recruit and activate Tel1 compared to the fusion proteins.

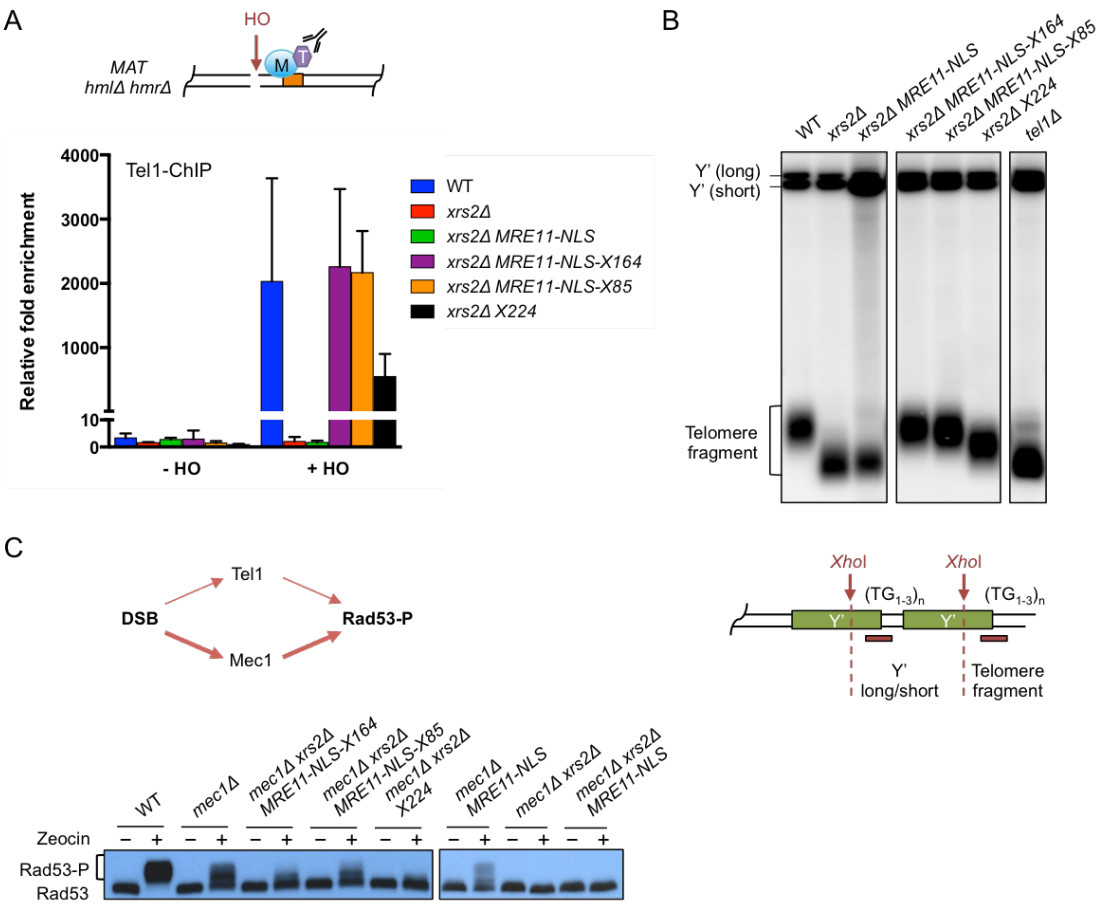

Figure 4-2. Verifying enforced recruitment and activation of Tel1 in *xrs2Δ* cells

(A) Schematic representation of the *MAT* locus used in ChIP experiments. The orange bar indicates the region amplified by qPCR. ChIP-qPCR for HA-Tel1 0.2 kb from an HO-induced DSB at the *MAT* locus in cells before (-HO) or 90 mins after HO induction (+HO). The error bars indicate SD (n = 3). (B) Southern blot of XhoI-digested genomic DNA hybridized with a Y' element probe for analysis of telomere lengths. Schematic representation of the telomeric Y' elements and TG repeats. *XhoI* digestion yield a terminal fragment of ~1.3 kb in WT strains. (C) Model of Rad53 phosphorylation (Rad53-P) in response to DNA damage. Tel1/ATM responds to MRX/N bound DSBs, whereas Mec1/ATR is activated by RPA bound to the ssDNA formed at resected DSBs. Western blot analysis showing Rad53-P in response to 1 hr of zeocin (500µg/ml) treatment.

4.3 Tel1 stabilizes Mre11 at DSB ends and enhances DNA damage resistance in the absence of Xrs2

MRE11-NLS xrs2Δ and *tel1Δ* strains show decreased retention of Mre11 at DSBs (Cassani et al., 2016; Gobbini et al., 2015; Oh et al., 2016). To address whether recruiting Tel1 to the MR

complex could restore enrichment of Mre11, we measured Mre11 binding to sequences adjacent to the HO cut site by ChIP. Consistently, expression of the fusion proteins, as well as the *X224* fragment, in the *xrs2Δ* mutant rescues the defective retention of Mre11 at DSBs (Figure 4-3A). Surprisingly, expression of all three constructs results in higher Mre11 enrichment than observed in WT cells. We speculated that the higher level of Mre11 is due to a role for Xrs2 in turnover of the complex. Since the FHA domain is missing in all three constructs, we measured Mre11 enrichment in the *xrs2-SH* mutant, which contains mutations of two conserved residues within the FHA domain. Indeed, the *xrs2-SH* mutant shows a similar increased enrichment of Mre11 to the fusion proteins and the *X224* fragment, suggesting that the FHA domain of Xrs2 plays a role in eviction of the MRX complex from DSB ends (Figure 4-3A). Deletion of *TEL1* in the *xrs2Δ X224* strain completely abolishes the restoration of Mre11 retention, indicating that Tel1 is responsible for the observed increased enrichment of Mre11 at DSBs (Figure 4-3A).

The severe genotoxin sensitivity of the *xrs2Δ* mutant is partially suppressed by *MRE11-NLS* (Oh et al., 2016; Tsukamoto et al., 2005). However, at a higher concentration of camptothecin (CPT) or methyl methanesulfonate (MMS), the *MRE11-NLS xrs2Δ* strain shows greatly reduced survival as compared to WT (Figure 4-3B,D). This is not due to the combined defects in Tel1 signaling and NHEJ since the *lif1Δ tel1Δ* double mutant is more resistant to CPT than the *MRE11-NLS xrs2Δ* strain. We hypothesized that the reduced DNA damage resistance of *MRE11-NLS xrs2Δ* cells could be due to failure to maintain Mre11 at DSBs. Indeed, the *MRE11-NLS-TID xrs2Δ* strains, which show restored Mre11 binding to DSBs, exhibit similar DNA damage resistance to WT cells. The restoration of CPT resistance is dependent on Tel1 but is partially independent of the Tel1 kinase activity, consistent with Tel1 contributing in a structural manner to stabilize Mre11 at DSBs. Since deletion of *TEL1* confers CPT sensitivity only in the absence of *XRS2*, it suggests that Tel1 can compensate for Xrs2 in promoting DNA damage resistance (Figure 4-3B).

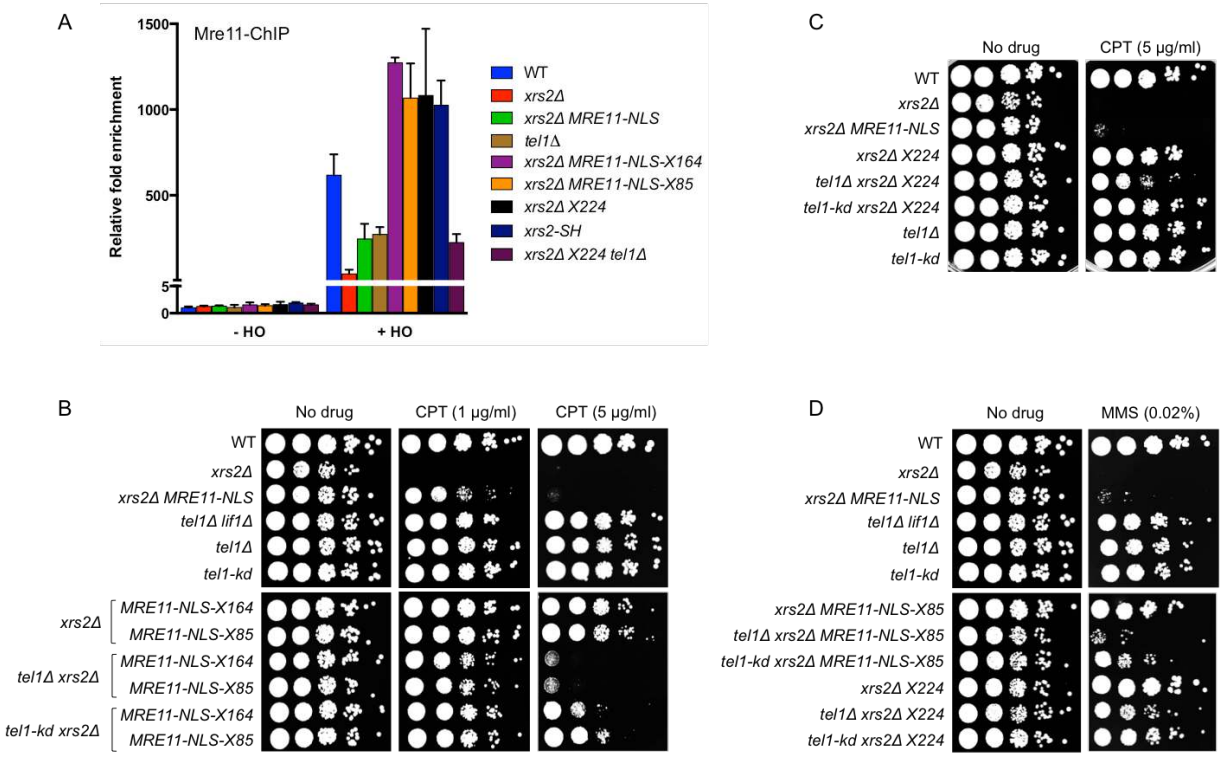

Figure 4-3. Tel1 promotes stable binding of Mre11 to DSBs and enhances DNA damage resistance

(A) ChIP-qPCR for Mre11 0.2 kb from the HO-induced DSB. The error bars indicate SD (n = 3). (B), (C) 10-fold serial dilutions of the indicated strains spotted onto rich medium with or without CPT at indicated concentrations. (D) 10-fold serial dilutions of the indicated strains spotted onto rich medium with or without MMS at indicated concentration.

The *X224* fragment also restores DNA damage resistance to the WT level; however, unlike the fusion proteins, the restoration is independent of Tel1 (Figure 4-3C). This suggests that the Mre11 binding domain present in the 224 aa Xrs2 fragment, but not in the fusion proteins, promotes DNA damage resistance in the absence of Tel1. In agreement with our previous study, normal growth and DNA damage resistance of the *xrs2Δ* strains expressing either the Mre11-TID fusions or X224 fragment is dependent on *SAE2* (Fig 4-4A,B), indicating that the MR end resection function is critical for proliferation and DNA damage resistance in Xrs2-deficient cells.

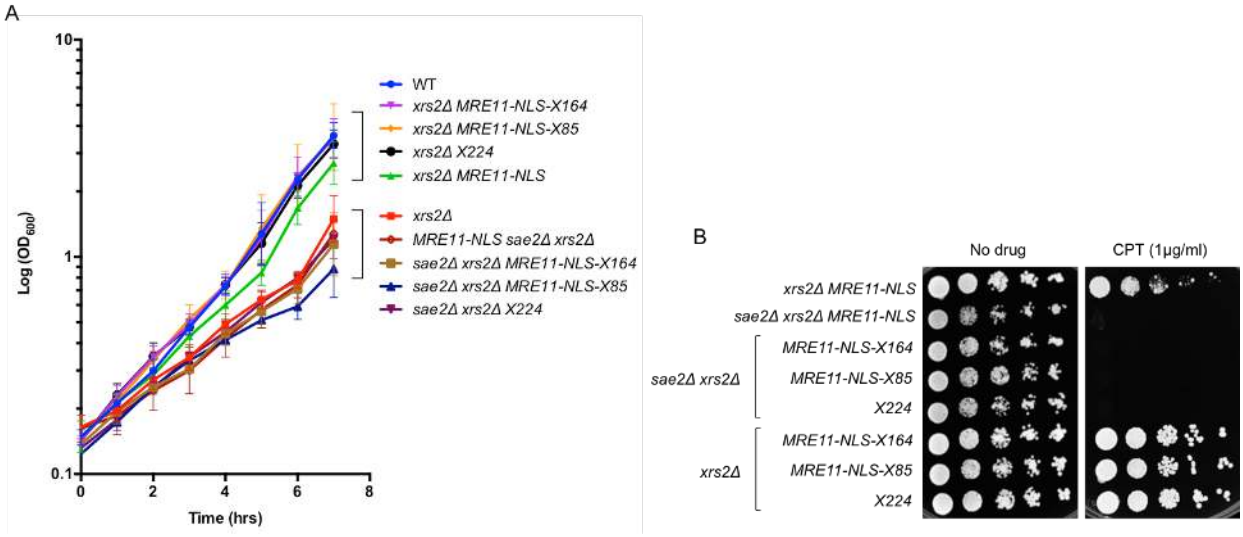

Figure 4-4. Complementation of the growth and DNA damage resistance defects of xrs2Δ by the Mre11 fusions and X224 fragment is dependent on SAE2

(A) Growth curves representing cell concentration measured by OD600 at the indicated time points. Error bars indicate SD (n=3). (B) 10-fold serial dilutions of the indicated strains spotted onto rich medium with our without CPT.

4.4 Tel1 rescues the DNA bridging defect of *MRE11-NLS xrs2Δ* cells

The finding that restoring Mre11 enrichment at DSBs enhances DNA damage resistance of the *xrs2Δ* mutant prompted us to examine the structural role of the MRX complex in bridging DSB ends and tethering sister chromatids. *In vitro*, Mre11-Rad50 is sufficient for end-bridging activity (Deshpande et al., 2014), and the role of Xrs2 in this process has not been investigated. To monitor DSB tethering, we inserted lacO and tetO arrays on opposite sides of an I-SceI cut site on chromosome V of haploid cells (Figure 4-5A). In this strain, I-SceI is expressed from a galactose-inducible promoter, LacI-YFP and TetR-RFP are constitutively expressed, and a Rad52-CFP fusion is used to monitor DSB formation. It is important to note that the DSB is effectively “irreparable”: HR cannot be employed because I-SceI is expected to cut both sister

chromatids in S/G2 phase cells, and imprecise NHEJ to mutate the I-SceI cut site is rare in yeast (Deng et al., 2014).

Four hr after I-SceI induction, the DSB can be visualized by appearance of a Rad52-CFP focus that co-localizes with YFP and/or RFP. For a tethered DSB we cannot distinguish between one and two Rad52 foci (Figure 4-5B). However, for untethered DSBs we observe some cells with two Rad52 foci, each associated with RFP or YFP, and others with a Rad52 focus associated with only one end (Figure 4-5B,C). The distance between YFP and RFP foci was measured in at least 100 cells with co-localizing Rad52 foci. Consistent with previous studies using similar assays, most WT cells exhibit co-localizing YFP and RFP foci (Figure 3B, D) (Cassani et al., 2016; Kaye et al., 2004; Lobachev et al., 2004; Seeber et al., 2016). We observed a significant increase in DSB end-to-end separation in *xrs2Δ* cells and *MRE11-NLS* is unable to rescue this defect. In agreement with previous studies, the *tel1Δ* mutant shows a slight increase in DSB end separation (Cassani et al., 2016; Lee et al., 2008), but in contrast to the Lee et al study (Lee et al., 2008), we find comparable end tethering in *tel1-kd* and WT cells (Figure 4-5E). Retention of Mre11 at DSBs is independent of Tel1 kinase activity (Gobbini et al., 2015), correlating with the end-tethering function. As expected if Mre11 retention at DSBs facilitates end tethering, the Mre11-NLS-X85 fusion protein and Xrs2 fragment are able to significantly rescue the end-tethering defect of *xrs2Δ* cells (Figure 4-5D). The recovery of end tethering in *xrs2Δ MRE11-NLS-X85* cells is Tel1 dependent, while loss of Tel1 in *xrs2Δ X224* cells reduces end tethering to the same level as observed in the *tel1Δ* mutant. These data mirror the CPT resistance of the strains and indicate separable roles of Xrs2 binding to Mre11 and Tel1-mediated stabilization of Mre11 DNA association in promoting end tethering and genotoxin resistance. The enhanced end tethering in *xrs2Δ MRE11-NLS-X85* and *xrs2Δ X224* is partially dependent on the kinase activity of Tel1 (Figure 4-5E) suggesting that Tel1 contributes in both a kinase-dependent and -independent manner in these mutant contexts.

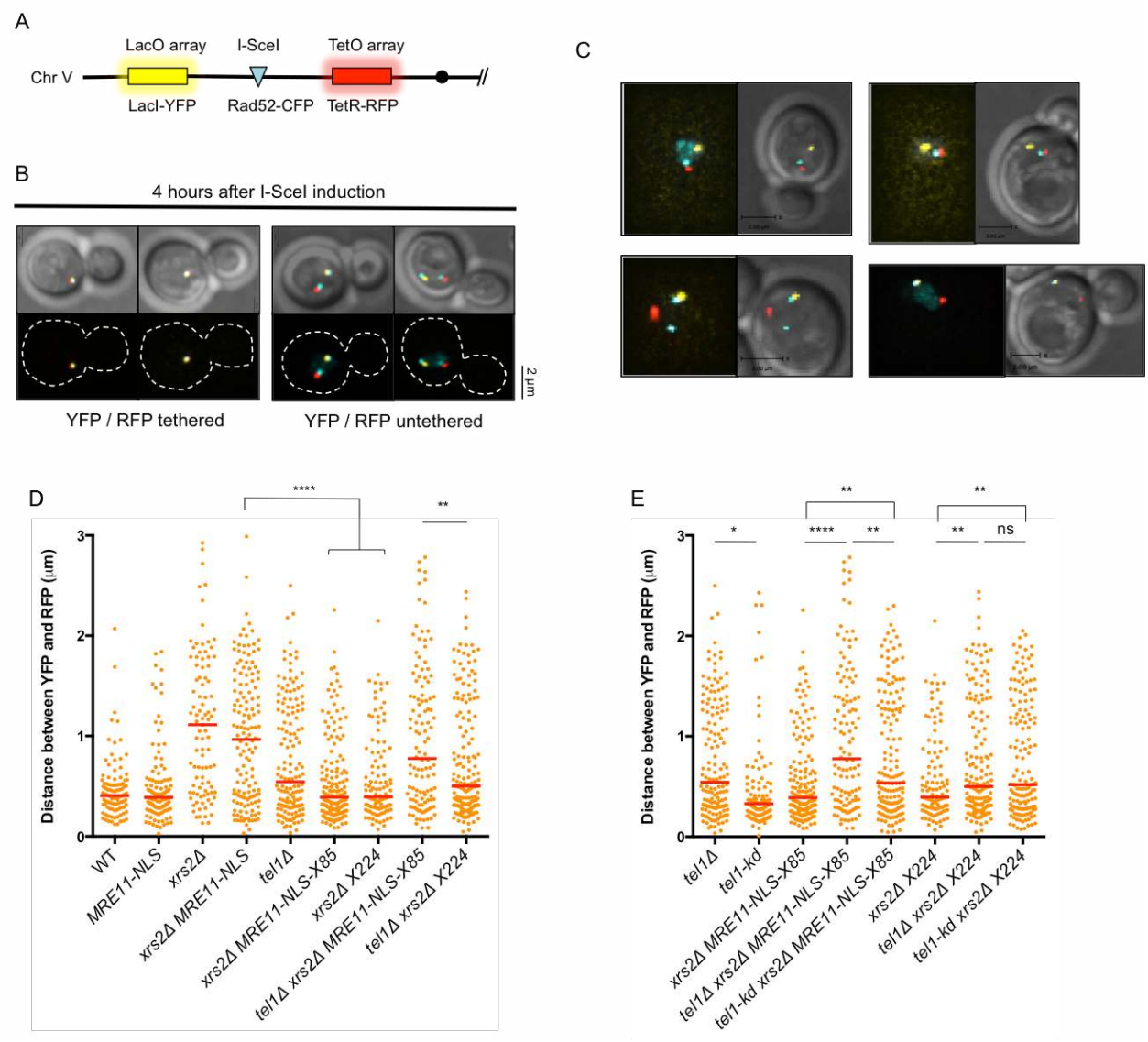

Figure 4-5. Tel1 promotes the DNA end-to-end bridging function of the Mre11-Rad50 complex

(A) Schematic representation of the DSB end-tethering assay system. (B) Examples of cells with YFP and RFP foci that are together or separated 4 hr after I-SceI induction. (C) Additional examples of cells with YFP and RFP foci that are separated 4 hr after I-SceI induction. Note that Rad52-CFP is not always visible at both ends. (D) Distribution of the distance between YFP and RFP foci. Red lines indicate median values. Cells in G2/M with Rad52 foci were scored (n ≥ 100). ** P ≤ 0.01, **** P ≤ 0.0001. (E) Distribution of the distance between YFP and RFP foci in *tel1Δ* and *tel1-kd* derivatives.). * P ≤ 0.05, ** P ≤ 0.001, **** P ≤ 0.0001, ns = not significant (P ≥ 0.05).

In late S and G2 phases, when the sister chromatid is present, the MRX complex also holds sisters together at DSBs (Seeber et al., 2016). Cells with two foci of the same fluorescence indicate sister-chromatid separation. The *xrs2Δ* and *MRE11-NLS xrs2Δ* strains show increased sister chromatid separation, which again is rescued by the fusion proteins and *X224* fragment (Figure 4-6A). These data demonstrate that Tel1 recruitment is crucial to stabilize Mre11 at DSBs to facilitate the DNA bridging function of the complex, especially when Xrs2 is not present. Cohesin, an SMC complex that normally keeps sister chromatids paired during G2 and cell division, also contributes to DSB and stalled replication fork repair, presumably by maintaining sister chromatids in a conformation that favors HR (Heidinger-Pauli et al., 2008; Kim et al., 2002; Sjogren and Nasmyth, 2001; Tittel-Elmer et al., 2012). Mre11 and Tel1 are involved in recruitment of DNA damage-induced cohesin around DSBs and stalled forks (Strom et al., 2007; Strom and Sjogren, 2007; Tittel-Elmer et al., 2012; Unal et al., 2004; Unal et al., 2007). To assess cohesion binding, enrichment of Scc1, one of the subunits of the cohesin complex, was measured at sequences 1 kb from HO induced DSB. The reduced Scc1 binding observed in *xrs2Δ* and *xrs2Δ MRE11-NLS* cells is rescued by expression of the fusion protein as well as *X224* fragment (Figure 4-6B). This observation suggests that the sister chromatid separation in *xrs2Δ* could be due to reduced cohesin recruitment resulting from low enrichment of Mre11 at DSB ends.

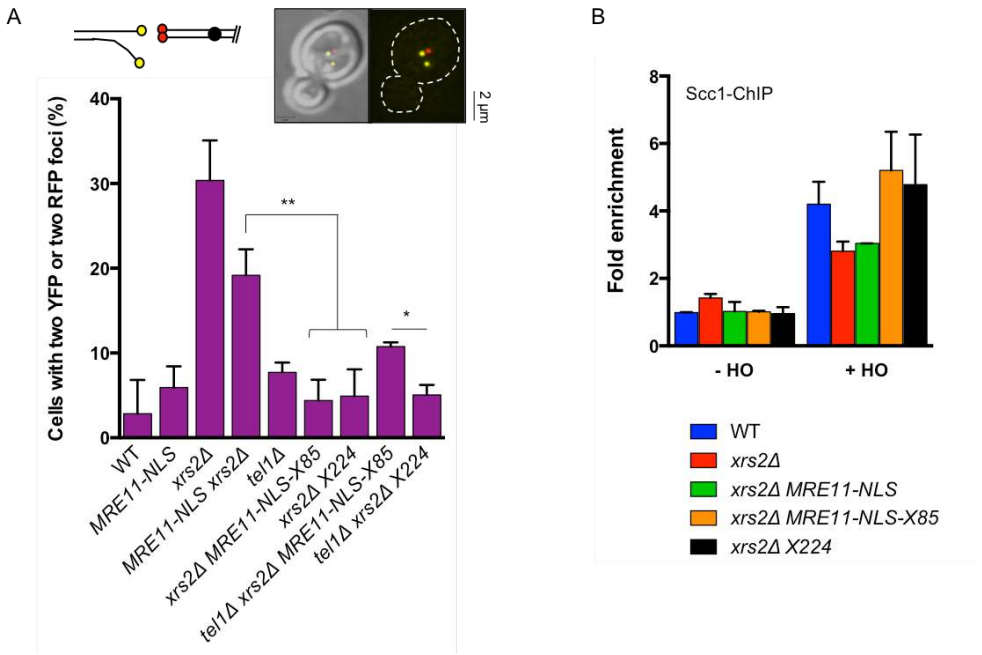

Figure 4-6. Tel1 promotes the sister-chromatid bridging function of the Mre11-Rad50 complex

(A) Cartoon of sister-chromatid separation after DSB formation and image of a cell with two YFP foci, indicating sister-chromatid separation. Graph shows the percentage of cells with either two YFP or two RFP foci. Cells in G2/M were scored (n ≥ 100). * P ≤ 0.05, ** P ≤ 0.01. (B) ChIP-qPCR for Scc1-Pk 1 kb from the HO-induced DSB. The error bars indicate SD (n=2).

4.5 End tethering by MRX is not required for DSB-induced recombination

Previous studies have suggested that the end tethering function of MRX is important for NHEJ and HR (Cassani et al., 2018; Cassani et al., 2016; Chen et al., 2001; Deshpande et al., 2014). We tested whether NHEJ is restored in *xrs2Δ* cells expressing the fusion proteins or *X224* fragment since end-to-end tethering is significantly increased in these cells. Using a plasmid-ligation assay we found that NHEJ is at the same low level in all of the *xrs2Δ* derivatives (Figure 4-7), indicating that restoration of end tethering is not sufficient for NHEJ, and interaction between the Xrs2 FHA domain and Lif1 is required for this repair mechanism (Chen et al., 2001; Matsuzaki et al., 2008; Oh et al., 2016; Palmbos et al., 2008).

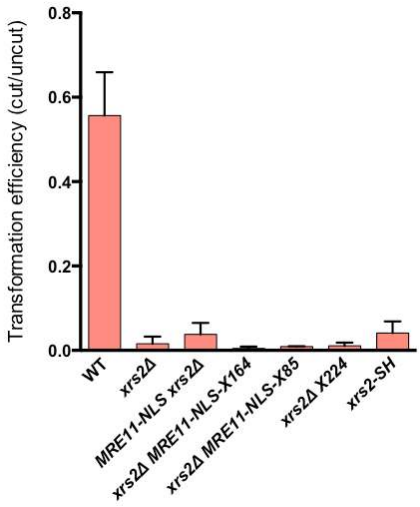

Figure 4-7. Restoration of DNA end tethering is not sufficient for NHEJ

Frequency of NHEJ measured by the ratio of transformants recovered from cut plasmid relative to uncut plasmid for the indicated strains. Error bars indicate SD (n=3).

Next, we used a direct repeat recombination reporter to determine how end tethering affects DSB-induced HR. In this system, an I-SceI induced DSB at the *ade2-I* locus is repaired using the intact *ade2-n* allele (Figure 4-8A) (Mozlin et al., 2008). In *RAD51* cells, repair occurs mainly by gene conversion (GC) maintaining the *TRP1* marker located between the repeats; whereas single strand annealing (SSA), which results in deletion of *TRP1* and one of the repeats, is *RAD51*-independent. We observe no significant change in *RAD51*-dependent GC or *RAD51*-independent SSA in *MRE11-NLS xrs2Δ* compared to WT (Figure 4-8B), indicating that end tethering is not required for homology-dependent DSB repair in this context.

Null mutation of genes encoding the MRX complex results in an increased rate of spontaneous recombination between heteroalleles in diploid cells (Ajimura et al., 1993; Ivanov et al., 1992; Malone et al., 1990). One mechanism suggested for the hyper-recombination phenotype is by channeling lesions from the sister chromatid to the homologue for repair due to disruption of sister-chromatid tethering (Hohl et al., 2015; Symington et al., 2014). We measured the rate of spontaneous recombination using diploid cells with *ade2-I* and *ade2-n* heteroalleles

(Figure 4-8C). Consistent with a previous study, the *xrs2Δ* mutant displays a 5-fold increase in the rate of Ade^{+} recombinants (Ivanov et al., 1992). Surprisingly, this phenotype is suppressed by *MRE11-NLS*, indicating that defective sister chromatid tethering is not responsible for the hyper-recombination phenotype (Figure 4-8D). However, when *SAE2* is deleted in this strain, the triple mutant again shows hyper-recombination suggesting that the hyper-rec phenotype is due to defective end resection, reducing co-conversion of the markers (Figure 4-8D).

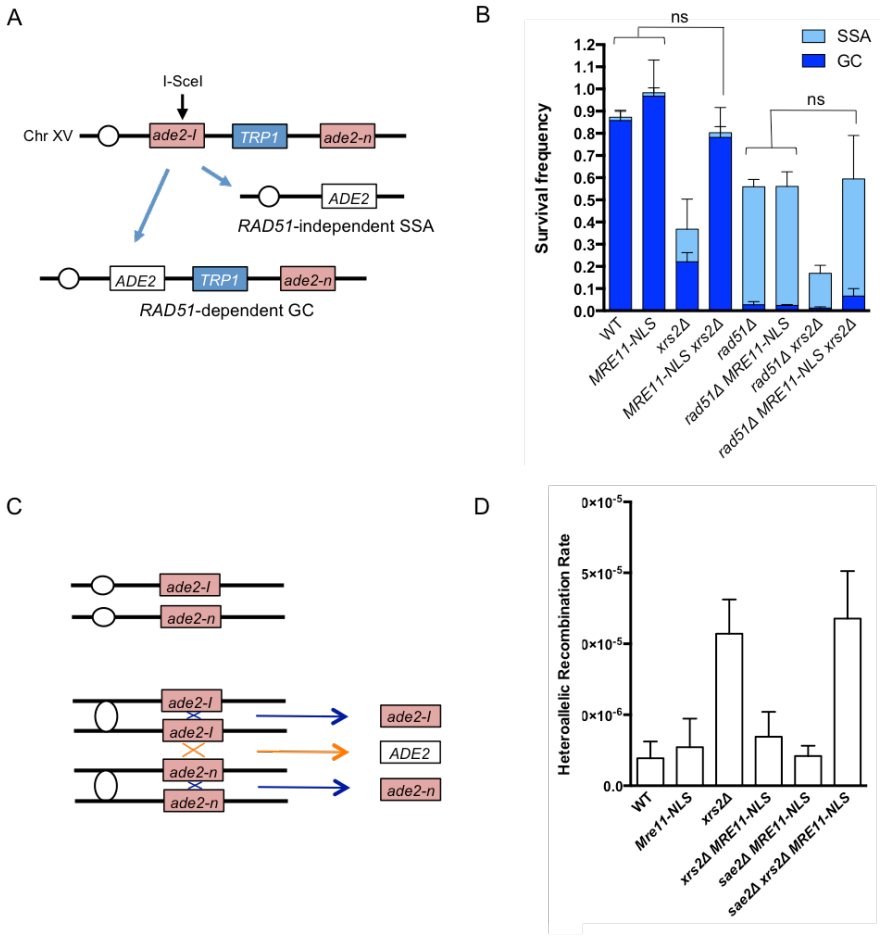

Figure 4-8. DNA end tethering is not required for HR

(A) Schematic of the *ade2* direct repeat recombination reporter. Repair of the I-SceI induced DSB occurs mostly by gene conversion with no accompanying crossover retaining *TRP1*. SSA, a *RAD51*-independent process, results in loss of one of the repeats and the intervening *TRP1* marker. (B) The frequencies of DSB-induced GC and SSA repair for the indicated strains. Error bars indicate SD (n=3). ns = not significant (P ≥ 0.05). (C) Schematic of the diploid recombination assay. In G2 phase cells, spontaneous lesions can be repaired from the sister chromatid resulting in no genetic alteration, or between non-sisters resulting in restoration of *ADE2*. (D) Rate of Ade+ recombinants in the indicated strains. Error bars indicate SD (n=3).

4.6 Suppression of chromosome rearrangements by MRX

Previous studies reported a 600-fold increase in the rate of gross chromosome rearrangements (GCRs) in the absence of MRX (Chen and Kolodner, 1999). By contrast, loss of Tel1 signaling or Mre11 nuclease activity causes no increase or modest increase in GCRs, respectively (Deng et al., 2015; Myung et al., 2001a; Smith et al., 2005). We measured the spontaneous GCR rate using an assay that detects simultaneous loss of two markers on the left arm of chromosome V (Chen and Kolodner, 1999) (Figure 4-9A). Consistent with previous studies, the *xrs2Δ* mutant shows a 664-fold increase in GCR accumulation compared to WT. *MRE11-NLS* lowers the GCR rate of *xrs2Δ* cells ~16-fold, but this rate is still ~42-fold higher than observed for WT (Figure 4-9B). However, expression of the *MRE11-NLS-X85* fusion protein or *X224* fragment in the *xrs2Δ* mutant led to a complete suppression of the hyper-GCR phenotype in a Tel1 dependent manner.

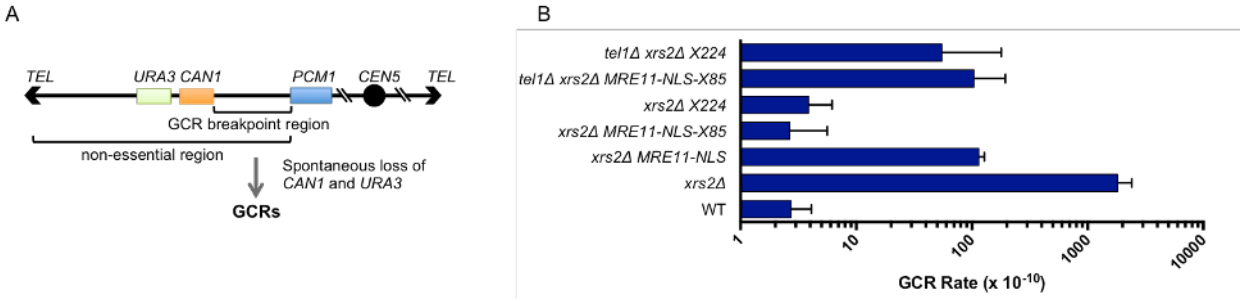

Figure 4-9. DNA end tethering is required to suppress GCRs

(A) Schematic of the GCR assay. Simultaneous loss of *URA3* and *CAN1* (selected by growth of cells on medium containing 5-FOA and canavanine) is due to loss of the terminal chromosome region followed by telomere addition, interstitial deletion, non-reciprocal translocation of hairpin-mediated inverted duplication. (B) GCR rates measured by simultaneous loss of *CAN1* and *URA3*. Error bars indicate 95% confidence interval (n ≥ 10).

4.7 Tel1 rescues the stalled replication fork instability of *MRE11-NLS xrs2Δ* cells

We noticed a significant increase in cells with spontaneous Rad52-CFP foci in *xrs2Δ* and *MRE11-NLS xrs2Δ* strains (Figure 4-10A). This observation, along with the increased rate of GCRs and sensitivity to hydroxyurea (HU) (Figure 4-10B), suggests more replication-associated DNA damage. The MRX complex is recruited to stalled replication forks and has been shown to stabilize the association of essential replisome components (Seeber et al., 2016; Tittel-Elmer et al., 2009). This function is independent of the S-phase checkpoint and the nuclease activity of Mre11, indicating a structural contribution of the complex in stabilizing stalled replication forks (Tittel-Elmer et al., 2009).

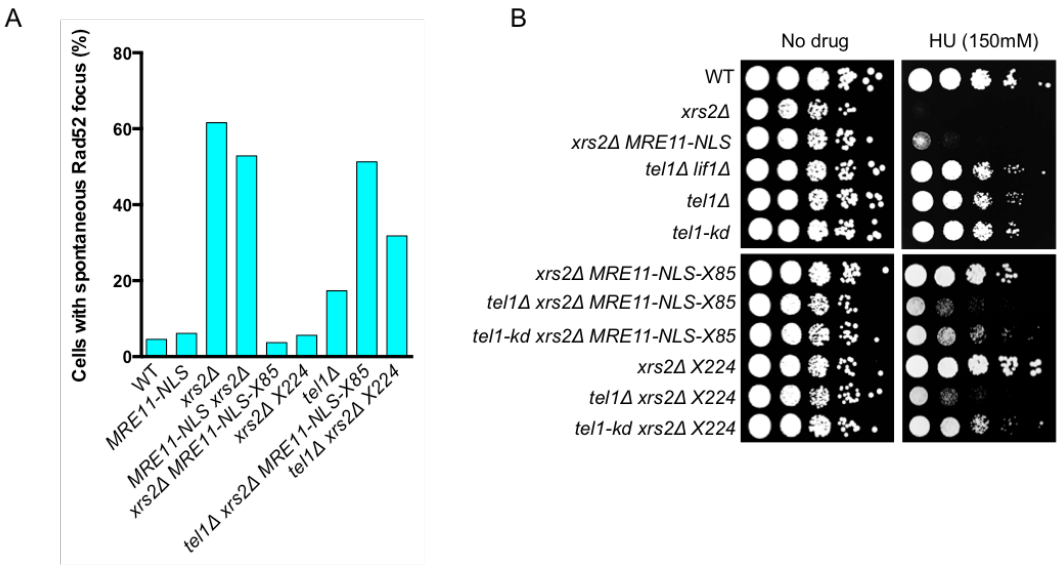

Figure 4-10. Tel1 suppresses replication-associated DNA damage in *MRE11-NLS xrs2Δ* cells

(A) Percentage of cells with a spontaneous Rad52 focus. (n ≥ 100). (B) 10-fold serial dilutions of the indicated strains spotted onto YPD medium with or without HU at indicated the concentration.

To address whether the DNA bridging function of MRX correlates with the replisome stability function, we measured the presence of Mre11 and DNA Polymerase α (Polα) near an early firing origin (*ARS607*) by ChIP after releasing G1 synchronized cells into 0.2 M HU. As

anticipated, the strains with DNA tethering defects, *xrs2Δ* and *MRE11-NLS xrs2Δ,* show loss of Mre11 and Polα enrichment compared to WT (Figure 4-11A). Consistently, expression of *MRE11-NLS-X85*, as well as the *X224* fragment, completely rescues Mre11 and Polα enrichment at stalled replication forks and HU sensitivity of *xrs2Δ* cells, as well as reducing the number of cells with spontaneous Rad52 foci (Figure 4-10A,B, 4-11A). Unlike the response to CPT and MMS, we find HU resistance of the *xrs2Δ X224* mutant requires Tel1. Therefore, we also measured Polα and Mre11 enrichment at *ARS607* in *tel1Δ* derivatives. Polα enrichment in *tel1Δ* cells is comparable to WT cells, while Mre11 enrichment is reduced, similar to that observed at DSBs. The rescue of Polα enrichment is completely Tel1-dependent in *xrs2Δ MRE11-NLS-X85* cells (Figure 4-11A), consistent with the end tethering data, suppression of spontaneous Rad52 foci, and GCRs. At the 40 min time point, Polα retention at *ARS607* in *xrs2Δ X224* cells is partially Tel1 dependent, but at 60 min, Polα enrichment is lost in the *tel1Δ* derivative, correlating with GCR results. These data suggest that Tel1 stabilization of Mre11 at stalled forks is important to prevent fork collapse and suppression of GCRs in cells lacking Xrs2.

In order to visualize replication fork progression in the presence of replicative stress, DNA combing was performed. Genomic DNA obtained from S phase cells pulse labeled with BrdU for 3 hr in the presence of 0.2M HU were stretched and newly synthesized DNA tracts were detected with anti-BrdU (Figure 4-11B). Consistent with the DNA Polα ChIP data, *xrs2Δ* and *MRE11-NLS xrs2Δ* had shorter tract lengths compared to WT, which was rescued by the *MRE11-NLS-X85* fusion protein or the *X224* fragment (Figure 4-11C). Collectively, these data show that loss of MR-mediated end tethering correlates with increased replisome fragility and elevated genomic instability.

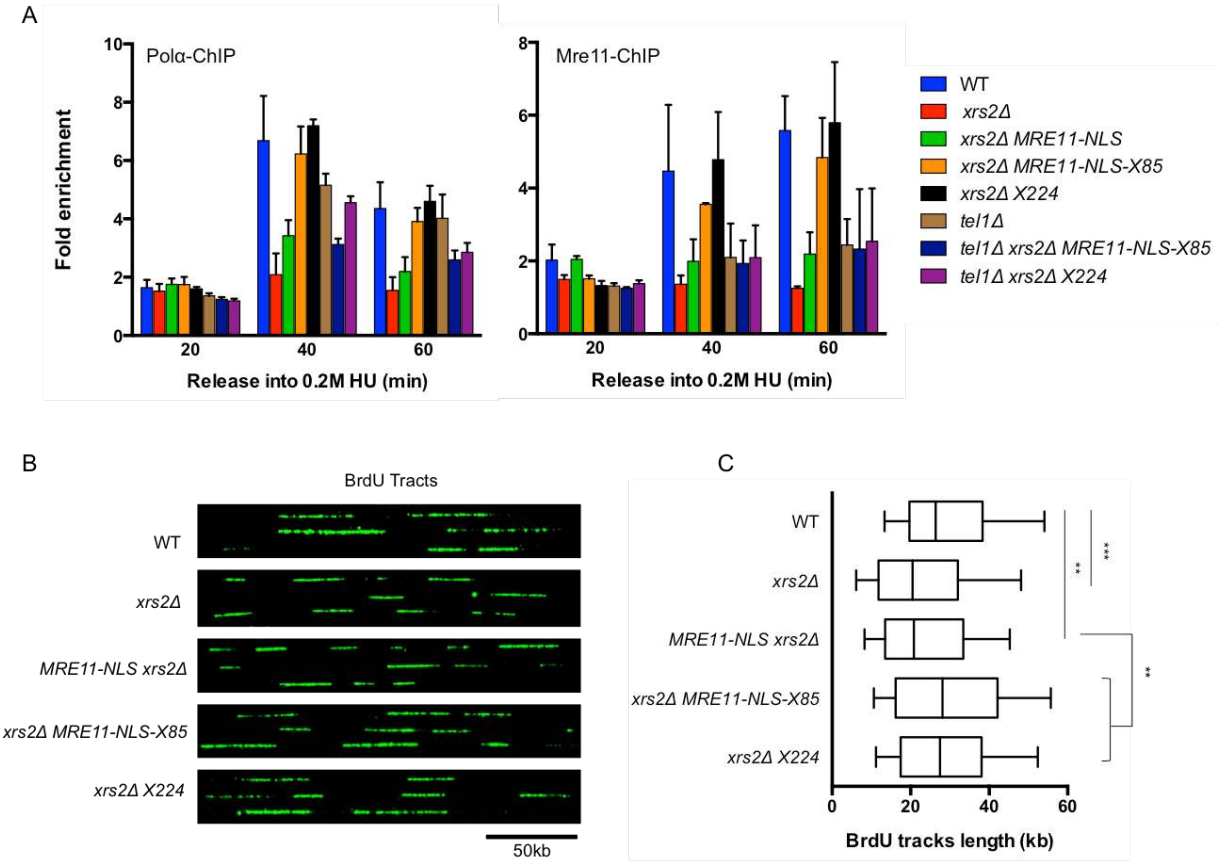

Figure 4-11. Tel1 promotes the stalled-replication fork stability in *MRE11-NLS xrs2Δ* cells

(A) ChIP-qPCR for Polα-Flag and Mre11 at early firing origin *ARS607* following release of cells from G1 arrest into medium containing 0.2M HU. The error bars indicate SD (n=3). (B) Representative DNA fibers after combing and detection of BrdU tracts in green. Genomic DNA was obtained from S phase cells labeled for 3 hr with BrdU in the presence of 0.2M HU. (C) Distribution of BrdU tract lengths in HU-treated cells. Box: 25-75-percentile range. Whiskers: 10-90-percentile range. Vertical bars indicate median values. ** P ≤ 0.01, *** P ≤ 0.001 (Mann-Whitney rank sum test).

4.8 Discussion

MRX functions in telomere maintenance and DNA damage checkpoint signaling by recruiting and activating the Tel1 kinase. Although the Tel1 binding domain within the C-terminal region of $Xrs2^{Nbs1}$ is required for Tel1 activation in vivo (Nakada et al., 2003; You et al., 2005), ATM activation can occur independently of the C-terminal ATM-interaction domain of Nbs1 (Kim et al., 2017; Lee and Paull, 2005). Moreover, ATP-induced conformational changes to the MR complex are critical for ATM activation (Al-Ahmadie et al., 2014; Deshpande et al., 2014; Morales et al., 2005). Here, we show that fusing the Tel1 interaction domain from Xrs2 to Mre11-NLS restores Tel1 activation, supporting the hypothesis that Tel1 recruitment and activation are separate functions of the MRX complex. Our studies further refine the Tel1 binding domain to the last 84 amino acids of Xrs2, encompassing an acidic patch and FXF/Y motif that were previously shown to be essential for $Tel1^{ATM}$ signaling in other systems (Falck et al., 2005; Limbo et al., 2018; You et al., 2005).

Unexpectedly, our studies identified a structural role for Tel1 in maintaining Mre11 association with DSBs that becomes physiologically relevant in the absence of Xrs2. Previous studies have shown reduced association of Mre11 with DSBs in the *tel1Δ* mutant, but not in cells lacking Tel1 kinase activity (Gobbini et al., 2016; Gobbini et al., 2015; Oh et al., 2016). The *tel1Δ* mutant shows far greater resistance to genotoxins than *mre11Δ*, indicating that reduced binding of Mre11 at damage sites does not grossly impair the DNA repair function of Mre11. Nbs1 binding to Mre11 extends the dimer interface and stabilizes the dimeric form of Mre11 (Schiller et al., 2012). We find that expression of an Xrs2-derived peptide encompassing the Mre11 and Tel1 binding domains is highly effective in suppressing CPT resistance and Mre11 retention at DSBs in *xrs2Δ* cells, suggesting that stabilization of the Mre11 dimer is a critical function of Xrs2. Supporting our findings, Kim et al (2017) found that expression of a 108 amino acid fragment of Nbs1, encompassing the Mre11 binding domain, is sufficient to restore

proliferation to Nbs1-deficient mouse cells. Our data suggest that Tel1 and Xrs2 independently contribute to Mre11 activity at DNA ends. While loss of Tel1 stabilization alone does not have a strong impact on DNA damage resistance, Tel1 can compensate for Xrs2-mediated Mre11 dimer stabilization to promote repair. The Tel1 stabilization function is critical for HU resistance and suppression of GCRs, even when the Xrs2-Mre11 interaction interface is restored, suggesting an additional function of Xrs2 during replication stress. Interestingly, the murine *Nbs1*$^{\Delta B/\Delta B}$ mutation, which deletes the N-terminal FHA and BRCT domains but retains Mre11 interactions, is synthetically lethal with ATM deficiency, suggesting that compensation between Nbs1 and ATM is conserved in mammals (Williams et al., 2002). We propose that the quantity and quality of the MRX complex compensate each other. Optimally stabilized Mre11 complex may engage in sufficient DNA tethering with minimal quantity while suboptimal complex may exhibit reduced ability to hold DNA together and thus require a higher local concentration. It remains unclear how Tel1 facilitates Mre11 retention at DSBs because no direct interaction between MR and Tel1 has been reported.

Our findings indicate that Mre11 stabilization at ends is critical for the end tethering function of MRX, and the previously reported reduction in end tethering of the *tel1Δ* mutant is a consequence of lower retention of Mre11 at DSBs. Retention of Mre11 at DSBs, end tethering and DNA damage resistance are highly correlated, raising the question of how end tethering facilitates genome integrity. Although end tethering is restored in *xrs2Δ MRE11-NLS-X85* cells, NHEJ remains defective indicating that end tethering is not sufficient for this mode of repair. Previous studies have suggested that end tethering is important for DSB-induced gene conversion and for SSA (Cassani et al., 2018; Cassani et al., 2016; Ferrari et al., 2015). However, we found both gene conversion and SSA to be restored to wild type frequencies in *xrs2Δ MRE11-NLS* cells, which are defective for end tethering. Because the assay we used measures intra-chromatid recombination or recombination between misaligned sister

chromatids, we cannot rule out the possibility that MRX bridging is important for precise sister chromatid recombination.

Our data suggest that CPT and MMS sensitivity of *xrs2Δ MRE11-NLS* cells is due to failure to maintain tethering during DNA replication. Loss of tethering results in an increase in spontaneous Rad52 foci and increased rates of GCRs, indicators of replication stress. The strains with reduced end tethering show lower Mre11 association with stalled replication forks, replisome instability and shorter DNA synthesis tracts in response to replication stress. This phenotype could be caused by loss of cohesin since a previous study showed that *rad50* mutants defective for tethering have reduced cohesin bound at stalled replication forks (Tittel-Elmer et al., 2012). Consistently, we show that cohesin enrichment mirrors Mre11 enrichment at DSB ends. The MR complex is known to associate with chromatin during S-phase and co-localizes to stressed and unstressed replication forks (Mirzoeva and Petrini, 2003; Sirbu et al., 2011; Tittel-Elmer et al., 2009). MR could use its intrinsic DNA binding activity to travel with the replisome, associate with the end produced by fork reversal or could be indirectly associated with DNA via RPA interaction (Seeber et al., 2016). Our data indicate that failure of MR to stably associate with DNA during replication stress results in fork collapse and ultimately to chromosome rearrangements (Figure 4-12).

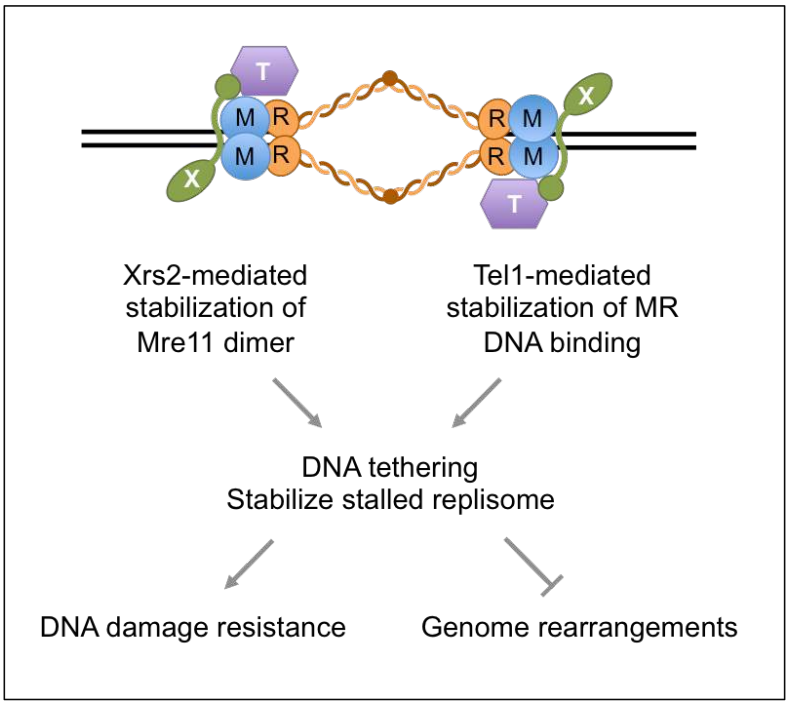

Figure 4-12. Summary of how Xrs2- and Tel1-mediated stabilization the Mre11 complex protect genome integrity

Xrs2 and Tel1 independently contribute to the DNA tethering function of the Mre11 complex, which in turn is important for stalled replication fork stability and genome integrity. In addition to responding to DSBs, the MRX complex and Tel1 actively prevent spontaneous DNA damage.

Chapter 5: Biochemical and genetic analysis of Mre11 nuclease

5.1 Introduction

This chapter compiles preliminary data collected in an attempt to decipher the functional significance of the Mre11 3'-5' dsDNA exonuclease activity in DSB repair. As mentioned in Chapter 1, Mre11 confers both exo- and endonuclease activities and coordinates with the Exo1 and Sgs1-Dna2 nucleases to create long tracts of ssDNA. The endonucleolytic cleavage by MRX-Sae2 is critical for removing hairpin-capped ends or protein blocks, such as Spo11, Ku, RPA, and nucleosomes (Lobachev et al., 2002; Reginato et al., 2017; Wang et al., 2017). However, the significance of the Mre11 exonuclease activity in DSB repair is not fully understood. Understanding the mechanistic significance of the Mre11 exonuclease activity in DSB repair is particularly challenging because the two nucleases of Mre11 work closely together and the endonuclease acts upstream of the exonuclease. A study in mammalian cells using small molecules that inhibit either the exo- or the endonuclease activities of Mre11 demonstrated that nuclease-specific inhibition confer distinct DSB repair phenotypes: inhibition of endonuclease activity channeled cells to repair by NHEJ in lieu of HR while inhibition of exonuclease activity resulted in repair defect, suggesting that both nuclease activities of Mre11 are crucial for repair and pathway choice (Shibata et al., 2014).

Structural examination of *Pyrococcus furiosus* Mre11 dimer bound to DNA suggests distinct, structure-specific, DNA alignment requirements for Mre11 dsDNA 3'-5' exonuclease and ssDNA endonuclease activities (Williams et al., 2008). Since ssDNA backbone is inherently flexible and accessible, the investigators hypothesized that ssDNA endonucleolytic cleavage should not require phosphate rotation that is required to access dsDNA backbone. Indeed, mutating a stringently conserved Histidine residue in the phosphoesterase domain that drives the phosphate rotation for the exonucleolytic activity (H52S) completely eliminated the 3'-5' exonuclease activity while the endonuclease activity was only slightly diminished (Williams et al., 2008). The equivalent mutation in *S. pombe* (H68S) showed a milder IR sensitivity than

Mre11 nuclease deficient (*mre11-nd)* mutants, suggesting that the exonuclease activity of Mre11 is less crucial for DSB repair than the endonuclease activity is. However, the extent of each nuclease activity of *mre11-H68S* was not analyzed in this study (Williams et al., 2008). The corresponding mutation was also made in *S. cerevisiae* Mre11 (H59S) and showed proficient endonuclease activity and reduced, but not abolished, 3'-5' exonuclease activity (Garcia et al., 2011). In another study, the equivalent Histidine (H63) residue in human MRE11 was mutated to Serine or Asparagine. Biochemical assays revealed that H63S has essentially a WT level of exonuclease activity while H63N showed much reduced activity (Chanut et al., 2016).

Here, we carried out biochemical and genetic analyses of ScMre11 His59 mutants, mre11-H59S and mre11-H59N*,* in an attempt to decipher the functional relevance of the Mre11 3'-5' dsDNA exonuclease in DSB repair. Our preliminary data shows that the separation of nuclease activities is not as distinct as anticipated, and, thus, suggests the future use of these mutants and interpretation of experiments to be done with care.

5.2 Biochemical analysis of ScMre11 H59 mutants

As mentioned, one of the stringently conserved Histidine residues in the phosphoesterase nuclease motif II has been targeted in different organisms to generate exonuclease-deficient and endonuclease-proficient Mre11. Table 5-1 summarizes the mutant alleles made from different organisms and their respective nuclease activities.

Table 5-1. *MRE11* mutant alleles targeting the conserved Histidine residue in nuclease motif II

		Exonuclease activity	Endonuclease activity
WT		+++	+++
Pf Mre11-H52S	Williams, R., *et al., Cell* (2008)	-	++
Sp Mre11-H68S	Williams, R., *et al., Cell* (2008)	NA	NA
Sc Mre11-H59S	Garcia, V., *et al., Nature* (2011)	+	++
Hs Mre11-H63S	Chanut, P., *et al., Nature Comm.* (2016)	+++	NA
Hs Mre11-H63N	Chanut, P., *et al., Nature Comm.* (2016)	+	NA

NA: experiment not done

The corresponding Histidine in *S. cerevisiae* Mre11 was mutated to Serine (H59S) or Asparagine (H59N) on a plasmid expressing a GST-Mre11 fusion protein via site-directed mutagenesis. The two Mre11 mutants, along with WT and one of the complete-nuclease-dead versions of Mre11 (H125N) were overexpressed using the galactose-inducible *GAL1* promoter in yeast and were purified from crude cell extracts by affinity chromatography using a glutathione Sepharose matrix. The purification was confirmed by western blot with an anti-Mre11 antibody (Figure5-1).

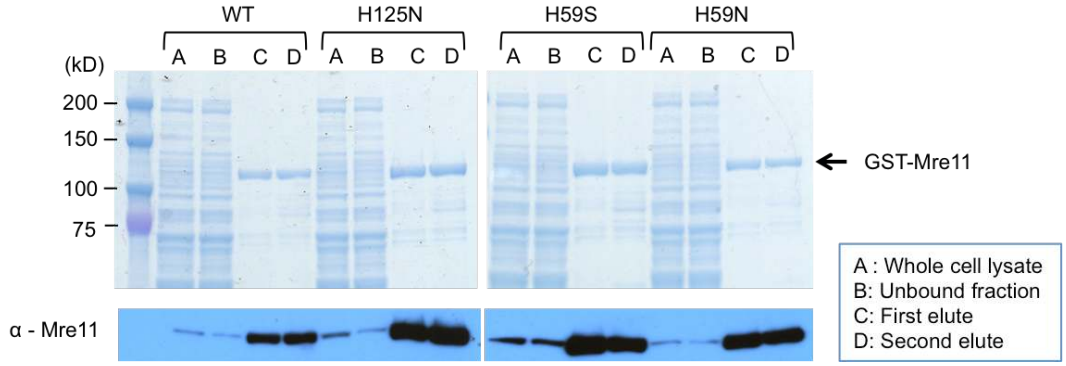

Figure 5-1. Purification of GST-Mre11 variants

Polyacrylamide gel electrophoresis showing representative purifications. Gel was stained with Coomassie brilliant blue. Western blot with anti-Mre11 antibodies was done for verification. kD = kilo Daltons

The endonuclease activity was measured by incubating the purified proteins with ΦX174 single-stranded circular DNA (Figure 5-2A). As expected, WT Mre11 proficiently cleaves ΦX174 within 30 minutes while Mre11^{H125N} shows no activity. To our surprise, Mre11^{H59S} also shows a very weak endonuclease activity, unlike reported in a previous study (Garcia et al., 2011). Mre11^{H59N} showed WT level of endonuclease activity. To examine the exonuclease activity, 55 bp duplex DNA radioactively labeled at one 5' end was incubated with recombinant Mre11 proteins. After 30 minutes, the reaction products were separated through a denaturing polyacrylamide gel (Figure 5-2B). As expected, Mre11^{H125N} shows no degradation and Mre11^{H59S} shows reduced exonuclease activity compared to WT. Mre11^{H59N}, however, appears to have no defect in exonuclease activity.

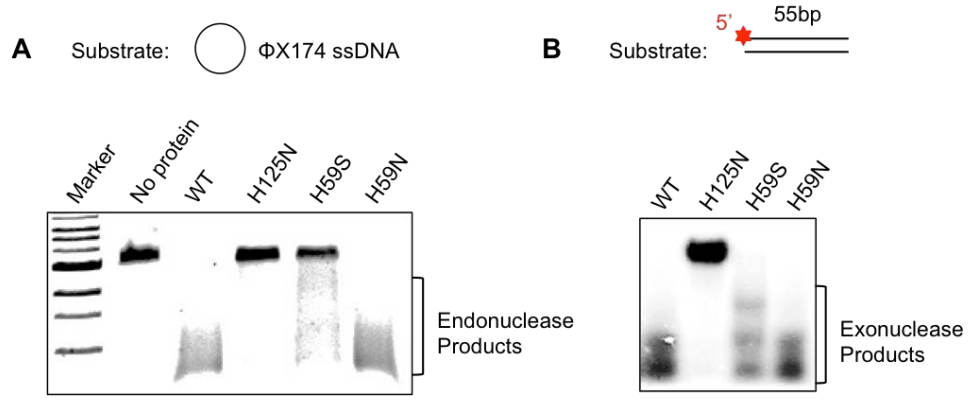

Figure 5-2. Nuclease analysis of purified Mre11

(A) Endonuclease assay performed with ΦX174 circular ssDNA (0.05 pmoles) for 30 minutes. Degraded ΦX174 are shown as smears on electrophoresis gel. (B) Exonuclease assay performed with 5'-labelled dsDNA substrate (2.5 pmoles) for 30 minutes. The products are separated on 12% Urea/Polyacrylamide gel.

Our biochemical analysis with purified Mre11 mutants shows that, *in vitro*, Mre11^{H59S} exhibits significantly reduced exo- and endonuclease activities while Mre11^{H59N} shows WT level of both nuclease activities. Thus, the separation of Mre11 nuclease activities in both mutant alleles was not as prominent as shown in previous studies.

5.3 Genetic analysis of ScMre11-H59S

In vivo, *mre11-H59S* appears to be proficient for endonuclease activity as Spo11-oligonucleotide complex are readily detected during meiosis at a comparable level to WT cells (Garcia et al., 2011). The oligonucleotides attached to Spo11 are longer in *mre11-H59S* cells, which was interpreted as a defect in the exonuclease activity (Garcia et al., 2011). However, if the Mre11^{H59S} mutant has compromised endonuclease then it is possible that the longer Spo11-oligos are a consequence of fewer endonucleolytic incisions of the 5' strands.

In order to examine the role of Mre11 exonuclease activity in mitotic DSB repair *in vivo*, various genetic analyses were performed with the *mre11-H59S* strain. The equivalent mutation in *S. pombe* (*mre11-H68S*) shows a milder IR sensitivity than *mre11-nd* mutants (Williams et al., 2008). Consistently, we also found that *mre11-H59S* is slightly sensitive to CPT but is more resistant than *mre11-H125N* (Figure 5-3A), suggesting that restoring Mre11 endonuclease activity slightly improves DDR. Based on the resection model, the endonuclease cleavage generates an entry site for extensive resection factors Exo1 and Dna2-Sgs1 to access the DNA. In the absence of the Mre11 exonuclease activity, the unprocessed short dsDNA remaining at break ends may possibly hinder Exo1 and Dna2-Sgs1 pathways. To understand the interplay between the Mre11 nuclease activities and the extensive resection pathways, *mre11-H59S* and *mre11-H125N* were combined with *exo1Δ* or *sgs1Δ*. *mre11-H125N exo1Δ* cells survive better than *mre11-H125N sgs1Δ* cells on CPT because Sgs1-Dna2 pathway can bypass the MRX-Sae2 nuclease initiation while Exo1 cannot unless Ku is eliminated (Balestrini et al., 2013; Foster et al., 2011; Mimitou and Symington, 2010; Shim et al., 2010). While *mre11-H59S exo1Δ* cells show equivalent sensitivity to CPT to *mre11-H125N exo1Δ*, *mre11-H59S sgs1Δ* cells are more resistant than *mre11-H125N sgs1Δ* cells (Figure 5-3A). This observation suggests that the MRX-Sae2 incision does not help the Sgs1-Dna2 pathway while it supports the Exo1 pathway. In *mre11-H125N*, deletion of *YKU70* promotes Exo1 activity, but not Sgs1-Dna2 activity,

presumably by revealing the DSB ends for Exo1 access (Mimitou and Symington, 2010). Interestingly, *yku70Δ* does not further alleviate the CPT sensitivity in both *mre11-H59S exo1Δ* and *mre11-H59S sgs1Δ* (Figure 5-3B). In fact, *yku70Δ sgs1Δ mre11-H125N*, *sgs1Δ mre11-H59S*, and *yku70Δ sgs1Δ mre11-H59S* all showed similar survival, suggesting that Exo1 activity is comparable whether it starts from Yku70-removed clean DSB ends or MRX-Sae2 generated nicks. Moreover, our data suggest that the inability to degrade the short dsDNA tract back towards the DSB ends does not significantly hinder the extensive resection pathway.

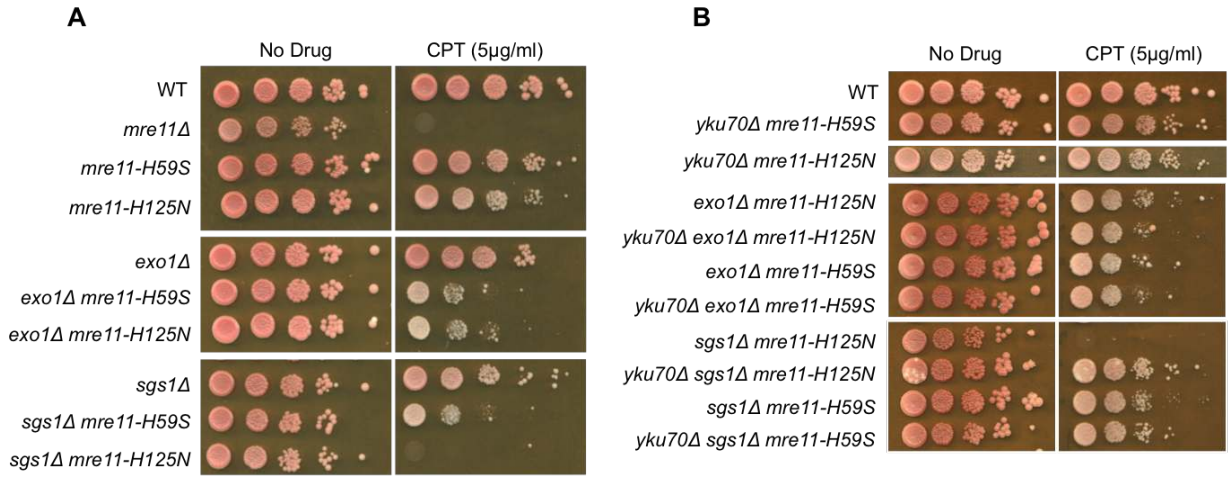

Figure 5-3. Interplay between Exo1, Sgs1-Dna2, and Mre11 nuclease activities

(A, B) Ten-fold serial dilutions of the indicative strains spotted onto rich medium without drug or medium containing 5μg/mL CPT.

Loss of Sae2 or the nuclease activity of Mre11 in the *exo1Δ sgs1Δ* background is lethal (Mimitou and Symington, 2008). We tested the viability of *exo1Δ sgs1Δ mre11-H59S* cells by dissecting spores from an *EXO1/exo1, SGS1/sgs1, mre11-H59S/MRE11* heterozygous diploid. Some triple mutants were able to grow, although they exhibited a severe growth defect (Figure 5-4A,B). The observation that some *exo1Δ sgs1Δ mre11-H59S* spores survive, while none of *exo1Δ sgs1Δ mre11-H125N* spores survive, highlights the importance of the Mre11

endonuclease activity in cell proliferation. Unfortunately, the growth defect of the *exo1Δ sgs1Δ mre11-H59S* strain hindered further genetic analysis.

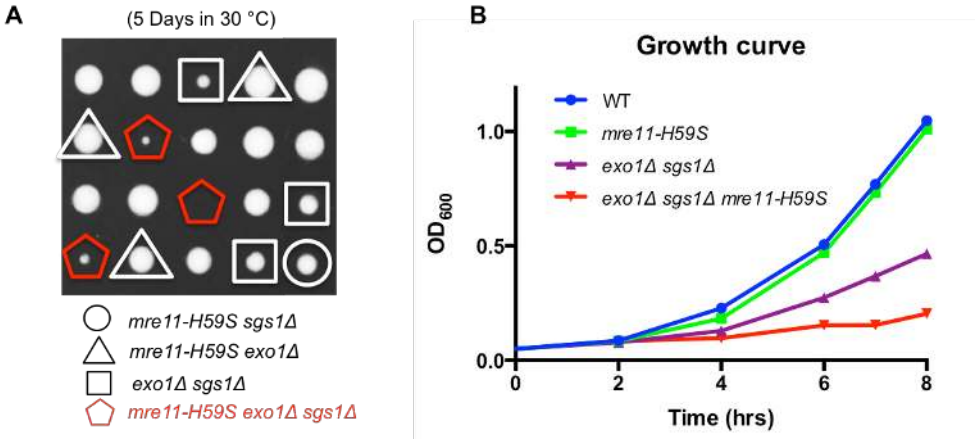

Figure 5-4. Some *exo1Δ sgs1Δ mre11-H59S* survive

(A) Spores derived from a diploid heterozygous for *EXO1, SGS1,* and *mre11-H59S.* (B) Growth curve representing cell concentration measured by OD_{600} at the indicated timepoints.

In the absence of the Mre11 nuclease activity, the MRX complex persists at DSB ends. In order to address whether Mre11 exonuclease activity is needed to remove the complex from DSB ends, enrichment of Mre11 at sequences 0.2kb away from an HO-induced DSB was measured by ChIP. As previously shown, *sae2Δ* and *mre11-H125N* cells show hyper-enrichment of Mre11 compared to WT cells (Clerici et al., 2006; Langerak et al., 2011). Similarly, $Mre11^{H59S}$ enrichment at DSB ends is significantly higher than Mre11 (P= 0.049 and P=0.016 at t1 and t3, respectively). The level was slightly lower than $Mre11^{H125N}$, but the difference is statistically not significant (Figure 5-5A), suggesting that the Mre11 exonuclease is required for proper turnover of the complex at DSB ends.

Initiation of resection prevents repair by NHEJ (Deng et al., 2014). To determine whether the exonuclease activity of Mre11 contributes to repair pathway choice, we measured imprecise NHEJ at an inverted duplication of I-SceI cut sites within the ade2 locus on chromosome XV

(Deng et al., 2014). Consistent with the MRX-Sae2 dependent endonucleolytic cleavage antagonizing the NHEJ pathway, *sae2Δ* and *mre11-H125N* both show a 5-fold and 3-fold increase in survival frequency, respectively. *mre11-H59S* conferred the same NHEJ efficiency as *mre11-H125N*, suggesting that the endonuclease cleavage is not sufficient to prevent end joining and that the exonuclease activity may be important to remove Ku from DSB ends. Combining *exo1Δ* or *sgs1Δ* with *mre11-H59S* further increased NHEJ, demonstrating that the combined activities of different nucleases antagonize the NHEJ pathway (Figure 5-5B).

The endonuclease activity of the Mre11 complex is also required to resolve hairpin-capped DNA ends. We used the genetic assay that measures ectopic recombination rate at locus inserted with inverted Alu elements to assess hairpin resolution ability (Lobachev et al., 2002). As previously shown, *mre11Δ* and *mre11-H125N* show more than 100-fold decrease in the rate of Lys^+ recombinants. The Lys+ recombination rate of the *mre11-H59S* mutant is intermediate between WT and *mre11-H125N* (Figure 5-5C). This may reflect the reduced endonuclease activity of Mre11-H59S observed *in vitro* (Figure 5-2A), or it may reflect the importance of the exonuclease activity of Mre11 in later steps of the recombination process after the hairpin is cleaved. Unfortunately, there is no good way to specifically measure the endo- or the exo-nuclease activities in mitotic cells *in vivo*.

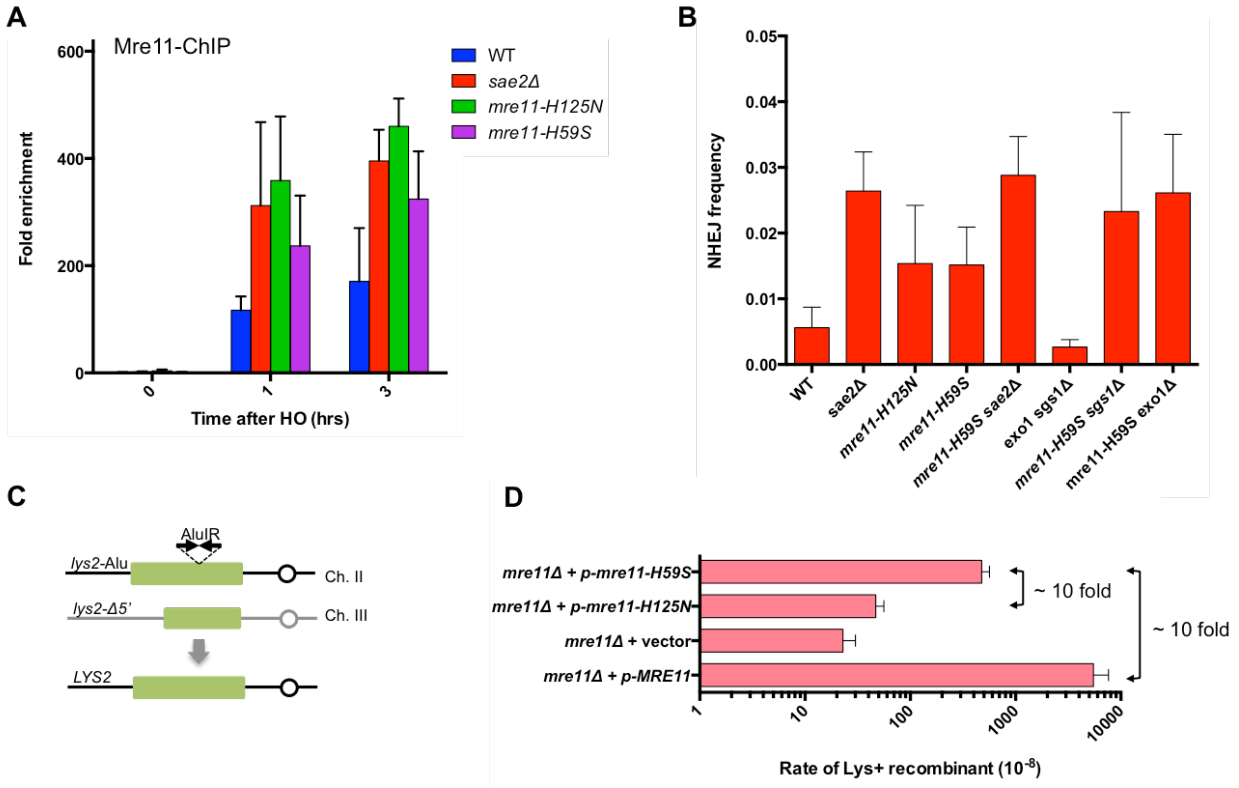

Figure 5-5. In vivo assays with *mre11-H59S*

(A) ChIP-qPCR for Mre11 0.2 kb from the HO-induced DSBs. The error bars indicate SD (n=3). (B) Frequency of chromosomal NHEJ. The error bars indicate SD (n=3). (C) Cartoon representation of the *lys2-AluIR* ectopic recombination assay. (D) Recombination frequencies of strains with the *lys2-AluIR* and *lys2-Δ5'* ectopic recombination reporter system. The rate of Lys^+ recombinants was derived from the median recombination frequency determined from eight different isolates of each strain. The error bars indicate SD (n=3).

5.4 Discussion

The biochemical analysis of recombinant ScMre11^{H59S} and ScMre11^{H59N} did not demonstrate a distinct separation of nuclease activities, in contrast to previous reports. We found Mre11^{H59S} to be largely defective in both endo- and exonuclease activities, while Mre11^{H59N} behaves essentially the same as Mre11. Garcia et al., 2011 previously reported that Mre11^{H59S} is proficient for endonuclease activity and defective for 3'-5' exonuclease activity; furthermore, Spo11-oligo complexes are released during meiosis in the *mre11-H59S* homozygous diploid, suggesting Mre11 endonuclease is proficient *in vivo*. The reason for the discrepancies between our *in vitro* data and those reported by Garcia et al. are currently unclear. In each case, Mre11 and mutant derivatives were purified as GST fusion proteins from yeast cells, and similar DNA substrates were used for *in vitro* assays (Garcia et al., 2011). Further analysis would need to be done to clarify the discrepancy.

We initially made the Mre11-H59N allele because the equivalent mutation in human showed a more defective exonuclease activity when mutated to Asparagine than to Serine (Chanut et al., 2016). However, it was later reported that the article incorrectly referred to the exonuclease mutant as H63N when, in fact, it was H63D (Chanut et al., 2017). It would be interesting to characterize the Sc.Mre11-H59D mutant to see if it confers a clear separation of nuclease activities.

In vivo, the *mre11-H59S* mutant clearly shows different phenotype compared with *mre11-H125N*. It is more resistant to genotoxic agents than *mre11-H125N* and while combination with *exo1Δ* results in comparable sensitivity, *mre11-H59S sgs1Δ* cells survive better than *mre11-H125N sgs1Δ* on CPT. Moreover, deletion of *YKU70* does not change *mre11-H59S sgs1Δ* sensitivity whereas it greatly alleviates *mre11-H125N sgs1Δ* sensitivity. These observations are consistent with the current model of end resection where 5' strand cleavage by MRX-Sae2 removes Ku and generates an entry site for Exo1 to access DNA

whereas Sgs1-Dna2 pathway can bypass the MRX-Sae2 activity to antagonize Ku and initiate resection itself.

Because there is no good way to quantitatively measure the extent of Mre11 exo- or endo-nuclease activities *in vivo* and since we did not see a distinct separation of nuclease activities *in vitro*, interpretation of the genetic data with *mre11-H59S* is difficult. The phenotype conferred by *mre11-H59S* may be reflecting the exonuclease deficiency or the combined reduced activities of both exo- and endo-nucleases. For example, the fact that we observe about 10-fold lower recombination rate with hairpin capped ends may represent either reduced Mre11 endonuclease activity or the defect in Mre11 exonuclease activity resulting in a recombination defect after hairpin cleavage. Similarly, we cannot conclude that the higher enrichment of Mre11 at DSB ends and increased NHEJ efficiency in *mre11-H59S* cells compared WT cells reflect the importance of Mre11 exonuclease activity in complex turnover and NHEJ.

Garcia et al., 2011 were able to study meiotic DSB processing in the mre11-H59S mutant because it is possible to separate the Spo11-oligonucleotide complex intermediates that are generated after the initial Mre11 endonuclease cleavage. Immunoprecipitation of Spo11 brings along the cleaved oligonucleotide to which it is covalently bound. In this case, even if the Mre11 endonuclease is slightly defective, the analysis is not affected because only the collected intermediates downstream of the endonucleolytic cleavage are examined. However, because there is currently no good way to separate resection intermediates from cycling cells, our studies likely reflect both of the Mre11 nuclease activities. To complete this study, we would need to generate an Mre11 mutant that has a clear separation of nuclease activities. The Histidine residue targeted in this study is based on the structure of *P. furiosus* Mre11 dimer (Williams et al., 2008). Since then, *S. pombe* Mre11 dimer has been solved (Schiller et al., 2012). Homology modeling based on the structure of *S. pombe* ortholog and molecular

dynamics simulations could help reveal a better amino acid to target for the generation of an Mre11 mutant with exo-proficient and endo-deficient nuclease activity.

Chapter 6: Conclusions and Perspectives

The MRX/N complex orchestrates the cellular response to DNA damage. It detects DSBs, recruits factors to the lesion, and structurally tethers the broken DNA molecules. The complex plays an enzymatic role in initiating end resection process and is the key to repair pathway choice. Furthermore, it is involved in DNA damage signal transduction by recruiting and activating Tel1/ATM checkpoint kinase. Owing to its importance in genome maintenance, the Mre11 complex has been an active area of research over the years. Still, many questions regarding the precise molecular details of how this highly conserved, multifunctional complex regulates DDR remains to be solved. The overarching focus of this thesis is to further expand our understanding of the molecular mechanism and regulation of the MRX complex in its various roles during DDR. Specifically, the thesis aims to decipher the roles of Xrs2, Tel1, and Mre11 exonuclease in regulating the Mre11 complex.

6.1 Roles of Xrs2 in regulating the Mre11 complex

6.1.1 Xrs2/Nbs1 regulates the subcellular localization of the Mre11 complex

One of the main responsibilities of Xrs2/Nbs1 is the translocation of Mre11-Rad50 into the nucleus. In NBS cells with truncated nibrin or in *xrs2Δ* cells, Mre11 and Rad50 still interact but are confined to the cytoplasm (Carney et al., 1998; Tsukamoto et al., 2005). There are two putative NLS sequences in Xrs2, a monopartite NLS at residues 350-360 and a bipartite NLS located at the C-terminus (residues 816-849) of the protein (predicted by cNLS Mapper). In Chapter 4, we demonstrated that the bipartite NLS alone is able to facilitate nuclear localization of MRX. In mouse nibrin, three NLS sequences were identified that were each capable of directing nuclear localization of MRN ($KRER_{468}$, $RKRK_{550}$, and $KKPR_{592}$) (Vissinga et al., 2009). Multiple redundant NLS sequences highlight the importance of nuclear localization of the MRX/N complex. Interestingly, Nbs1 also consists of an active nuclear export sequence (NES)

(Vissinga et al., 2009), suggesting a more dynamic subcellular localization of the complex than observed in static images.

The significance of the subcellular localization regulation by Xrs2/Nbs1 has not been thoroughly examined. In normally resting cells, a bulk of Mre11 and Rad50 are uniformly distributed in the nuclei. As Chapter 3 and other studies demonstrate, the nuclear Mre11-Rad50 complex can carry out some DDR independently of Xrs2/Nbs1 (Kim et al., 2017; Oh et al., 2016; Tsukamoto et al., 2005). Based on these observations, one could wonder why Mre11 or Rad50 never developed a nuclear localization sequence of its own. One possible explanation for this is for Mre11-Rad50 to have a cytoplasmic role. Supporting this hypothesis, Mre11-Rad50 has been identified as a sensor for exogenous dsDNA, which is required for STING trafficking and type I interferon (IFN) induction (Kondo et al., 2013). Nbs1, however, is not necessary for this cytosolic DNA response and exogenous DNA-induced STING pathway (Kondo et al., 2013). Consistently, a cell line derived from an ATLD patient with compromised DNA binding properties of MRE11 has a defect in IFN production (Kondo et al., 2013). This aspect of the Mre11 complex provides a linkage between DNA repair and innate immunity, which is of great importance for current biomedicine to explore and expand on. It is also plausible that Nbs1's NES is a means for cells to downregulate MR complex and Tel1/ATM kinase activities after DNA damage response is complete. Supporting this view, ATM-dependent phosphorylation of human Nbs1 at DSBs trigger relocalization of the protein to the nucleoplasm (Lukas et al., 2003).

6.1.2 Xrs2/Nbs1 influences the architecture of the Mre11 complex

In addition to the subcellular localization, Xrs2/Nbs1 influences the overall assembly and stability of the Mre11 complex. The basis for Mre11-Xrs2/Nbs1 interaction is the eukaryotic-specific latching loop that extends the dimer interface distal to the DNA-Rad50 binding cleft (Schiller et al., 2012). This loop marks the structural difference between prokaryotes and

eukaryotes, which may be the source for the necessity of the third component of the complex – Xrs2/Nbs1. Mutations in the loop are associated with ATLD and NBSLD, demonstrating that this region is critical for Mre11 function and/or stability. Nbs1 binding across both latching loops in the Mre11 dimer via its Mre11-interaction domain 2 is suggested to stabilize Mre11 dimer (Kim et al., 2017; Schiller et al., 2012). Our data in Chapter 4 also supports such stabilization effect of Xrs2 on Mre11 complex: expressing an Xrs2 fragment that encompasses the Mre11-interaction domain 2 and Tel1-interaction domain (*X224*) in *xrs2Δ* cells enhanced DNA damage resistance and DNA tethering independently of Tel1. To further verify the stabilization effect of Xrs2, expression of a smaller Xrs2 fragment just consisting the Mre11-interaction domain 2 should be analyzed.

In a similar study, expression of just a 108 amino acid fragment encompassing the Mre11 interaction domain was sufficient to rescue viability and ATM activation in cultured mouse cells and supported differentiation of hematopoietic cells *in vivo* (Kim et al., 2017). Interestingly, the stabilization effect of Xrs2/Nbs1 seems to be more important in higher eukaryotes than in budding yeast. Expression of nuclear Mre11 (Mre11-NLS) in *xrs2Δ* restored DNA damage resistance in a Rad50-dependent manner in budding yeast whereas expression of *Mre11-NLS* in *Nbs1*$^{-/-}$ mouse embryonic fibroblasts and human cells did not restore nuclear localization of Rad50 (Kim et al., 2017; Lakdawala et al., 2008). Moreover, while the purified yeast MR complex showed endonucleolytic cleavage activity in the presence of Sae2, CtIP was unable to stimulate purified human MR complex (Kim et al., 2017). These results suggest that mammalian Nbs1 has a larger influence on the assembly and disposition of the complex than Xrs2. A recent *in vitro* study also found that yeast Mre11-Rad50 complex can carry out endonucleolytic cleavage, but the addition of Xrs2 lead to a marked stimulation of reaction efficiency (Wang et al., 2017), suggesting that different reaction conditions, such as salt concentration, may influence the stability of the complex. Scanning force microscopy analysis revealed that binding of Nbs1 causes rearrangement of MR conformation and influences the flexibility of the Rad50

coiled coils (Kim et al., 2017). It would be interesting to examine the binding effect of Xrs2 in yeast MR architecture using the same scanning force microscopy method to compare the extent of Xrs2- and Nbs1-influences on the overall architecture of the complex. Also, structure analysis detailing the interaction between human Mre11 and Nbs1 would be helpful in solving how Nbs1 regulates the overall complex architecture. Furthermore, it would be interesting to swap the interface domain of eukaryotic and prokaryotic Mre11 to explore the contribution of the latching loop and the Mre11-Xrs2/Nbs2 interaction in Mre11 dimerization.

6.1.3 Xrs2 is dispensable for the nuclease functions of the Mre11 complex

In Chapter 3, we demonstrated that Xrs2 is dispensable for the nuclease functions of the Mre11 complex. Nuclear Mre11 (*MRE11-NLS)* suppresses many of the *xrs2Δ* defects, including slow growth, resistance to clastogens, end resection, and meiosis. These functions are dependent on the Mre11 nuclease and Sae2. In addition, we showed that the MR complex is as competent for initiation of resection at protein-blocked ends as the MRX complex *in vitro*, and this reaction requires Sae2, consistent with our *in vivo* studies. These data are surprising because phosphorylated Sae2/Ctp1/CtIP interacts with the FHA domain of Xrs2/Nbs1 and this interaction had been suggested to target Ctp1 to damaged sites (Williams et al, 2009; Lloyd et al, 2009). Interestingly, in the absence of Xrs2, Mre11-NLS partially restores hairpin opening and this is mostly independent of Sae2 but still requires the Mre11 nuclease activity. This result is most consistent with Sae2/CtIP regulating Mre11 nuclease at different end structures rather than acting directly as a nuclease.

The underlying molecular mechanism of how Sae2 promotes the catalytic activity of Mre11 is still unknown. While several studies have mutagenized *MRE11* and found alleles that suppress *sae2Δ,* none of them are self-activating Mre11 (Chen et al., 2015; Puddu et al., 2015). This suggests that Sae2 might activate Mre11 indirectly, perhaps by providing architectural and DNA binding support through interaction with Rad50. Consistent with this model, *rad50S* mutant

confers similar phenotype as *sae2Δ* and *mre11-nd.* However, no physical interaction between Rad50 and Sae2 has been reported to this day, leaving the question unanswered.

The Xrs2-independent resection and DNA damage resistance in *MRE11-NLS xrs2Δ* cells is completely dependent on *SAE2* even though resection is only mildly impacted by the *sae2Δ* mutation in budding yeast. Our initial explanation for this observation was that resection initiation by Sgs1-Dna2 is compromised due to the reduced retention of Mre11 and Dna2 at DSB ends in *MRE11-NLS sae2Δ xrs2Δ* cells. However, even though *MRE11-NLS-TID* restored retention of Mre11 at DSB ends in *xrs2Δ* cells, the restoration of DNA damage resistance remained Sae2-dependent. This suggests that Sae2 may play a direct role in promoting Sgs1-Dna2 activity. Indeed, a recent study reported biochemical evidence that CtIP promotes BLM-DNA2 pathway by directly interacting with BLM and enhancing its helicase activity (Daley et al., 2017). Consistently, an epistatic relationship between CtIP and Dna2 has been reported in chicken DT40, human cells, and *Xenopus* extracts (Hoa et al., 2015; Peterson et al., 2013).

Unlike Xrs2, human Nbs1 is required to promote Mre11 endonuclease activity. Purified human MR complex with CtIP does not show endonucleolytic cleavage activity on blocked DNA ends and hairpin substrates *in vitro* (Deshpande et al., 2016; Deshpande et al., 2017; Kim et al., 2017; Paull and Gellert, 1999). The differential requirement for Xrs2 and Nbs1 in regulating the nuclease activity of the Mre11 complex may be due to the bigger influence Nbs1 plays in the proper architecture of the complex, as mentioned in the previous section.

6.1.4 Xrs2/Nbs1 is a scaffold protein

Another crucial role of Xrs2/Nbs1 is in connecting the Mre11 complex with different repair proteins. The FHA domain interacts with phosphorylated Sae2/CtIP and Lif1/Xrcc4 (Chen et al., 2001; Liang et al., 2015; Lloyd et al., 2009; Matsuzaki et al., 2008; Palmbos et al., 2008; Wang et al., 2013; Williams et al., 2009). As shown in Chapter 3, the *xrs2Δ MRE11-NLS* strain

remains defective for NHEJ, similarly to the *xrs2-SH* mutant, consistent with Xrs2-Lif1 interaction being critical for NHEJ.

The observation that Sae2-Xrs2 interaction is dispensable for end resection prompts the question what is the Xrs2-Sae2 interaction for? In Chapter 4, we found that the FHA domain mutant of Xrs2 (*xrs2-SH*) shows hyper-enrichment of Mre11 at DSB ends, similarly to *sae2Δ* cells. This suggests that the Xrs2-Sae2 interaction may mediate turnover of Mre11 at the damaged site. It is unclear whether MRX resides at dsDNA or ssDNA when it persists at break ends and whether resection is sufficient for the eviction of the complex from break ends. *sae2Δ* and *mre11-H125N* both confer hyper-enrichment of Mre11 while they only show very mild resection defect, suggesting that MRX may persist on ssDNA even after resection initiates. Prolonged MRX accumulation at DNA ends causes persistent checkpoint activation and cell cycle arrest, eventually leading to cell death (Chen et al., 2015; Puddu et al., 2015). By simultaneously interacting with Tel1 and Sae2, Xrs2 may be a means to efficiently couple checkpoint activation and MRX removal from DSB ends. Intriguingly, *xrs2-SH, xrs2Δ MRE11-NLS-TID*, and *xrs2Δ X224* cells all confer hyper-enrichment of Mre11 at DSB ends but are not sensitive to DNA damaging agents (Shima et al., 2005). This suggests that the level of Mre11 at break ends does not directly correlate with DNA damage sensitivity, and it may reflect Sae2's additional function in attenuating checkpoint signaling for cell survival.

Consistent with previous studies, we confirmed in Chapter 3 that Tel1 recruitment to DSBs requires a direct interaction with Xrs2 (Nakada et al., 2003; Tsukamoto et al., 2005; You et al., 2005). In Chapter 4, we further demonstrated that enforced recruitment of Tel1 to Mre11 is sufficient to restore telomere elongation and Tel1 signaling in Xrs2-deficient cells. Similarly, in fission yeast, Tel1 overexpression bypasses the requirement for Nbs1 in Tel1-dependent signaling and telomere maintenance (Limbo et al., 2018) and a minimal Nbs1 fragment comprising the Mre11 interface but not the ATM interacting domain is sufficient to rescue ATM activation in mammalian cells (Kim et al., 2017). These data indicate that Xrs2/Nbs1 functions

only to recruit Tel1/ATM and that Mre11 and/or Rad50 directly mediate kinase activation. *In vitro*, Rad50 mediated recruitment of ATM has been observed, although its kinase activity was not stimulated without Nbs1 (Lee and Paull, 2005). Also, some genetic and biochemical analysis have shown that mutation in Rad50 influences the activation of ATM and Tel1 (Deshpande et al., 2014; Hohl et al., 2011). Based on these observations, it is speculated that Rad50-mediated conformation change regulates Tel1/ATM activation.

6.2 Roles of Tel1 in regulating the Mre11 complex

6.2.1 Kinase-independent role of Tel1

Once recruited to DSBs, Tel1 provides a positive feedback loop by stabilizing MRX association at DNA ends (Cassani et al., 2016; Oh et al., 2016). This function is independent of its kinase activity, implying that it structurally stabilizes MRX retention to DSBs. In Chapter 4, we extended the analysis of this structural role of Tel1 and its functional significance. We show that Tel1-mediated positive feedback loop also acts at replication forks as it does at DSB ends. Furthermore, we provide evidence that the structural contribution of Tel1 is compensatory to Xrs2-mediated stabilization of the Mre11 dimer in DNA damage resistance and DNA tethering. These findings suggest that the quantity and quality of the MRX complex compensate each other. Optimally stabilized Mre11 complex may engage in sufficient DNA tethering with minimal quantity while suboptimal complex may exhibit reduced ability to hold DNA together and thus require higher local concentration.

Interestingly, the abundance of MRX and the Xrs2-dependent stabilization both have little impact on end resection. Disrupting dimerization of *P. furiosus* Mre11 does not decrease exo- and endonuclease catalysis (Williams et al., 2008), suggesting that Mre11 catalytic and architectural functions are separate. Furthermore, *tel1Δ* cells are proficient in end resection, hairpin resolution, and meiosis (Carballo et al., 2008; Cartagena-Lirola et al., 2006; Oh et al.,

2016), indicating that abundant retention of the complex at its substrate is not a prerequisite for the enzymatic activity of Mre11. However, the quality and quantity of the MRX complex may be important for meiotic DSB formation and/or processing. While *MRE11-NLS xrs2Δ* diploids sporulate about 3 fold less than WT diploids, *MRE11-NLS-TID xrs2Δ* and *X224 xrs2Δ* diploids restore sporulation to WT level (Appendix 2).

It is unclear how Tel1 structurally stabilize the MR-DNA association. The Tel1-interacting domain of Xrs2 is immediately downstream of this Mre11-interacting domain, implying that Tel1 would sit right below the Mre11-Rad50 globular domain. Since Tel1 is a large protein with a molecular weight of 322 kDa, it is possible that it makes some contact with the DNA-bound globular domain and locks the complex onto its substrate. No direct interaction between Tel1 and Mre11 or Rad50 has been identified. However, in fission yeast, Mre11-Rad50-dependent, Nbs1-independent recruitment of Tel1 to DNA ends has been observed when Tel1 is overexpressed (Limbo et al., 2018), suggesting a weak but direct interaction between Mre11-Rad50 and Tel1. Crystal structure of the Tel1/ATM in association with the Mre11 complex would need to be solved and analyzed to reveal the contribution of the Tel1/ATM interaction in Mre11-Rad50 architecture.

6.2.2 Kinase-dependent role of Tel1

The kinase activity of Tel1 is redundant with Mec1 in DNA damage signaling and appears to be a backup pathway in yeast. Deletion of Tel1 does not significantly sensitize cells to genotoxic agents as long as Mec1 is present (Mantiero et al., 2007; Sanchez et al., 1996). In addition to the structural role of Tel1, our data demonstrate a kinase-dependent role of Tel1 in regulating Mre11 complex functions. *xrs2Δ MRE11-NLS-X85 tel1-kd* cells are slightly more sensitive than *xrs2Δ MRE11-NLS-X85* to genotoxic agents. Similarly, the recovery of end tethering in *xrs2Δ MRE11-NLS-X85* and *xrs2Δ X224* is partially dependent on the kinase activity of Tel1. These observations indicating that the kinase activity of Tel1 has at least some contributes to the DNA

damage resistance and DNA tethering functions of the complex in these mutant contexts. Tel1 phosphorylates Mre11 and Xrs2 in response to DNA damage (D'Amours and Jackson, 2001; Usui et al., 2001) but whether this modification has any functional relevance is unclear. Elimination of all the possible Tel1 target sites in Xrs2 does not confer any defect in DDR or telomere length maintenance (Mallory et al., 2003). It is possible that the Tel1-mediated phosphorylation of Mre11 and/or Xrs2 influences the complex quality and that this influence only becomes relevant in our mutant contexts while it is functionally irrelevance in an otherwise WT background. One way to verify this hypothesis is to eliminate the SQ/TQ motifs in Mre11-NLS-X85 and assess the DNA damage sensitivity in the *xrs2Δ* background. If the hypothesis is true, such strain should confer similar sensitivity as in *MRE11-NLS-TID xrs2Δ tel1-kd* cells.

6.3 MRX safeguards genome integrity through various means

In this thesis, we used a number of different assays to tweak out and analyze specific functions of the MRX complex in DDR. This allowed us to understand which of the various responsibilities of the complex actually have a consequential impact on its ability to safeguard genome integrity. We show that loss of NHEJ and Tel1 signaling has little affect on DNA damage resistance. This is expected since in budding yeast, HR is a more prominent repair pathway than NHEJ, and Mec1 is redundant with Tel1 in checkpoint signaling. Consistently, DNA end resection, which is essential for HR and Mec1 checkpoint activation, is critical for DNA damage resistance. Through analysis of *xrs2Δ MRE11-NLS* and *sae2Δ xrs2Δ MRE11-NLS* cells, we demonstrated the importance of end resection in cell proliferation and in resistance to DNA damage.

We found that the residual DNA damage sensitivity in *xrs2Δ MRE11-NLS* cells is due to its reduced DNA tethering ability. It appears that while a slight defect in DNA bridging is tolerable, as in *tel1Δ* cells, once the extent of defect crosses some threshold, it becomes a source for DNA damage sensitivity. The significance of DNA tethering in genome integrity is not

fully understood. We found that end tethering by itself is not sufficient for NHEJ and that cells with reduced end tethering can still undergo proficient intra-chromatid recombination or recombination between misaligned sister chromatids. Other studies suggest that DSB tethering may be particularly important for SDSA and SSA repair pathways (Cassani et al., 2016; Clerici et al., 2005). We also provide evidence that the hyper spontaneous heteroallelic recombination observed in MRX-null diploids is not due to defect in sister chromatid bridging. In fact, the increase in heteroallelic recombination rate correlates with the decrease in resection efficiency. This observation aligns with the hypothesis that slow resection yields shorter heteroduplex tracts, resulting in more prototrophs and an apparent increase heteroallelic recombination (Haber, 1998). A possible way to further explore the chromatin dynamics during recombination would be to follow both ends of a repairable DSB simultaneously with its homologous donor using a high-speed and super-resolution imagining. Such a study could uncover different modes of DNA tethering during homology search, pairing, and synthesis, as well as after dissociation.

Our data suggest that one way DNA tethering promotes genome integrity is by stabilizing the replisome at stalled forks and minimizing spontaneously arising damages during S phase. The structural integrity of MRX mediates the replisome stability function independently of Mre11 nuclease activity and S phase checkpoint (Tittel-Elmer et al., 2009). By maintaining the sister chromatids together, MRX preserves the architecture of the replisome, thus promoting replication recovery and restart. This function of MRX is likely shared with cohesin complex. Indeed, the combined loss of Mre11 and cohesin complex results in severe sensitivity to replication stress (Tittel-Elmer et al., 2009). CPT, MMS, and HU all induce replication stresses. Top1 poisoning prevents DNA uncoiling and covalently traps Top1 complex on DNA while MMS alkylates DNA, both presenting an obstacle to replication fork progression (Koster et al., 2007; Ray Chaudhuri et al., 2012). HU inhibits ribonucleotide reductase, decreasing the basal dNTP pool and thus blocking replication fork progression (Koc et al., 2004). Mre11 enrichment, end tethering, and survival on CPT and MMS are highly correlated. Xrs2 and Tel1 independently

contribute to these functions by regulating the Mre11 complex, and the two effects can compensate each other, which is evident by expression of X224 fragment rescuing *xrs2Δ* cells independently of Tel1. On the contrary, the presence of Tel1 is required for survival on HU in *xrs2Δ X224* cells. This suggests that Tel1 and/or MRX functions differently based on the genotoxic agents and that it may play an additional role in overcoming cytotoxicity of HU. Our data uncovered an important role of DNA bridging during replication in suppressing GCR formation. Spontaneously arising damage during replication is likely to initiate GCR events. Indeed, stalling a replication fork at a protein barrier leads to elevated ectopic recombination resulting in GCRs (Lambert et al., 2005). By ensuring replication stability, MRX minimizes the initiating lesions that could potentially resolve as GCRs. Alternatively, the structural function of the Mre11 complex might be important for suppressing intermediates of inappropriate ectopic recombination. To further explore the subject of how MRX structurally suppresses large chromosomal rearrangements, classification of GCR events should be done and intermediates should be analyzed.

6.4 The unanswered role of Mre11 exonuclease in DSB repair

DNA end resection is a key step in HR-mediate repair; the process determines the repair pathway choice and ensures the activation of checkpoint signaling. Mre11 exerts both endo- and exonuclease activities during this highly regulated process. The goal of Chapter 5 was to decipher the functional significance of the Mre11 exonuclease using mre11 mutant alleles that have been reported to impair the exo but not the endonuclease activity. Unfortunately, the mutant alleles did not show a clear separation of nuclease activities *in vitro*, which made the *in vivo* analysis difficult to interpret. To this end, several questions remain to be answered regarding the role of Mre11 exonuclease in DSB repair. Is Mre11-dependent exonucleolytic degradation required for the extensive resection machinery to access DNA from the nick

generated by Mre11 endonuclease? Is it required for the eviction of MRX and Ku from DSB ends? Can Rad51 load onto ssDNA with unprocessed dsDNA at break ends? Is Mre11 exonuclease necessary to remove proteins bound to the break ends? Is it required to prevent NHEJ or to promote MMEJ? Does it have any role in the resolution of hairpin structures? Answers to these questions will provide important mechanistic insights into the precise role of Mre11 nuclease activities during resection and thereby expand our understanding of the regulation of repair pathway choice. To address these questions *in vivo*, an Mre11 allele with a clear separation of nuclease activities needs to be generated. Structural modeling with the solved *S. pombe* ortholog could be helpful in identifying such a mutant allele.

6.5 Conclusions

As a central orchestrator of the DNA damage response, the Mre11 complex manages several pivotal responsibilities for the protection of the genome integrity. Its various activities during DDR are regulated by multiple means to ensure fidelity of repair outcomes. This thesis defines the regulatory role of Xrs2 in the Mre11 complex functions. Our data support the idea that Xrs2 is a scaffold protein that connects MR complex to Tel1 signaling and NHEJ through discrete binding motifs but plays only a minor role in the nuclease function of the MR complex. This is consistent with prokaryotic homolog SbcCD functioning independently of an Xrs2-like protein to process hairpin-capped ends in *E.coli.* Furthermore, we provide insights on how Tel1 regulates MRX activity and its functional relevance. We propose a model whereby Xrs2 and Tel1 independently contribute to Mre11 complex stabilization at DSBs and stalled replication forks to promote genome integrity through efficient DNA bridging. The thesis establishes the importance of the replisome stability and DNA tethering functions of MRX in the suppression of gross chromosome rearrangements thereby supporting the idea that the MRX functions as a fundamental replisome component. Altogether, this thesis expands our understanding of the molecular mechanism of the MRX complex and highlights its role in actively preventing spontaneous DNA damage in addition to responding to DSBs.

References

Aguilera, A., and Gomez-Gonzalez, B. (2008). Genome instability: a mechanistic view of its causes and consequences. Nat Rev Genet *9*, 204-217.

Ajimura, M., Leem, S.H., and Ogawa, H. (1993). Identification of new genes required for meiotic recombination in Saccharomyces cerevisiae. Genetics *133*, 51-66.

Al-Ahmadie, H., Iyer, G., Hohl, M., Asthana, S., Inagaki, A., Schultz, N., Hanrahan, A.J., Scott, S.N., Brannon, A.R., McDermott, G.C.*, et al.* (2014). Synthetic lethality in ATM-deficient RAD50-mutant tumors underlies outlier response to cancer therapy. Cancer Discov *4*, 1014-1021.

Alani, E., Padmore, R., and Kleckner, N. (1990). Analysis of wild-type and rad50 mutants of yeast suggests an intimate relationship between meiotic chromosome synapsis and recombination. Cell *61*, 419-436.

Amberg, D.C., Burke, D. J. & Strathern, J. N. (2005). Methods in Yeast Genetics: A Cold Spring Harbor Laboratory Course Manual. Cold spring Harbor Laboratory Press.

Anand, R., Ranjha, L., Cannavo, E., and Cejka, P. (2016). Phosphorylated CtIP Functions as a Co-factor of the MRE11-RAD50-NBS1 Endonuclease in DNA End Resection. Molecular cell *64*, 940-950.

Andres, S.N., Appel, C.D., Westmoreland, J.W., Williams, J.S., Nguyen, Y., Robertson, P.D., Resnick, M.A., and Williams, R.S. (2015). Tetrameric Ctp1 coordinates DNA binding and DNA bridging in DNA double-strand-break repair. Nat Struct Mol Biol *22*, 158-166.

Arthur, L.M., Gustausson, K., Hopfner, K.P., Carson, C.T., Stracker, T.H., Karcher, A., Felton, D., Weitzman, M.D., Tainer, J., and Carney, J.P. (2004). Structural and functional analysis of Mre11-3. Nucleic acids research *32*, 1886-1893.

Bakkenist, C.J., and Kastan, M.B. (2003). DNA damage activates ATM through intermolecular autophosphorylation and dimer dissociation. Nature *421*, 499-506.

Balestrini, A., Ristic, D., Dionne, I., Liu, X.Z., Wyman, C., Wellinger, R.J., and Petrini, J.H. (2013). The Ku heterodimer and the metabolism of single-ended DNA double-strand breaks. Cell Rep *3*, 2033-2045.

Barlow, J.H., Lisby, M., and Rothstein, R. (2008). Differential regulation of the cellular response to DNA double-strand breaks in G1. Mol Cell *30*, 73-85.

Baroni, E., Viscardi, V., Cartagena-Lirola, H., Lucchini, G., and Longhese, M.P. (2004). The functions of budding yeast Sae2 in the DNA damage response require Mec1- and Tel1-dependent phosphorylation. Molecular and cellular biology *24*, 4151-4165.

Becker, E., Meyer, V., Madaoui, H., and Guerois, R. (2006). Detection of a tandem BRCT in Nbs1 and Xrs2 with functional implications in the DNA damage response. Bioinformatics *22*, 1289-1292.

Bennardo, N., Cheng, A., Huang, N., and Stark, J.M. (2008). Alternative-NHEJ is a mechanistically distinct pathway of mammalian chromosome break repair. PLoS Genet *4*, e1000110.

Boboila, C., Alt, F.W., and Schwer, B. (2012). Classical and alternative end-joining pathways for repair of lymphocyte-specific and general DNA double-strand breaks. Adv Immunol *116*, 1-49.

Bonetti, D., Villa, M., Gobbini, E., Cassani, C., Tedeschi, G., and Longhese, M.P. (2015). Escape of Sgs1 from Rad9 inhibition reduces the requirement for Sae2 and functional MRX in DNA end resection. EMBO reports *16*, 351-361.

Borde, V. (2007). The multiple roles of the Mre11 complex for meiotic recombination. Chromosome research : an international journal on the molecular, supramolecular and evolutionary aspects of chromosome biology *15*, 551-563.

Boulton, S.J., and Jackson, S.P. (1998). Components of the Ku-dependent non-homologous end-joining pathway are involved in telomeric length maintenance and telomeric silencing. EMBO J *17*, 1819-1828.

Bressan, D.A., Baxter, B.K., and Petrini, J.H. (1999). The Mre11-Rad50-Xrs2 protein complex facilitates homologous recombination-based double-strand break repair in Saccharomyces cerevisiae. Mol Cell Biol *19*, 7681-7687.

Budd, M.E., and Campbell, J.L. (2009). Interplay of Mre11 nuclease with Dna2 plus Sgs1 in Rad51-dependent recombinational repair. PloS one *4*, e4267.

Buis, J., Wu, Y., Deng, Y., Leddon, J., Westfield, G., Eckersdorff, M., Sekiguchi, J.M., Chang, S., and Ferguson, D.O. (2008). Mre11 nuclease activity has essential roles in DNA repair and genomic stability distinct from ATM activation. Cell *135*, 85-96.

Cannavo, E., and Cejka, P. (2014). Sae2 promotes dsDNA endonuclease activity within Mre11-Rad50-Xrs2 to resect DNA breaks. Nature *514*, 122-125.

Carballo, J.A., Johnson, A.L., Sedgwick, S.G., and Cha, R.S. (2008). Phosphorylation of the axial element protein Hop1 by Mec1/Tel1 ensures meiotic interhomolog recombination. Cell *132*, 758-770.

Carney, J.P., Maser, R.S., Olivares, H., Davis, E.M., Le Beau, M., Yates, J.R., 3rd, Hays, L., Morgan, W.F., and Petrini, J.H. (1998). The hMre11/hRad50 protein complex and Nijmegen breakage syndrome: linkage of double-strand break repair to the cellular DNA damage response. Cell *93*, 477-486.

Cartagena-Lirola, H., Guerini, I., Viscardi, V., Lucchini, G., and Longhese, M.P. (2006). Budding Yeast Sae2 is an In Vivo Target of the Mec1 and Tel1 Checkpoint Kinases During Meiosis. Cell cycle *5*, 1549-1559.

Cassani, C., Gobbini, E., Vertemara, J., Wang, W., Marsella, A., Sung, P., Tisi, R., Zampella, G., and Longhese, M.P. (2018). Structurally distinct Mre11 domains mediate MRX functions in resection, end-tethering and DNA damage resistance. Nucleic acids research.

Cassani, C., Gobbini, E., Wang, W., Niu, H., Clerici, M., Sung, P., and Longhese, M.P. (2016). Tel1 and Rif2 Regulate MRX Functions in End-Tethering and Repair of DNA Double-Strand Breaks. PLoS biology *14*, e1002387.

Celli, G.B., and de Lange, T. (2005). DNA processing is not required for ATM-mediated telomere damage response after TRF2 deletion. Nat Cell Biol *7*, 712-718.

Chamankhah, M., and Xiao, W. (1999). Formation of the yeast Mre11-Rad50-Xrs2 complex is correlated with DNA repair and telomere maintenance. Nucleic acids research *27*, 2072-2079.

Chan, J.E., and Kolodner, R.D. (2011). A genetic and structural study of genome rearrangements mediated by high copy repeat Ty1 elements. PLoS Genet *7*, e1002089.

Chan, S.H., Yu, A.M., and McVey, M. (2010). Dual roles for DNA polymerase theta in alternative end-joining repair of double-strand breaks in Drosophila. PLoS Genet *6*, e1001005.

Chanut, P., Britton, S., Coates, J., Jackson, S.P., and Calsou, P. (2016). Coordinated nuclease activities counteract Ku at single-ended DNA double-strand breaks. Nat Commun *7*, 12889.

Chanut, P., Britton, S., Coates, J., Jackson, S.P., and Calsou, P. (2017). Corrigendum: Coordinated nuclease activities counteract Ku at single-ended DNA double-strand breaks. Nature communications *8*, 15917.

Chaudhuri, A.R., Callen, E., Ding, X., Gogola, E., Duarte, A.A., Lee, J.E., Wong, N., Lafarga, V., Calvo, J.A., Panzarino, N.J.*, et al.* (2016). Erratum: Replication fork stability confers chemoresistance in BRCA-deficient cells. Nature *539*, 456.

Chen, C., and Kolodner, R.D. (1999). Gross chromosomal rearrangements in Saccharomyces cerevisiae replication and recombination defective mutants. Nat Genet *23*, 81-85.

Chen, H., Donnianni, R.A., Handa, N., Deng, S.K., Oh, J., Timashev, L.A., Kowalczykowski, S.C., and Symington, L.S. (2015). Sae2 promotes DNA damage resistance by removing the Mre11-Rad50-Xrs2 complex from DNA and attenuating Rad53 signaling. Proc Natl Acad Sci U S A *112*, E1880-1887.

Chen, H., Lisby, M., and Symington, L.S. (2013). RPA coordinates DNA end resection and prevents formation of DNA hairpins. Molecular cell *50*, 589-600.

Chen, L., Trujillo, K., Ramos, W., Sung, P., and Tomkinson, A.E. (2001). Promotion of Dnl4-catalyzed DNA end-joining by the Rad50/Mre11/Xrs2 and Hdf1/Hdf2 complexes. Molecular cell *8*, 1105-1115.

Chen, P.L., Liu, F., Cai, S., Lin, X., Li, A., Chen, Y., Gu, B., Lee, E.Y., and Lee, W.H. (2005). Inactivation of CtIP leads to early embryonic lethality mediated by G1 restraint and to tumorigenesis by haploid insufficiency. Molecular and cellular biology *25*, 3535-3542.

Chen, X., Niu, H., Chung, W.H., Zhu, Z., Papusha, A., Shim, E.Y., Lee, S.E., Sung, P., and Ira, G. (2011). Cell cycle regulation of DNA double-strand break end resection by Cdk1-dependent Dna2 phosphorylation. Nat Struct Mol Biol *18*, 1015-1019.

Chiruvella, K.K., Liang, Z., and Wilson, T.E. (2013). Repair of double-strand breaks by end joining. Cold Spring Harbor perspectives in biology *5*, a012757.

Chung, W.H., Zhu, Z., Papusha, A., Malkova, A., and Ira, G. (2010). Defective resection at DNA double-strand breaks leads to de novo telomere formation and enhances gene targeting. PLoS Genet *6*, e1000948.

Clerici, M., Mantiero, D., Guerini, I., Lucchini, G., and Longhese, M.P. (2008). The Yku70-Yku80 complex contributes to regulate double-strand break processing and checkpoint activation during the cell cycle. EMBO reports *9*, 810-818.

Clerici, M., Mantiero, D., Lucchini, G., and Longhese, M.P. (2005). The Saccharomyces cerevisiae Sae2 protein promotes resection and bridging of double strand break ends. J Biol Chem *280*, 38631-38638.

Clerici, M., Mantiero, D., Lucchini, G., and Longhese, M.P. (2006). The Saccharomyces cerevisiae Sae2 protein negatively regulates DNA damage checkpoint signalling. EMBO reports *7*, 212-218.

Connelly, J.C., and Leach, D.R. (1996). The sbcC and sbcD genes of Escherichia coli encode a nuclease involved in palindrome inviability and genetic recombination. Genes to cells : devoted to molecular & cellular mechanisms *1*, 285-291.

Connelly, J.C., and Leach, D.R. (2002). Tethering on the brink: the evolutionarily conserved Mre11-Rad50 complex. Trends Biochem Sci *27*, 410-418.

Costanzo, V., Robertson, K., Bibikova, M., Kim, E., Grieco, D., Gottesman, M., Carroll, D., and Gautier, J. (2001). Mre11 protein complex prevents double-strand break accumulation during chromosomal DNA replication. Mol Cell *8*, 137-147.

D'Amours, D., and Jackson, S.P. (2001). The yeast Xrs2 complex functions in S phase checkpoint regulation. Genes Dev *15*, 2238-2249.

D'Amours, D., and Jackson, S.P. (2002). The Mre11 complex: at the crossroads of dna repair and checkpoint signalling. Nat Rev Mol Cell Biol *3*, 317-327.

Daley, J.M., Jimenez-Sainz, J., Wang, W., Miller, A.S., Xue, X., Nguyen, K.A., Jensen, R.B., and Sung, P. (2017). Enhancement of BLM-DNA2-Mediated Long-Range DNA End Resection by CtIP. Cell Rep *21*, 324-332.

Daley, J.M., Palmbos, P.L., Wu, D., and Wilson, T.E. (2005). Nonhomologous end joining in yeast. Annual review of genetics *39*, 431-451.

Davies, O.R., Forment, J.V., Sun, M., Belotserkovskaya, R., Coates, J., Galanty, Y., Demir, M., Morton, C.R., Rzechorzek, N.J., Jackson, S.P.*, et al.* (2015). CtIP tetramer assembly is required for DNA-end resection and repair. Nat Struct Mol Biol *22*, 150-157.

de Jager, M., Trujillo, K.M., Sung, P., Hopfner, K.P., Carney, J.P., Tainer, J.A., Connelly, J.C., Leach, D.R., Kanaar, R., and Wyman, C. (2004). Differential arrangements of conserved building blocks among homologs of the Rad50/Mre11 DNA repair protein complex. J Mol Biol *339*, 937-949.

de Jager, M., van Noort, J., van Gent, D.C., Dekker, C., Kanaar, R., and Wyman, C. (2001). Human Rad50/Mre11 is a flexible complex that can tether DNA ends. Mol Cell *8*, 1129-1135.

Deem, A., Keszthelyi, A., Blackgrove, T., Vayl, A., Coffey, B., Mathur, R., Chabes, A., and Malkova, A. (2011). Break-induced replication is highly inaccurate. PLoS biology *9*, e1000594.

Demuth, I., Frappart, P.O., Hildebrand, G., Melchers, A., Lobitz, S., Stockl, L., Varon, R., Herceg, Z., Sperling, K., Wang, Z.Q.*, et al.* (2004). An inducible null mutant murine model of Nijmegen breakage syndrome proves the essential function of NBS1 in chromosomal stability and cell viability. Hum Mol Genet *13*, 2385-2397.

Deng, S.K., Gibb, B., de Almeida, M.J., Greene, E.C., and Symington, L.S. (2014). RPA antagonizes microhomology-mediated repair of DNA double-strand breaks. Nat Struct Mol Biol *21*, 405-412.

Deng, S.K., Yin, Y., Petes, T.D., and Symington, L.S. (2015). Mre11-Sae2 and RPA Collaborate to Prevent Palindromic Gene Amplification. Mol Cell *60*, 500-508.

Deriano, L., Stracker, T.H., Baker, A., Petrini, J.H., and Roth, D.B. (2009). Roles for NBS1 in alternative nonhomologous end-joining of V(D)J recombination intermediates. Mol Cell *34*, 13-25.

Desai-Mehta, A., Cerosaletti, K.M., and Concannon, P. (2001). Distinct functional domains of nibrin mediate Mre11 binding, focus formation, and nuclear localization. Mol Cell Biol *21*, 2184-2191.

Deshpande, R.A., Lee, J.H., Arora, S., and Paull, T.T. (2016). Nbs1 Converts the Human Mre11/Rad50 Nuclease Complex into an Endo/Exonuclease Machine Specific for Protein-DNA Adducts. Mol Cell *64*, 593-606.

Deshpande, R.A., Lee, J.H., and Paull, T.T. (2017). Rad50 ATPase activity is regulated by DNA ends and requires coordination of both active sites. Nucleic acids research *45*, 5255-5268.

Deshpande, R.A., Williams, G.J., Limbo, O., Williams, R.S., Kuhnlein, J., Lee, J.H., Classen, S., Guenther, G., Russell, P., Tainer, J.A.*, et al.* (2014). ATP-driven Rad50 conformations regulate DNA tethering, end resection, and ATM checkpoint signaling. EMBO J *33*, 482-500.

Di Virgilio, M., Ying, C.Y., and Gautier, J. (2009). PIKK-dependent phosphorylation of Mre11 induces MRN complex inactivation by disassembly from chromatin. DNA Repair (Amst) *8*, 1311-1320.

Difilippantonio, S., Celeste, A., Kruhlak, M.J., Lee, Y., Difilippantonio, M.J., Feigenbaum, L., Jackson, S.P., McKinnon, P.J., and Nussenzweig, A. (2007). Distinct domains in Nbs1 regulate irradiation-induced checkpoints and apoptosis. J Exp Med *204*, 1003-1011.

Dynan, W.S., and Yoo, S. (1998). Interaction of Ku protein and DNA-dependent protein kinase catalytic subunit with nucleic acids. Nucleic acids research *26*, 1551-1559.

Eykelenboom, J.K., Blackwood, J.K., Okely, E., and Leach, D.R. (2008). SbcCD causes a double-strand break at a DNA palindrome in the Escherichia coli chromosome. Molecular cell *29*, 644-651.

Falck, J., Coates, J., and Jackson, S.P. (2005). Conserved modes of recruitment of ATM, ATR and DNA-PKcs to sites of DNA damage. Nature *434*, 605-611.

Feldser, D., Strong, M.A., and Greider, C.W. (2006). Ataxia telangiectasia mutated (Atm) is not required for telomerase-mediated elongation of short telomeres. Proc Natl Acad Sci U S A *103*, 2249-2251.

Ferguson, D.O., and Holloman, W.K. (1996). Recombinational repair of gaps in DNA is asymmetric in Ustilago maydis and can be explained by a migrating D-loop model. Proc Natl Acad Sci U S A *93*, 5419-5424.

Ferrari, M., Dibitetto, D., De Gregorio, G., Eapen, V.V., Rawal, C.C., Lazzaro, F., Tsabar, M., Marini, F., Haber, J.E., and Pellicioli, A. (2015). Functional interplay between the 53BP1-ortholog Rad9 and the Mre11 complex regulates resection, end-tethering and repair of a double-strand break. PLoS genetics *11*, e1004928.

Fishman-Lobell, J., Rudin, N., and Haber, J.E. (1992). Two alternative pathways of double-strand break repair that are kinetically separable and independently modulated. Mol Cell Biol *12*, 1292-1303.

Forment, J.V., Jackson, S.P., and Pellegrini, L. (2015). When two is not enough: a CtIP tetramer is required for DNA repair by Homologous Recombination. Nucleus *6*, 344-348.

Foster, S.S., Balestrini, A., and Petrini, J.H. (2011). Functional interplay of the Mre11 nuclease and Ku in the response to replication-associated DNA damage. Mol Cell Biol *31*, 4379-4389.

Frank-Vaillant, M., and Marcand, S. (2002). Transient stability of DNA ends allows nonhomologous end joining to precede homologous recombination. Mol Cell *10*, 1189-1199.

Fu, Q., Chow, J., Bernstein, K.A., Makharashvili, N., Arora, S., Lee, C.F., Person, M.D., Rothstein, R., and Paull, T.T. (2014). Phosphorylation-regulated transitions in an oligomeric state control the activity of the Sae2 DNA repair enzyme. Molecular and cellular biology *34*, 778-793.

Fukunaga, K., Kwon, Y., Sung, P., and Sugimoto, K. (2011). Activation of protein kinase Tel1 through recognition of protein-bound DNA ends. Molecular and cellular biology *31*, 1959-1971.

Furuse, M., Nagase, Y., Tsubouchi, H., Murakami-Murofushi, K., Shibata, T., and Ohta, K. (1998). Distinct roles of two separable in vitro activities of yeast Mre11 in mitotic and meiotic recombination. EMBO J *17*, 6412-6425.

Garcia, V., Phelps, S.E., Gray, S., and Neale, M.J. (2011). Bidirectional resection of DNA double-strand breaks by Mre11 and Exo1. Nature *479*, 241-244.

Ghodke, I., and Muniyappa, K. (2013). Processing of DNA double-stranded breaks and intermediates of recombination and repair by Saccharomyces cerevisiae Mre11 and its stimulation by Rad50, Xrs2, and Sae2 proteins. J Biol Chem *288*, 11273-11286.

Girard, C., Roelens, B., Zawadzki, K.A., and Villeneuve, A.M. (2018). Interdependent and separable functions of Caenorhabditis elegans MRN-C complex members couple formation and repair of meiotic DSBs. Proc Natl Acad Sci U S A *115*, E4443-E4452.

Gnugge, R., Liphardt, T., and Rudolf, F. (2016). A shuttle vector series for precise genetic engineering of Saccharomyces cerevisiae. Yeast *33*, 83-98.

Gnugge, R., Oh, J., and Symington, L.S. (2018). Processing of DNA Double-Strand Breaks in Yeast. Methods Enzymol *600*, 1-24.

Gobbini, E., Cassani, C., Villa, M., Bonetti, D., and Longhese, M.P. (2016). Functions and regulation of the MRX complex at DNA double-strand breaks. Microbial cell *3*, 329-337.

Gobbini, E., Cesena, D., Galbiati, A., Lockhart, A., and Longhese, M.P. (2013). Interplays between ATM/Tel1 and ATR/Mec1 in sensing and signaling DNA double-strand breaks. DNA Repair *12*, 791-799.

Gobbini, E., Villa, M., Gnugnoli, M., Menin, L., Clerici, M., and Longhese, M.P. (2015). Sae2 Function at DNA Double-Strand Breaks Is Bypassed by Dampening Tel1 or Rad53 Activity. PLoS genetics *11*, e1005685.

Goedhart, J., von Stetten, D., Noirclerc-Savoye, M., Lelimousin, M., Joosen, L., Hink, M.A., van Weeren, L., Gadella, T.W., Jr., and Royant, A. (2012). Structure-guided evolution of cyan fluorescent proteins towards a quantum yield of 93%. Nat Commun *3*, 751.

Gravel, S., Chapman, J.R., Magill, C., and Jackson, S.P. (2008). DNA helicases Sgs1 and BLM promote DNA double-strand break resection. Genes Dev *22*, 2767-2772.

Haber, J.E. (1998). The many interfaces of Mre11. Cell *95*, 583-586.

Harper, J.W., and Elledge, S.J. (2007). The DNA damage response: ten years after. Mol Cell *28*, 739-745.

Hashimoto, Y., Ray Chaudhuri, A., Lopes, M., and Costanzo, V. (2010). Rad51 protects nascent DNA from Mre11-dependent degradation and promotes continuous DNA synthesis. Nat Struct Mol Biol *17*, 1305-1311.

Hector, R.E., Shtofman, R.L., Ray, A., Chen, B.R., Nyun, T., Berkner, K.L., and Runge, K.W. (2007). Tel1p preferentially associates with short telomeres to stimulate their elongation. Mol Cell *27*, 851-858.

Heidinger-Pauli, J.M., Unal, E., Guacci, V., and Koshland, D. (2008). The kleisin subunit of cohesin dictates damage-induced cohesion. Mol Cell *31*, 47-56.

Hélène Tourrière, J.S., Armelle Lengronne and Philippe Pasero (2017). Single-molecule Analysis of DNA Replication Dynamics in Budding Yeast and Human Cells by DNA Combing. Bio-protocol *7*, 17.

Hirano, Y., Fukunaga, K., and Sugimoto, K. (2009). Rif1 and rif2 inhibit localization of tel1 to DNA ends. Mol Cell *33*, 312-322.

Hoa, N.N., Akagawa, R., Yamasaki, T., Hirota, K., Sasa, K., Natsume, T., Kobayashi, J., Sakuma, T., Yamamoto, T., Komatsu, K.*, et al.* (2015). Relative contribution of four nucleases, CtIP, Dna2, Exo1 and Mre11, to the initial step of DNA double-strand break repair by homologous recombination in both the chicken DT40 and human TK6 cell lines. Genes to cells : devoted to molecular & cellular mechanisms *20*, 1059-1076.

Hohl, M., Kochanczyk, T., Tous, C., Aguilera, A., Krezel, A., and Petrini, J.H. (2015). Interdependence of the rad50 hook and globular domain functions. Mol Cell *57*, 479-491.

Hohl, M., Kwon, Y., Galvan, S.M., Xue, X., Tous, C., Aguilera, A., Sung, P., and Petrini, J.H. (2011). The Rad50 coiled-coil domain is indispensable for Mre11 complex functions. Nat Struct Mol Biol *18*, 1124-1131.

Hopfner, K.P., Craig, L., Moncalian, G., Zinkel, R.A., Usui, T., Owen, B.A., Karcher, A., Henderson, B., Bodmer, J.L., McMurray, C.T.*, et al.* (2002a). The Rad50 zinc-hook is a structure joining Mre11 complexes in DNA recombination and repair. Nature *418*, 562-566.

Hopfner, K.P., Karcher, A., Craig, L., Woo, T.T., Carney, J.P., and Tainer, J.A. (2001). Structural biochemistry and interaction architecture of the DNA double-strand break repair Mre11 nuclease and Rad50-ATPase. Cell *105*, 473-485.

Hopfner, K.P., Karcher, A., Shin, D.S., Craig, L., Arthur, L.M., Carney, J.P., and Tainer, J.A. (2000). Structural biology of Rad50 ATPase: ATP-driven conformational control in DNA double-strand break repair and the ABC-ATPase superfamily. Cell *101*, 789-800.

Hopfner, K.P., Putnam, C.D., and Tainer, J.A. (2002b). DNA double-strand break repair from head to tail. Curr Opin Struct Biol *12*, 115-122.

Huertas, P., Cortes-Ledesma, F., Sartori, A.A., Aguilera, A., and Jackson, S.P. (2008). CDK targets Sae2 to control DNA-end resection and homologous recombination. Nature *455*, 689-692.

Huertas, P., and Jackson, S.P. (2009). Human CtIP mediates cell cycle control of DNA end resection and double strand break repair. J Biol Chem *284*, 9558-9565.

Ivanov, E.L., Korolev, V.G., and Fabre, F. (1992). XRS2, a DNA repair gene of Saccharomyces cerevisiae, is needed for meiotic recombination. Genetics *132*, 651-664.

Ivanov, E.L., Sugawara, N., White, C.I., Fabre, F., and Haber, J.E. (1994). Mutations in XRS2 and RAD50 delay but do not prevent mating-type switching in Saccharomyces cerevisiae. Mol Cell Biol *14*, 3414-3425.

Iwasaki, D., Hayashihara, K., Shima, H., Higashide, M., Terasawa, M., Gasser, S.M., and Shinohara, M. (2016). The MRX Complex Ensures NHEJ Fidelity through Multiple Pathways Including Xrs2-FHA-Dependent Tel1 Activation. PLoS genetics *12*, e1005942.

Johzuka, K., and Ogawa, H. (1995). Interaction of Mre11 and Rad50: two proteins required for DNA repair and meiosis-specific double-strand break formation in Saccharomyces cerevisiae. Genetics *139*, 1521-1532.

Kanellis, P., Gagliardi, M., Banath, J.P., Szilard, R.K., Nakada, S., Galicia, S., Sweeney, F.D., Cabelof, D.C., Olive, P.L., and Durocher, D. (2007). A screen for suppressors of gross chromosomal rearrangements identifies a conserved role for PLP in preventing DNA lesions. PLoS Genet *3*, e134.

Karathanasis, E., and Wilson, T.E. (2002). Enhancement of Saccharomyces cerevisiae end-joining efficiency by cell growth stage but not by impairment of recombination. Genetics *161*, 1015-1027.

Karlsson, K.H., and Stenerlow, B. (2004). Focus formation of DNA repair proteins in normal and repair-deficient cells irradiated with high-LET ions. Radiat Res *161*, 517-527.

Kaye, J.A., Melo, J.A., Cheung, S.K., Vaze, M.B., Haber, J.E., and Toczyski, D.P. (2004). DNA breaks promote genomic instability by impeding proper chromosome segregation. Current biology : CB *14*, 2096-2106.

Keelagher, R.E., Cotton, V.E., Goldman, A.S., and Borts, R.H. (2011). Separable roles for Exonuclease I in meiotic DNA double-strand break repair. DNA Repair (Amst) *10*, 126-137.

Keeney, S., and Kleckner, N. (1995). Covalent protein-DNA complexes at the 5' strand termini of meiosis-specific double-strand breaks in yeast. Proc Natl Acad Sci U S A *92*, 11274-11278.

Kim, H.S., Vijayakumar, S., Reger, M., Harrison, J.C., Haber, J.E., Weil, C., and Petrini, J.H. (2008). Functional interactions between Sae2 and the Mre11 complex. Genetics *178*, 711-723.

Kim, J.H., Grosbart, M., Anand, R., Wyman, C., Cejka, P., and Petrini, J.H. (2017). The Mre11-Nbs1 Interface Is Essential for Viability and Tumor Suppression. Cell Rep *18*, 496-507.

Kim, J.S., Krasieva, T.B., LaMorte, V., Taylor, A.M., and Yokomori, K. (2002). Specific recruitment of human cohesin to laser-induced DNA damage. J Biol Chem *277*, 45149-45153.

Koc, A., Wheeler, L.J., Mathews, C.K., and Merrill, G.F. (2004). Hydroxyurea arrests DNA replication by a mechanism that preserves basal dNTP pools. J Biol Chem *279*, 223-230.

Kolinjivadi, A.M., Sannino, V., De Antoni, A., Zadorozhny, K., Kilkenny, M., Techer, H., Baldi, G., Shen, R., Ciccia, A., Pellegrini, L.*, et al.* (2017). Smarcal1-Mediated Fork Reversal Triggers Mre11-Dependent Degradation of Nascent DNA in the Absence of Brca2 and Stable Rad51 Nucleofilaments. Mol Cell *67*, 867-881 e867.

Kondo, T., Kobayashi, J., Saitoh, T., Maruyama, K., Ishii, K.J., Barber, G.N., Komatsu, K., Akira, S., and Kawai, T. (2013). DNA damage sensor MRE11 recognizes cytosolic double-stranded DNA and induces type I interferon by regulating STING trafficking. Proc Natl Acad Sci U S A *110*, 2969-2974.

Koster, D.A., Palle, K., Bot, E.S., Bjornsti, M.A., and Dekker, N.H. (2007). Antitumour drugs impede DNA uncoiling by topoisomerase I. Nature *448*, 213-217.

Krogh, B.O., Llorente, B., Lam, A., and Symington, L.S. (2005). Mutations in Mre11 phosphoesterase motif I that impair Saccharomyces cerevisiae Mre11-Rad50-Xrs2 complex stability in addition to nuclease activity. Genetics *171*, 1561-1570.

Krogh, B.O., and Symington, L.S. (2004). Recombination proteins in yeast. Annual review of genetics *38*, 233-271.

Lakdawala, S.S., Schwartz, R.A., Ferenchak, K., Carson, C.T., McSharry, B.P., Wilkinson, G.W., and Weitzman, M.D. (2008). Differential requirements of the C terminus of Nbs1 in suppressing adenovirus DNA replication and promoting concatemer formation. J Virol *82*, 8362-8372.

Lambert, S., Watson, A., Sheedy, D.M., Martin, B., and Carr, A.M. (2005). Gross chromosomal rearrangements and elevated recombination at an inducible site-specific replication fork barrier. Cell *121*, 689-702.

Lammens, K., Bemeleit, D.J., Mockel, C., Clausing, E., Schele, A., Hartung, S., Schiller, C.B., Lucas, M., Angermuller, C., Soding, J.*, et al.* (2011). The Mre11:Rad50 structure shows an ATP-dependent molecular clamp in DNA double-strand break repair. Cell *145*, 54-66.

Langerak, P., Mejia-Ramirez, E., Limbo, O., and Russell, P. (2011). Release of Ku and MRN from DNA ends by Mre11 nuclease activity and Ctp1 is required for homologous recombination repair of double-strand breaks. PLoS genetics *7*, e1002271.

Lee, J.H., Ghirlando, R., Bhaskara, V., Hoffmeyer, M.R., Gu, J., and Paull, T.T. (2003). Regulation of Mre11/Rad50 by Nbs1: effects on nucleotide-dependent DNA binding and association with ataxia-telangiectasia-like disorder mutant complexes. J Biol Chem *278*, 45171-45181.

Lee, J.H., Mand, M.R., Deshpande, R.A., Kinoshita, E., Yang, S.H., Wyman, C., and Paull, T.T. (2013). Ataxia telangiectasia-mutated (ATM) kinase activity is regulated by ATP-driven conformational changes in the Mre11/Rad50/Nbs1 (MRN) complex. J Biol Chem *288*, 12840-12851.

Lee, J.H., and Paull, T.T. (2005). ATM activation by DNA double-strand breaks through the Mre11-Rad50-Nbs1 complex. Science *308*, 551-554.

Lee, K., Zhang, Y., and Lee, S.E. (2008). Saccharomyces cerevisiae ATM orthologue suppresses break-induced chromosome translocations. Nature *454*, 543-546.

Lee, S.E., Moore, J.K., Holmes, A., Umezu, K., Kolodner, R.D., and Haber, J.E. (1998). Saccharomyces Ku70, mre11/rad50 and RPA proteins regulate adaptation to G2/M arrest after DNA damage. Cell *94*, 399-409.

Lee-Theilen, M., Matthews, A.J., Kelly, D., Zheng, S., and Chaudhuri, J. (2011). CtIP promotes microhomology-mediated alternative end joining during class-switch recombination. Nat Struct Mol Biol *18*, 75-79.

Lemacon, D., Jackson, J., Quinet, A., Brickner, J.R., Li, S., Yazinski, S., You, Z., Ira, G., Zou, L., Mosammaparast, N.*, et al.* (2017). MRE11 and EXO1 nucleases degrade reversed forks and elicit MUS81-dependent fork rescue in BRCA2-deficient cells. Nat Commun *8*, 860.

Lempiainen, H., and Halazonetis, T.D. (2009). Emerging common themes in regulation of PIKKs and PI3Ks. EMBO J *28*, 3067-3073.

Lengsfeld, B.M., Rattray, A.J., Bhaskara, V., Ghirlando, R., and Paull, T.T. (2007). Sae2 is an endonuclease that processes hairpin DNA cooperatively with the Mre11/Rad50/Xrs2 complex. Molecular cell *28*, 638-651.

Levy, D.L., and Blackburn, E.H. (2004). Counting of Rif1p and Rif2p on Saccharomyces cerevisiae telomeres regulates telomere length. Mol Cell Biol *24*, 10857-10867.

Liang, J., Suhandynata, R.T., and Zhou, H. (2015). Phosphorylation of Sae2 Mediates Forkhead-associated (FHA) Domain-specific Interaction and Regulates Its DNA Repair Function. J Biol Chem *290*, 10751-10763.

Lim, D.S., Kim, S.T., Xu, B., Maser, R.S., Lin, J., Petrini, J.H., and Kastan, M.B. (2000). ATM phosphorylates p95/nbs1 in an S-phase checkpoint pathway. Nature *404*, 613-617.

Lim, H.S., Kim, J.S., Park, Y.B., Gwon, G.H., and Cho, Y. (2011). Crystal structure of the Mre11-Rad50-ATPgammaS complex: understanding the interplay between Mre11 and Rad50. Genes Dev *25*, 1091-1104.

Limbo, O., Chahwan, C., Yamada, Y., de Bruin, R.A., Wittenberg, C., and Russell, P. (2007). Ctp1 is a cell-cycle-regulated protein that functions with Mre11 complex to control double-strand break repair by homologous recombination. Molecular cell *28*, 134-146.

Limbo, O., Yamada, Y., and Russell, P. (2018). Mre11-Rad50-dependent activity of ATM/Tel1 at DNA breaks and telomeres in the absence of Nbs1. Mol Biol Cell *29*, 1389-1399.

Lisby, M., Barlow, J.H., Burgess, R.C., and Rothstein, R. (2004). Choreography of the DNA damage response: spatiotemporal relationships among checkpoint and repair proteins. Cell *118*, 699-713.

Lisby, M., Mortensen, U.H., and Rothstein, R. (2003). Colocalization of multiple DNA double-strand breaks at a single Rad52 repair centre. Nat Cell Biol *5*, 572-577.

Lisby, M., Rothstein, R., and Mortensen, U.H. (2001). Rad52 forms DNA repair and recombination centers during S phase. Proc Natl Acad Sci U S A *98*, 8276-8282.

Lloyd, J., Chapman, J.R., Clapperton, J.A., Haire, L.F., Hartsuiker, E., Li, J., Carr, A.M., Jackson, S.P., and Smerdon, S.J. (2009). A supramodular FHA/BRCT-repeat architecture mediates Nbs1 adaptor function in response to DNA damage. Cell *139*, 100-111.

Lobachev, K., Vitriol, E., Stemple, J., Resnick, M.A., and Bloom, K. (2004). Chromosome fragmentation after induction of a double-strand break is an active process prevented by the RMX repair complex. Curr Biol *14*, 2107-2112.

Lobachev, K.S., Gordenin, D.A., and Resnick, M.A. (2002). The Mre11 complex is required for repair of hairpin-capped double-strand breaks and prevention of chromosome rearrangements. Cell *108*, 183-193.

Lobachev, K.S., Stenger, J.E., Kozyreva, O.G., Jurka, J., Gordenin, D.A., and Resnick, M.A. (2000). Inverted Alu repeats unstable in yeast are excluded from the human genome. EMBO J *19*, 3822-3830.

Lukas, C., Falck, J., Bartkova, J., Bartek, J., and Lukas, J. (2003). Distinct spatiotemporal dynamics of mammalian checkpoint regulators induced by DNA damage. Nat Cell Biol *5*, 255-260.

Luo, G., Yao, M.S., Bender, C.F., Mills, M., Bladl, A.R., Bradley, A., and Petrini, J.H. (1999). Disruption of mRad50 causes embryonic stem cell lethality, abnormal embryonic development, and sensitivity to ionizing radiation. Proc Natl Acad Sci U S A *96*, 7376-7381.

Ma, J.L., Kim, E.M., Haber, J.E., and Lee, S.E. (2003). Yeast Mre11 and Rad1 proteins define a Ku-independent mechanism to repair double-strand breaks lacking overlapping end sequences. Mol Cell Biol *23*, 8820-8828.

Ma, Y., Pannicke, U., Schwarz, K., and Lieber, M.R. (2002). Hairpin opening and overhang processing by an Artemis/DNA-dependent protein kinase complex in nonhomologous end joining and V(D)J recombination. Cell *108*, 781-794.

Majka, J., Binz, S.K., Wold, M.S., and Burgers, P.M. (2006). Replication protein A directs loading of the DNA damage checkpoint clamp to 5'-DNA junctions. J Biol Chem *281*, 27855-27861.

Makharashvili, N., Tubbs, A.T., Yang, S.H., Wang, H., Barton, O., Zhou, Y., Deshpande, R.A., Lee, J.H., Lobrich, M., Sleckman, B.P*., et al.* (2014). Catalytic and noncatalytic roles of the CtIP endonuclease in double-strand break end resection. Molecular cell *54*, 1022-1033.

Mallory, J.C., Bashkirov, V.I., Trujillo, K.M., Solinger, J.A., Dominska, M., Sung, P., Heyer, W.D., and Petes, T.D. (2003). Amino acid changes in Xrs2p, Dun1p, and Rfa2p that remove the preferred targets of the ATM family of protein kinases do not affect DNA repair or telomere length in Saccharomyces cerevisiae. DNA Repair (Amst) *2*, 1041-1064.

Malone, R.E., Ward, T., Lin, S., and Waring, J. (1990). The RAD50 gene, a member of the double strand break repair epistasis group, is not required for spontaneous mitotic recombination in yeast. Current genetics *18*, 111-116.

Mantiero, D., Clerici, M., Lucchini, G., and Longhese, M.P. (2007). Dual role for Saccharomyces cerevisiae Tel1 in the checkpoint response to double-strand breaks. EMBO reports *8*, 380-387.

Maser, R.S., Mirzoeva, O.K., Wells, J., Olivares, H., Williams, B.R., Zinkel, R.A., Farnham, P.J., and Petrini, J.H. (2001). Mre11 complex and DNA replication: linkage to E2F and sites of DNA synthesis. Mol Cell Biol *21*, 6006-6016.

Maser, R.S., Monsen, K.J., Nelms, B.E., and Petrini, J.H. (1997). hMre11 and hRad50 nuclear foci are induced during the normal cellular response to DNA double-strand breaks. Mol Cell Biol *17*, 6087-6096.

Matsuzaki, K., Shinohara, A., and Shinohara, M. (2008). Forkhead-associated domain of yeast Xrs2, a homolog of human Nbs1, promotes nonhomologous end joining through interaction with a ligase IV partner protein, Lif1. Genetics *179*, 213-225.

McKee, A.H., and Kleckner, N. (1997a). A general method for identifying recessive diploid-specific mutations in Saccharomyces cerevisiae, its application to the isolation of mutants blocked at intermediate stages of meiotic prophase and characterization of a new gene SAE2. Genetics *146*, 797-816.

McKee, A.H., and Kleckner, N. (1997b). Mutations in Saccharomyces cerevisiae that block meiotic prophase chromosome metabolism and confer cell cycle arrest at pachytene identify two new meiosis-specific genes SAE1 and SAE3. Genetics *146*, 817-834.

Melo, J.A., Cohen, J., and Toczyski, D.P. (2001). Two checkpoint complexes are independently recruited to sites of DNA damage in vivo. Genes Dev *15*, 2809-2821.

Menin, L., Ursich, S., Trovesi, C., Zellweger, R., Lopes, M., Longhese, M.P., and Clerici, M. (2018). Tel1/ATM prevents degradation of replication forks that reverse after topoisomerase poisoning. EMBO reports.

Mijic, S., Zellweger, R., Chappidi, N., Berti, M., Jacobs, K., Mutreja, K., Ursich, S., Ray Chaudhuri, A., Nussenzweig, A., Janscak, P.*, et al.* (2017). Replication fork reversal triggers fork degradation in BRCA2-defective cells. Nat Commun *8*, 859.

Milman, N., Higuchi, E., and Smith, G.R. (2009). Meiotic DNA double-strand break repair requires two nucleases, MRN and Ctp1, to produce a single size class of Rec12 (Spo11)-oligonucleotide complexes. Molecular and cellular biology *29*, 5998-6005.

Mimitou, E.P., and Symington, L.S. (2008). Sae2, Exo1 and Sgs1 collaborate in DNA double-strand break processing. Nature *455*, 770-774.

Mimitou, E.P., and Symington, L.S. (2009). DNA end resection: many nucleases make light work. DNA Repair (Amst) *8*, 983-995.

Mimitou, E.P., and Symington, L.S. (2010). Ku prevents Exo1 and Sgs1-dependent resection of DNA ends in the absence of a functional MRX complex or Sae2. EMBO J *29*, 3358-3369.

Mimitou, E.P., Yamada, S., and Keeney, S. (2017). A global view of meiotic double-strand break end resection. Science *355*, 40-45.

Mirzoeva, O.K., and Petrini, J.H. (2003). DNA replication-dependent nuclear dynamics of the Mre11 complex. Mol Cancer Res *1*, 207-218.

Mitelman, F. (1991). Cancer Cytogenetics - an Overview. American journal of human genetics *49*, 74-74.

Mockel, C., Lammens, K., Schele, A., and Hopfner, K.P. (2012). ATP driven structural changes of the bacterial Mre11:Rad50 catalytic head complex. Nucleic acids research *40*, 914-927.

Mohapatra, S., Yannone, S.M., Lee, S.H., Hromas, R.A., Akopiants, K., Menon, V., Ramsden, D.A., and Povirk, L.F. (2013). Trimming of damaged 3' overhangs of DNA double-strand breaks by the Metnase and Artemis endonucleases. DNA Repair (Amst) *12*, 422-432.

Moore, J.K., and Haber, J.E. (1996). Cell cycle and genetic requirements of two pathways of nonhomologous end-joining repair of double-strand breaks in Saccharomyces cerevisiae. Molecular and cellular biology *16*, 2164-2173.

Morales, M., Theunissen, J.W., Kim, C.F., Kitagawa, R., Kastan, M.B., and Petrini, J.H. (2005). The Rad50S allele promotes ATM-dependent DNA damage responses and suppresses ATM deficiency: implications for the Mre11 complex as a DNA damage sensor. Genes Dev *19*, 3043-3054.

Moreau, S., Ferguson, J.R., and Symington, L.S. (1999). The nuclease activity of Mre11 is required for meiosis but not for mating type switching, end joining, or telomere maintenance. Mol Cell Biol *19*, 556-566.

Mozlin, A.M., Fung, C.W., and Symington, L.S. (2008). Role of the Saccharomyces cerevisiae Rad51 paralogs in sister chromatid recombination. Genetics *178*, 113-126.

Myler, L.R., Gallardo, I.F., Soniat, M.M., Deshpande, R.A., Gonzalez, X.B., Kim, Y., Paull, T.T., and Finkelstein, I.J. (2017). Single-Molecule Imaging Reveals How Mre11-Rad50-Nbs1 Initiates DNA Break Repair. Mol Cell *67*, 891-898 e894.

Myung, K., Chen, C., and Kolodner, R.D. (2001a). Multiple pathways cooperate in the suppression of genome instability in Saccharomyces cerevisiae. Nature *411*, 1073-1076.

Myung, K., Datta, A., and Kolodner, R.D. (2001b). Suppression of spontaneous chromosomal rearrangements by S phase checkpoint functions in Saccharomyces cerevisiae. Cell *104*, 397-408.

Nairz, K., and Klein, F. (1997). mre11S--a yeast mutation that blocks double-strand-break processing and permits nonhomologous synapsis in meiosis. Genes Dev *11*, 2272-2290.

Nakada, D., Hirano, Y., Tanaka, Y., and Sugimoto, K. (2005). Role of the C terminus of Mec1 checkpoint kinase in its localization to sites of DNA damage. Mol Biol Cell *16*, 5227-5235.

Nakada, D., Matsumoto, K., and Sugimoto, K. (2003). ATM-related Tel1 associates with double-strand breaks through an Xrs2-dependent mechanism. Genes Dev *17*, 1957-1962.

Narayanan, V., Mieczkowski, P.A., Kim, H.M., Petes, T.D., and Lobachev, K.S. (2006). The pattern of gene amplification is determined by the chromosomal location of hairpin-capped breaks. Cell *125*, 1283-1296.

Neale, M.J., Pan, J., and Keeney, S. (2005). Endonucleolytic processing of covalent protein-linked DNA double-strand breaks. Nature *436*, 1053-1057.

Neelsen, K.J., and Lopes, M. (2015). Replication fork reversal in eukaryotes: from dead end to dynamic response. Nat Rev Mol Cell Biol *16*, 207-220.

Nelms, B.E., Maser, R.S., MacKay, J.F., Lagally, M.G., and Petrini, J.H. (1998). In situ visualization of DNA double-strand break repair in human fibroblasts. Science *280*, 590-592.

Niu, H., Chung, W.H., Zhu, Z., Kwon, Y., Zhao, W., Chi, P., Prakash, R., Seong, C., Liu, D., Lu, L.*, et al.* (2010). Mechanism of the ATP-dependent DNA end-resection machinery from Saccharomyces cerevisiae. Nature *467*, 108-111.

Ogi, H., Goto, G.H., Ghosh, A., Zencir, S., Henry, E., and Sugimoto, K. (2015). Requirement of the FATC domain of protein kinase Tel1 for localization to DNA ends and target protein recognition. Mol Biol Cell *26*, 3480-3488.

Oh, J., Al-Zain, A., Cannavo, E., Cejka, P., and Symington, L.S. (2016). Xrs2 Dependent and Independent Functions of the Mre11-Rad50 Complex. Molecular cell *64*, 405-415.

Ohta, K., Nicolas, A., Furuse, M., Nabetani, A., Ogawa, H., and Shibata, T. (1998). Mutations in the MRE11, RAD50, XRS2, and MRE2 genes alter chromatin configuration at meiotic DNA double-stranded break sites in premeiotic and meiotic cells. Proc Natl Acad Sci U S A *95*, 646-651.

Olson, E., Nievera, C.J., Liu, E., Lee, A.Y., Chen, L., and Wu, X. (2007). The Mre11 complex mediates the S-phase checkpoint through an interaction with replication protein A. Mol Cell Biol *27*, 6053-6067.

Palm, W., and de Lange, T. (2008). How shelterin protects mammalian telomeres. Annual review of genetics *42*, 301-334.

Palmbos, P.L., Wu, D., Daley, J.M., and Wilson, T.E. (2008). Recruitment of Saccharomyces cerevisiae Dnl4-Lif1 complex to a double-strand break requires interactions with Yku80 and the Xrs2 FHA domain. Genetics *180*, 1809-1819.

Park, Y.B., Chae, J., Kim, Y.C., and Cho, Y. (2011). Crystal structure of human Mre11: understanding tumorigenic mutations. Structure *19*, 1591-1602.

Paull, T.T., and Gellert, M. (1998). The 3' to 5' exonuclease activity of Mre 11 facilitates repair of DNA double-strand breaks. Mol Cell *1*, 969-979.

Paull, T.T., and Gellert, M. (1999). Nbs1 potentiates ATP-driven DNA unwinding and endonuclease cleavage by the Mre11/Rad50 complex. Genes Dev *13*, 1276-1288.

Peterson, S.E., Li, Y., Wu-Baer, F., Chait, B.T., Baer, R., Yan, H., Gottesman, M.E., and Gautier, J. (2013). Activation of DSB processing requires phosphorylation of CtIP by ATR. Mol Cell *49*, 657-667.

Prinz, S., Amon, A., and Klein, F. (1997). Isolation of COM1, a new gene required to complete meiotic double-strand break-induced recombination in Saccharomyces cerevisiae. Genetics *146*, 781-795.

Puddu, F., Oelschlaegel, T., Guerini, I., Geisler, N.J., Niu, H., Herzog, M., Salguero, I., Ochoa-Montano, B., Vire, E., Sung, P.*, et al.* (2015). Synthetic viability genomic screening defines Sae2 function in DNA repair. EMBO J *34*, 1509-1522.

Putnam, C.D., Hayes, T.K., and Kolodner, R.D. (2009). Specific pathways prevent duplication-mediated genome rearrangements. Nature *460*, 984-989.

Putnam, C.D., and Kolodner, R.D. (2010). Determination of gross chromosomal rearrangement rates. Cold Spring Harb Protoc *2010*, pdb prot5492.

Rass, E., Grabarz, A., Plo, I., Gautier, J., Bertrand, P., and Lopez, B.S. (2009). Role of Mre11 in chromosomal nonhomologous end joining in mammalian cells. Nat Struct Mol Biol *16*, 819-824.

Rattray, A.J., McGill, C.B., Shafer, B.K., and Strathern, J.N. (2001). Fidelity of mitotic double-strand-break repair in Saccharomyces cerevisiae: a role for SAE2/COM1. Genetics *158*, 109-122.

Rattray, A.J., Shafer, B.K., Neelam, B., and Strathern, J.N. (2005). A mechanism of palindromic gene amplification in Saccharomyces cerevisiae. Genes Dev *19*, 1390-1399.

Ray Chaudhuri, A., Hashimoto, Y., Herrador, R., Neelsen, K.J., Fachinetti, D., Bermejo, R., Cocito, A., Costanzo, V., and Lopes, M. (2012). Topoisomerase I poisoning results in PARP-mediated replication fork reversal. Nat Struct Mol Biol *19*, 417-423.

Reginato, G., Cannavo, E., and Cejka, P. (2017). Physiological protein blocks direct the Mre11-Rad50-Xrs2 and Sae2 nuclease complex to initiate DNA end resection. Genes Dev *31*, 2325-2330.

Ritchie, K.B., and Petes, T.D. (2000). The Mre11p/Rad50p/Xrs2p complex and the Tel1p function in a single pathway for telomere maintenance in yeast. Genetics *155*, 475-479.

Robert, I., Dantzer, F., and Reina-San-Martin, B. (2009). Parp1 facilitates alternative NHEJ, whereas Parp2 suppresses IgH/c-myc translocations during immunoglobulin class switch recombination. J Exp Med *206*, 1047-1056.

Robison, J.G., Elliott, J., Dixon, K., and Oakley, G.G. (2004). Replication protein A and the Mre11.Rad50.Nbs1 complex co-localize and interact at sites of stalled replication forks. J Biol Chem *279*, 34802-34810.

Rogakou, E.P., Pilch, D.R., Orr, A.H., Ivanova, V.S., and Bonner, W.M. (1998). DNA double-stranded breaks induce histone H2AX phosphorylation on serine 139. J Biol Chem *273*, 5858-5868.

Ruff, P., Donnianni, R.A., Glancy, E., Oh, J., and Symington, L.S. (2016). RPA Stabilization of Single-Stranded DNA Is Critical for Break-Induced Replication. Cell Rep *17*, 3359-3368.

Saeki, T., Machida, I., and Nakai, S. (1980). Genetic control of diploid recovery after gamma-irradiation in the yeast Saccharomyces cerevisiae. Mutat Res *73*, 251-265.

Sakofsky, C.J., and Malkova, A. (2017). Break induced replication in eukaryotes: mechanisms, functions, and consequences. Crit Rev Biochem Mol Biol *52*, 395-413.

Sanchez, Y., Desany, B.A., Jones, W.J., Liu, Q., Wang, B., and Elledge, S.J. (1996). Regulation of RAD53 by the ATM-like kinases MEC1 and TEL1 in yeast cell cycle checkpoint pathways. Science *271*, 357-360.

Sarbajna, S., and West, S.C. (2014). Holliday junction processing enzymes as guardians of genome stability. Trends Biochem Sci *39*, 409-419.

Sartori, A.A., Lukas, C., Coates, J., Mistrik, M., Fu, S., Bartek, J., Baer, R., Lukas, J., and Jackson, S.P. (2007). Human CtIP promotes DNA end resection. Nature *450*, 509-514.

Schiller, C.B., Lammens, K., Guerini, I., Coordes, B., Feldmann, H., Schlauderer, F., Mockel, C., Schele, A., Strasser, K., Jackson, S.P.*, et al.* (2012). Structure of Mre11-Nbs1 complex yields insights into ataxia-telangiectasia-like disease mutations and DNA damage signaling. Nat Struct Mol Biol *19*, 693-700.

Schlacher, K., Christ, N., Siaud, N., Egashira, A., Wu, H., and Jasin, M. (2011). Double-strand break repair-independent role for BRCA2 in blocking stalled replication fork degradation by MRE11. Cell *145*, 529-542.

Seeber, A., Hegnauer, A.M., Hustedt, N., Deshpande, I., Poli, J., Eglinger, J., Pasero, P., Gut, H., Shinohara, M., Hopfner, K.P.*, et al.* (2016). RPA Mediates Recruitment of MRX to Forks and Double-Strand Breaks to Hold Sister Chromatids Together. Mol Cell *64*, 951-966.

Sfeir, A., and Symington, L.S. (2015). Microhomology-Mediated End Joining: A Back-up Survival Mechanism or Dedicated Pathway? Trends Biochem Sci *40*, 701-714.

Shibata, A., Moiani, D., Arvai, A.S., Perry, J., Harding, S.M., Genois, M.M., Maity, R., van Rossum-Fikkert, S., Kertokalio, A., Romoli, F.*, et al.* (2014). DNA double-strand break repair pathway choice is directed by distinct MRE11 nuclease activities. Mol Cell *53*, 7-18.

Shikano, T., Arioka, H., Kobayashi, R., Naito, H., and Ishikawa, Y. (1993). Jumping translocations of 1q in Burkitt lymphoma and acute nonlymphocytic leukemia. Cancer Genet Cytogenet *71*, 22-26.

Shiloh, Y. (1997). Ataxia-telangiectasia and the Nijmegen breakage syndrome: related disorders but genes apart. Annual review of genetics *31*, 635-662.

Shim, E.Y., Chung, W.H., Nicolette, M.L., Zhang, Y., Davis, M., Zhu, Z., Paull, T.T., Ira, G., and Lee, S.E. (2010). Saccharomyces cerevisiae Mre11/Rad50/Xrs2 and Ku proteins regulate association of Exo1 and Dna2 with DNA breaks. EMBO J *29*, 3370-3380.

Shima, H., Suzuki, M., and Shinohara, M. (2005). Isolation and characterization of novel xrs2 mutations in Saccharomyces cerevisiae. Genetics *170*, 71-85.

Sirbu, B.M., Couch, F.B., Feigerle, J.T., Bhaskara, S., Hiebert, S.W., and Cortez, D. (2011). Analysis of protein dynamics at active, stalled, and collapsed replication forks. Genes Dev *25*, 1320-1327.

Sjogren, C., and Nasmyth, K. (2001). Sister chromatid cohesion is required for postreplicative double-strand break repair in Saccharomyces cerevisiae. Current biology : CB *11*, 991-995.

Smith, C.E., Llorente, B., and Symington, L.S. (2007). Template switching during break-induced replication. Nature *447*, 102-105.

Smith, S., Gupta, A., Kolodner, R.D., and Myung, K. (2005). Suppression of gross chromosomal rearrangements by the multiple functions of the Mre11-Rad50-Xrs2 complex in Saccharomyces cerevisiae. DNA Repair (Amst) *4*, 606-617.

Stewart, G.S., Maser, R.S., Stankovic, T., Bressan, D.A., Kaplan, M.I., Jaspers, N.G., Raams, A., Byrd, P.J., Petrini, J.H., and Taylor, A.M. (1999). The DNA double-strand break repair gene hMRE11 is mutated in individuals with an ataxia-telangiectasia-like disorder. Cell *99*, 577-587.

Stracker, T.H., Morales, M., Couto, S.S., Hussein, H., and Petrini, J.H. (2007). The carboxy terminus of NBS1 is required for induction of apoptosis by the MRE11 complex. Nature *447*, 218-221.

Stracker, T.H., and Petrini, J.H. (2011). The MRE11 complex: starting from the ends. Nat Rev Mol Cell Biol *12*, 90-103.

Strom, L., Karlsson, C., Lindroos, H.B., Wedahl, S., Katou, Y., Shirahige, K., and Sjogren, C. (2007). Postreplicative formation of cohesion is required for repair and induced by a single DNA break. Science *317*, 242-245.

Strom, L., and Sjogren, C. (2007). Chromosome segregation and double-strand break repair - a complex connection. Curr Opin Cell Biol *19*, 344-349.

Svendsen, J.M., and Harper, J.W. (2010). GEN1/Yen1 and the SLX4 complex: Solutions to the problem of Holliday junction resolution. Genes Dev *24*, 521-536.

Symington, L.S., Rothstein, R., and Lisby, M. (2014). Mechanisms and regulation of mitotic recombination in Saccharomyces cerevisiae. Genetics *198*, 795-835.

Szostak, J.W., Orr-Weaver, T.L., Rothstein, R.J., and Stahl, F.W. (1983). The double-strand-break repair model for recombination. Cell *33*, 25-35.

Taglialatela, A., Alvarez, S., Leuzzi, G., Sannino, V., Ranjha, L., Huang, J.W., Madubata, C., Anand, R., Levy, B., Rabadan, R.*, et al.* (2017). Restoration of Replication Fork Stability in BRCA1- and BRCA2-Deficient Cells by Inactivation of SNF2-Family Fork Remodelers. Mol Cell *68*, 414-430 e418.

Takai, H., Smogorzewska, A., and de Lange, T. (2003). DNA damage foci at dysfunctional telomeres. Current biology : CB *13*, 1549-1556.

Tauchi, H., Kobayashi, J., Morishima, K., Matsuura, S., Nakamura, A., Shiraishi, T., Ito, E., Masnada, D., Delia, D., and Komatsu, K. (2001). The forkhead-associated domain of NBS1 is essential for nuclear foci formation after irradiation but not essential for hRAD50[middle dot]hMRE11[middle dot]NBS1 complex DNA repair activity. J Biol Chem *276*, 12-15.

Tittel-Elmer, M., Alabert, C., Pasero, P., and Cobb, J.A. (2009). The MRX complex stabilizes the replisome independently of the S phase checkpoint during replication stress. EMBO J *28*, 1142-1156.

Tittel-Elmer, M., Lengronne, A., Davidson, M.B., Bacal, J., Francois, P., Hohl, M., Petrini, J.H.J., Pasero, P., and Cobb, J.A. (2012). Cohesin association to replication sites depends on rad50 and promotes fork restart. Mol Cell *48*, 98-108.

Trujillo, K.M., Roh, D.H., Chen, L., Van Komen, S., Tomkinson, A., and Sung, P. (2003). Yeast xrs2 binds DNA and helps target rad50 and mre11 to DNA ends. J Biol Chem *278*, 48957-48964.

Trujillo, K.M., and Sung, P. (2001). DNA structure-specific nuclease activities in the Saccharomyces cerevisiae Rad50*Mre11 complex. J Biol Chem *276*, 35458-35464.

Truong, L.N., Li, Y., Shi, L.Z., Hwang, P.Y., He, J., Wang, H., Razavian, N., Berns, M.W., and Wu, X. (2013). Microhomology-mediated End Joining and Homologous Recombination share the initial end resection step to repair DNA double-strand breaks in mammalian cells. Proc Natl Acad Sci U S A *110*, 7720-7725.

Tseng, S.F., Lin, J.J., and Teng, S.C. (2006). The telomerase-recruitment domain of the telomere binding protein Cdc13 is regulated by Mec1p/Tel1p-dependent phosphorylation. Nucleic acids research *34*, 6327-6336.

Tsukamoto, Y., Mitsuoka, C., Terasawa, M., Ogawa, H., and Ogawa, T. (2005). Xrs2p regulates Mre11p translocation to the nucleus and plays a role in telomere elongation and meiotic recombination. Mol Biol Cell *16*, 597-608.

Unal, E., Arbel-Eden, A., Sattler, U., Shroff, R., Lichten, M., Haber, J.E., and Koshland, D. (2004). DNA damage response pathway uses histone modification to assemble a double-strand break-specific cohesin domain. Mol Cell *16*, 991-1002.

Unal, E., Heidinger-Pauli, J.M., and Koshland, D. (2007). DNA double-strand breaks trigger genome-wide sister-chromatid cohesion through Eco1 (Ctf7). Science *317*, 245-248.

Usui, T., Ogawa, H., and Petrini, J.H. (2001). A DNA damage response pathway controlled by Tel1 and the Mre11 complex. Mol Cell *7*, 1255-1266.

Usui, T., Ohta, T., Oshiumi, H., Tomizawa, J., Ogawa, H., and Ogawa, T. (1998). Complex formation and functional versatility of Mre11 of budding yeast in recombination. Cell *95*, 705-716.

Vallerga, M.B., Mansilla, S.F., Federico, M.B., Bertolin, A.P., and Gottifredi, V. (2015). Rad51 recombinase prevents Mre11 nuclease-dependent degradation and excessive PrimPol-mediated elongation of nascent DNA after UV irradiation. Proc Natl Acad Sci U S A *112*, E6624-6633.

van Attikum, H., Fritsch, O., Hohn, B., and Gasser, S.M. (2004). Recruitment of the INO80 complex by H2A phosphorylation links ATP-dependent chromatin remodeling with DNA double-strand break repair. Cell *119*, 777-788.

van der Linden, E., Sanchez, H., Kinoshita, E., Kanaar, R., and Wyman, C. (2009). RAD50 and NBS1 form a stable complex functional in DNA binding and tethering. Nucleic acids research *37*, 1580-1588.

Vialard, J.E., Gilbert, C.S., Green, C.M., and Lowndes, N.F. (1998). The budding yeast Rad9 checkpoint protein is subjected to Mec1/Tel1-dependent hyperphosphorylation and interacts with Rad53 after DNA damage. EMBO J *17*, 5679-5688.

Vissinga, C.S., Yeo, T.C., Warren, S., Brawley, J.V., Phillips, J., Cerosaletti, K., and Concannon, P. (2009). Nuclear export of NBN is required for normal cellular responses to radiation. Mol Cell Biol *29*, 1000-1006.

Vujanovic, M., Krietsch, J., Raso, M.C., Terraneo, N., Zellweger, R., Schmid, J.A., Taglialatela, A., Huang, J.W., Holland, C.L., Zwicky, K.*, et al.* (2017). Replication Fork Slowing and Reversal upon DNA Damage Require PCNA Polyubiquitination and ZRANB3 DNA Translocase Activity. Mol Cell *67*, 882-890 e885.

Wang, H., Li, Y., Truong, L.N., Shi, L.Z., Hwang, P.Y., He, J., Do, J., Cho, M.J., Li, H., Negrete, A.*, et al.* (2014). CtIP maintains stability at common fragile sites and inverted repeats by end resection-independent endonuclease activity. Molecular cell *54*, 1012-1021.

Wang, H., Shi, L.Z., Wong, C.C., Han, X., Hwang, P.Y., Truong, L.N., Zhu, Q., Shao, Z., Chen, D.J., Berns, M.W.*, et al.* (2013). The interaction of CtIP and Nbs1 connects CDK and ATM to regulate HR-mediated double-strand break repair. PLoS genetics *9*, e1003277.

Wang, W., Daley, J.M., Kwon, Y., Krasner, D.S., and Sung, P. (2017). Plasticity of the Mre11-Rad50-Xrs2-Sae2 nuclease ensemble in the processing of DNA-bound obstacles. Genes Dev *31*, 2331-2336.

Wellinger, R.J., and Zakian, V.A. (2012). Everything you ever wanted to know about Saccharomyces cerevisiae telomeres: beginning to end. Genetics *191*, 1073-1105.

Williams, B.R., Mirzoeva, O.K., Morgan, W.F., Lin, J., Dunnick, W., and Petrini, J.H. (2002). A murine model of Nijmegen breakage syndrome. Current biology : CB *12*, 648-653.

Williams, G.J., Lees-Miller, S.P., and Tainer, J.A. (2010). Mre11-Rad50-Nbs1 conformations and the control of sensing, signaling, and effector responses at DNA double-strand breaks. DNA Repair (Amst) *9*, 1299-1306.

Williams, R.S., Dodson, G.E., Limbo, O., Yamada, Y., Williams, J.S., Guenther, G., Classen, S., Glover, J.N., Iwasaki, H., Russell, P.*, et al.* (2009). Nbs1 flexibly tethers Ctp1 and Mre11-Rad50 to coordinate DNA double-strand break processing and repair. Cell *139*, 87-99.

Williams, R.S., Moncalian, G., Williams, J.S., Yamada, Y., Limbo, O., Shin, D.S., Groocock, L.M., Cahill, D., Hitomi, C., Guenther, G.*, et al.* (2008). Mre11 dimers coordinate DNA end bridging and nuclease processing in double-strand-break repair. Cell *135*, 97-109.

Wiltzius, J.J., Hohl, M., Fleming, J.C., and Petrini, J.H. (2005). The Rad50 hook domain is a critical determinant of Mre11 complex functions. Nat Struct Mol Biol *12*, 403-407.

Wotton, D., and Shore, D. (1997). A novel Rap1p-interacting factor, Rif2p, cooperates with Rif1p to regulate telomere length in Saccharomyces cerevisiae. Genes Dev *11*, 748-760.

Wu, D., Topper, L.M., and Wilson, T.E. (2008). Recruitment and dissociation of nonhomologous end joining proteins at a DNA double-strand break in Saccharomyces cerevisiae. Genetics *178*, 1237-1249.

Wu, L., and Hickson, I.D. (2003). The Bloom's syndrome helicase suppresses crossing over during homologous recombination. Nature *426*, 870-874.

Xiao, Y., and Weaver, D.T. (1997). Conditional gene targeted deletion by Cre recombinase demonstrates the requirement for the double-strand break repair Mre11 protein in murine embryonic stem cells. Nucleic acids research *25*, 2985-2991.

Xu, C., Wu, L., Cui, G., Botuyan, M.V., Chen, J., and Mer, G. (2008). Structure of a second BRCT domain identified in the nijmegen breakage syndrome protein Nbs1 and its function in an MDC1-dependent localization of Nbs1 to DNA damage sites. J Mol Biol *381*, 361-372.

Yan, C.T., Boboila, C., Souza, E.K., Franco, S., Hickernell, T.R., Murphy, M., Gumaste, S., Geyer, M., Zarrin, A.A., Manis, J.P.*, et al.* (2007). IgH class switching and translocations use a robust non-classical end-joining pathway. Nature *449*, 478-482.

Ying, S., Hamdy, F.C., and Helleday, T. (2012). Mre11-dependent degradation of stalled DNA replication forks is prevented by BRCA2 and PARP1. Cancer Res *72*, 2814-2821.

You, Z., Chahwan, C., Bailis, J., Hunter, T., and Russell, P. (2005). ATM activation and its recruitment to damaged DNA require binding to the C terminus of Nbs1. Molecular and cellular biology *25*, 5363-5379.

Young, J.A., Hyppa, R.W., and Smith, G.R. (2004). Conserved and nonconserved proteins for meiotic DNA breakage and repair in yeasts. Genetics *167*, 593-605.

Yu, A.M., and McVey, M. (2010). Synthesis-dependent microhomology-mediated end joining accounts for multiple types of repair junctions. Nucleic acids research *38*, 5706-5717.

Yu, C., Gan, H., Han, J., Zhou, Z.X., Jia, S., Chabes, A., Farrugia, G., Ordog, T., and Zhang, Z. (2014). Strand-specific analysis shows protein binding at replication forks and PCNA unloading from lagging strands when forks stall. Mol Cell *56*, 551-563.

Yu, X., and Gabriel, A. (2003). Ku-dependent and Ku-independent end-joining pathways lead to chromosomal rearrangements during double-strand break repair in Saccharomyces cerevisiae. Genetics *163*, 843-856.

Zakharyevich, K., Ma, Y., Tang, S., Hwang, P.Y., Boiteux, S., and Hunter, N. (2010). Temporally and biochemically distinct activities of Exo1 during meiosis: double-strand break resection and resolution of double Holliday junctions. Mol Cell *40*, 1001-1015.

Zhang, Y., and Jasin, M. (2011). An essential role for CtIP in chromosomal translocation formation through an alternative end-joining pathway. Nat Struct Mol Biol *18*, 80-84.

Zhao, S., Weng, Y.C., Yuan, S.S., Lin, Y.T., Hsu, H.C., Lin, S.C., Gerbino, E., Song, M.H., Zdzienicka, M.Z., Gatti, R.A.*, et al.* (2000). Functional link between ataxia-telangiectasia and Nijmegen breakage syndrome gene products. Nature *405*, 473-477.

Zhao, X., Muller, E.G., and Rothstein, R. (1998). A suppressor of two essential checkpoint genes identifies a novel protein that negatively affects dNTP pools. Molecular cell *2*, 329-340.

Zhu, J., Petersen, S., Tessarollo, L., and Nussenzweig, A. (2001). Targeted disruption of the Nijmegen breakage syndrome gene NBS1 leads to early embryonic lethality in mice. Current biology : CB *11*, 105-109.

Zhu, Z., Chung, W.H., Shim, E.Y., Lee, S.E., and Ira, G. (2008). Sgs1 helicase and two nucleases Dna2 and Exo1 resect DNA double-strand break ends. Cell *134*, 981-994.

Zierhut, C., and Diffley, J.F. (2008). Break dosage, cell cycle stage and DNA replication influence DNA double strand break response. EMBO J *27*, 1875-1885.

Zou, L., and Elledge, S.J. (2003). Sensing DNA damage through ATRIP recognition of RPA-ssDNA complexes. Science *300*, 1542-1548.

Appendix 1: Additional data for Chapter 3

The alleviation of DNA damage sensitivity in *xrs2Δ* cells by Mre11-NLS is Rad50 dependent in budding yeast (Figure 3-1C). However, expression of *Mre11-NLS* in *Nbs1*$^{-/-}$ mouse embryonic fibroblasts and human cells does not restore nuclear localization of Rad50 (Kim et al., 2017; Lakdawala et al., 2008), raising the possibility that the residual DNA damage sensitivity of *xrs2Δ MRE11-NLS* cells could be due to the limited Rad50 activity. To assess this possibility, Rad50 was overexpressed in *xrs2Δ MRE11-NLS* cells and CPT sensitivity was measured (Figure A1). We found that overexpression of Rad50 does not further alleviate the CPT sensitivity of *xrs2Δ MRE11-NLS* cells, indicating that Rad50 is not limiting for DNA repair.

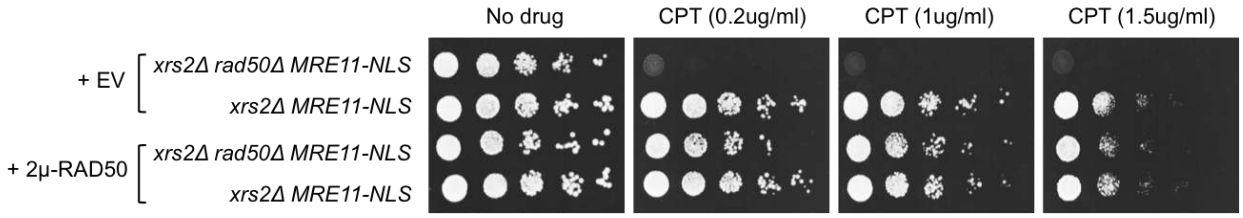

Figure A1. Rad50 is not limiting for DNA repair

Spot assay with the indicated strains transformed with empty vector or 2μ-RAD50.

Appendix 2: Additional data for Chapter 4

Expression of *MRE11-NLS* partially rescues the sporulation defect of *xrs2Δ* (7% of cells formed tetrads) (Figure 3-7A,B). Expression of *MRE11-NLS-TID* and *X224* both completely rescued the residual defect observed in *xrs2Δ MRE11-NLS*. This indicates that the quality and quantity of the MRX complex is important for meiotic DSB formation and/or processing.

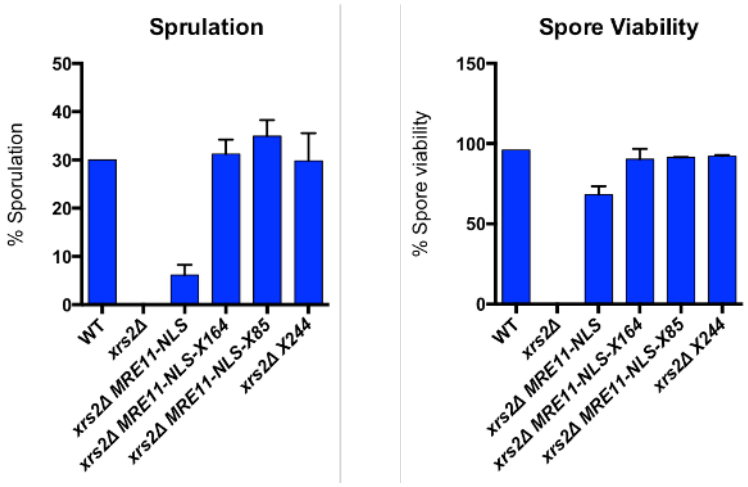

Figure A2. *MRE11-NLS-TID* and *X224* restores sporulation to WT level

Sporulation percentage determined by counting cells that contain three or four visible spores out of at least 700 total cells counted. Spore viability determined by dissection of asci and counting spores germinating to give visible colonies. No fewer than 50 asci were dissected for each strain.